Profiling the Insulin-like Growth Factor Receptor (IGF-1R) Signalling Pathway in Pancreatic Ductal Adenocarcinoma (PDAC) Cell Lines

Derushka Arnachellen

A dissertation submitted to the Faculty of Health Sciences, University of the Witwatersrand, Johannesburg, in fulfilment of the requirements for the degree of Master of Science in Medicine.

Johannesburg, 2021

DECLARATION

I, Derushka Arnachellen, declare that this Dissertation, which I hereby submit for the Degree of Master of Science in Medicine at the University of the Witwatersrand, Johannesburg, is my own, unaided work. This work has not been submitted before for any degree or examination at any other University.

……
Derushka Arnachellen

October 2021

ABSTRACT

Pancreatic ductal adenocarcinoma (PDAC) is the most common type of pancreatic cancers and accounts for 7 % of cancer-related mortalities worldwide. The disease has an overall 5year survival rate of less than 5 % and a median survival of 6 months, with mortalities caused by the disease being almost equal to the incidence each year. The poor prognosis associated with PDAC is attributed to its mostly asymptomatic nature and lack of specific biomarkers in the early stages of the disease, thus most cases are diagnosed at an advanced stage where metastasis has already occurred. Despite perceived improvements in chemotherapeutic and biological agent strategies, the prognosis of advanced PDAC remains dismal. This study investigated the role of the insulin-like growth factor 1 receptor (IGF-1R) pathway in PDAC *in vitro.* The baseline expression the IGF-1R and downstream signalling was determined in control and PDAC cell lines, which represented normal, early-, intermediate and late-stages of the disease. Further assessment of the role of IGF-1R signalling was assessed through modulation of the pathway with IGF-1, a stimulatory compound; and NVP-AEW541 and Picropodophyllotoxin (PPP) IGF-1R inhibitors. Diluent controls of DMSO and BSA were also used.

The HPDE, PANC-1. Mia PaCa-2 and CF PAC-1 cell lines were used. These cell lines are representative of the tumours from which they were derived, i.e., PANC-1, Mia PaCa-2 and CF PAC-1 cells represent the early, intermediate, and late stages of PDAC, and HPDE cells represent a normal, healthy pancreatic ductal cells. The cytotoxic potential of the NVPAEW541 and Picropodophyllotoxin inhibitors were determined using the Trypan blue exclusion method. The WST-1 assay was used to compare proliferation between the cell lines. Clonogenic and migration phenotypic assays were used to evaluate the survival and migratory capacity of the PDAC cells. Alterations in gene expression was assessed using quantitative real-time polymerase chain reaction (qRT-PCR). In Mia PaCa-2 cells, protein expression of downstream members of the IGF-1R pathway was assessed using a western blot analysis technique.

Across all cell lines the IC_{50} of NVP-AEW541 was found to be between 2.5 µM and 2.7 µM, and between 0.65 µM and 4 µM for the Picropodophyllotoxin inhibitor. NVP-AEW541 and Picropodophyllotoxin was found to significantly decrease cell proliferation in the HPDE, PANC-1 and CF PAC-1 cell lines. In addition, HPDE cells appeared to be the most sensitive cell line to the different treatment groups when compared to the other cell lines. Colony

counts were significantly decreased in all cell lines when treated with the DMSO diluent, with Picropodophyllotoxin being more effective than NVP-AEW541 in preventing large colony formations. Migration was significantly decreased in all cell lines when treated with DMSO, NVP-AEW541 and Picropodophyllotoxin. Analysis of gene expression data of genes involved in the IGF-1R pathway showed that NVP-AEW541 increased the expression of these genes in HPDE and CF PAC-1 cells. In PANC-1 and Mia PaCa-2 cells the expression of these genes was downregulated in cultures treated with NVP-AEW541.

Picropodophyllotoxin either decreased or had a minimal effect on gene expression in all cell lines. Protein expression of IGF-1R was found to be constant across all treatment groups in the Mia PaCa-2 cell line.

This study found that even though IGF-1R was not a predominant signalling cascade in the Mia PaCa-2 cell line which represents the intermediate stage of PDAC, and it is hypothesized that the cytotoxic effects of the compounds used may have been metabolised by these cells at a later point. It was further shown that PDAC cells responds differently at different stages of its progression, showing that a single treatment for all stages of the disease is not sufficient in improving overall patient survival. This demonstrates an urgent need for molecular subtyping of tumours which may lead to more tailored therapies for PDAC.

ACKNOWLEDGEMENTS

I would like to thank the following people, without which, this work would not have been possible.

My supervisors,

Prof Raquel Duarte, words cannot express how grateful I am to you for your continuous patience, understanding, advice and motivation. I have grown so much as a person and as a scientist working under your supervision. I am so grateful to have been given the opportunity for such growth. Thank you for all your help in ensuring my success.

Prof Martin Brand, for the advice, conceptualisation, and proof reading of this dissertation. Without you, this dissertation would not have been possible.

The Oncology Research Group.
Dr Caroline Dickens for always making time to assist me and for all the help with teaching me new techniques. Thérèse Dix-Peek, for being always willing to assist me with anything I needed. I appreciate your help and assistance so much.
Nomthandazo Twala and Confidence Magope for your friendship, encouragement, support and keeping me company during those long lab days.

The School of Anatomical Sciences and Mrs Hasiena Ali for use of the tissue culture facilities. I am so grateful for the support and assistance I continue to receive from this department.

The National Research Foundation (NRF) and the University of the Witwatersrand for their financial support during this study.

My amazing support group,
Dr Tanya Augustine, for your support, encouragement, and advice throughout the years. Your support and wisdom is always appreciated. You truly are an inspiration!
Sapna Kalyan, for your unconditional support, advice, patience, and wisdom during all our car rides home. Thank you for listening to my complaints and helping me to stay grounded. Your wisdom and advice have kept me centred throughout the past few years.

My ‘Anam Cara’, Nalencia Naidoo, Nadine Stock, Kgabo Tsheshene, Candice Pillay, Janisha Thakordas, Phumla Zitha and Trevolen Govender. Your friendship and support have helped me through some of my darkest days. The bond I share with each one of you is a special one and one which I hold extremely close to my heart. I am both honoured and humbled to call you all my soul friends.

Lastly, and most importantly, my amazing family. Your patience, love and support drive me to be a better person and a better scientist. Thank you for always encouraging my curiosity and allowing me the opportunity to do what I love. I will forever be indebted to you. My sister, Denisha, for all the love and encouragement, it means more to me than you will ever know. I hope I have made you all proud.

TABLE OF CONTENTS

DECLARATION i

ABSTRACT ii

ACKNOWLEDGEMENTS iv

LIST OF FIGURES ix

LIST OF TABLES xii

ABBREVIATIONS, ACRONYMS AND SYMBOLS xiii

CHAPTER 1: INTRODUCTION 1

1.1. Pancreatic Ductal Adenocarcinoma: Overview 1

1.1.1. Biology 1

1.1.2. Symptoms 4

1.1.3. Detection and staging 4

1.1.4. Treatment of PDAC 5

1.1.4.1. Surgery 5

1.1.4.2. Adjuvant therapy after resection 6

1.1.4.3. Treatment of metastatic disease 6

1.2. Hallmarks of Cancer 7

1.2.1. Sustaining Proliferative Signalling 7

1.2.2. Evading growth suppressors 8

1.2.3. Enabling infinite replicative potential 8

1.2.4. Genome instability and mutation 9

1.2.5. Angiogenesis 9

1.2.6. Inflammation and immune evasion 9

1.2.7. Metabolic rewiring 10

1.2.8. Invasion and metastasis 10

1.2.9. Evasion of apoptosis 11

1.3. Signal Transduction 12

1.3.1. Signalling pathways in PDAC 13

1.3.1.1. Epidermal Growth Factor Receptor (EGFR) pathway 13

1.3.1.2. Insulin-like Growth Factor Receptor (IGFR) pathway 14

1.3.1.3. Potential crosstalk between the EGFR and IGF-1R pathways in PDAC 16

1.4. Study Rationale 17

1.5. Aim: 18

1.6. Objectives: 18

CHAPTER 2: METHODOLOGY 19

2.1 Cell lines and cell maintenance 19

2.1.1. Cell lines 19
2.1.2. Cell culture and cell maintenance 19
2.1.3 Modulation of IGF-1R signalling 20
2.2. IC_{50} 21
2.2.1. Analysis 22
2.3. Assessment of cell proliferation 22
2.3.1. Water Soluble Tetrazolium Salts (WST)-1 Assay 22
2.3.1.2. Analysis 23
2.4. Clonogenic Assay 23
2.4.1. Crystal Violet Staining 23
2.4.2. Imaging and Analysis 24
2.5. Migration Assay 24
2.5.1. Scratch Assay 24
2.5.2. Imaging and Analysis 24
2.6. Apoptosis Assay ..... **Error! Bookmark not defined.**
2.6.1. Annexin V Human ELISA ..... **Error! Bookmark not defined.**
2.6.2. Analysis ..... **Error! Bookmark not defined.**
2.7. Quantitative real-time Polymerase Chain Reaction (qRT-PCR) 25
2.7.1. Primer design 25
2.7.2. RNA extraction 27
2.7.3 cDNA synthesis 27
2.7.4. Quantitative Real-Time Polymerase Chain Reaction (qRT-PCR) 28
2.7.5. Analysis 28
2.8. Western Blot Analysis 29
2.8.1. Total protein extraction 29
2.8.2. Protein Quantification 29
2.8.3. Dot Blot 29
2.8.4. Electrophoresis 30
2.9. Statistical Analysis 33
CHAPTER 3: RESULTS 34
3.1. IC_{50} 34
3.1.1. HPDE 35
3.1.2. PANC-1 36
3.1.3. Mia PaCa-2 37
3.1.4. CF PAC-1 38
3.2. Morphology 39

3.2.1. HPDE 39
3.2.2. PANC-1 41
3.2.3. Mia PaCa-2 41
3.2.4. CF PAC-1 42
3.3. WST-1 Proliferation Assay 43
3.4. Clonogenic Assays 47
3.5. Migration Assay 52
3.5.1. HPDE 52
3.5.2. PANC-1 54
3.5.3. Mia PaCa-2 56
3.5.4. CF PAC-1 58
3.6. Apoptosis ..... **Error! Bookmark not defined.**
3.7. Quantitative Real Time PCR 61
3.7.1. HPDE 61
3.7.2. PANC-1 62
3.7.3. Mia PaCa-2 63
3.7.4. CF PAC-1 63
3.7.5. BAX/BCL2 64
3.8. Western Blot Analysis 71
CHAPTER 4: DISCUSSION 72
4.1. IC_{50} ..... **Error! Bookmark not defined.**
4.2. The effects of IGF-1R modulation on PDAC cells ..... **Error! Bookmark not defined.**
4.2.1. The phenotypic effects of IGF-1R modulation ..... **Error! Bookmark not defined.**
4.2.1.1. Apoptosis ..... **Error! Bookmark not defined.**
4.2.2. The effects of IGF-1R modulation on gene expression ..... **Error! Bookmark not defined.**
4.3. Potential crosstalk between the IGF-1R and EGFR pathways..... **Error! Bookmark not defined.**
4.3. The effect of DMSO on PDAC cell lines ..... **Error! Bookmark not defined.**
4.4. Western Blotting troubleshooting ..... **Error! Bookmark not defined.**
4.5. Further Studies and Limitations ..... **Error! Bookmark not defined.**
CHAPTER 5: CONCLUSION ..... **Error! Bookmark not defined.**
REFERENCES 85
APPENDICES 102
Appendix A: Ethics Waiver 102
Appendix B: Solutions 103
Appendix C: Supplementary data 107
Appendix D: Turnitin Report 119

LIST OF FIGURES

CHAPTER 1: INTRODUCTION

Figure 1.1: A cross-section of the pancreas**……..2**

Figure 1.2: The development of normal pancreatic cells to a tumour**……3**

Figure 1.3: Therapeutic options of the different stages of PDAC**…….……7**

Figure 1.4: The Hallmarks of Cancer as described by Hanahan *et al.,* 2011**……..……...12**

Figure 1.5: The interaction of IGF-1R and its major downstream signalling cascades**…..…16**

Figure 1.6: The role of EGFR and IGFR in cancer progression**…..……..……..17**

CHAPTER 2: METHODOLOGY

Figure 2.1: Experimental set-up for spotting of samples in a dot blot**……29**

Figure 2.2: Schematic demonstrating the assembly of western blotting equipment for protein transfer**……..……...31**

CHAPTER 3: RESULTS

Figure 3.1: IC_{50} values of a) NVP-AEW541 and b) Picropodophyllotoxin (PPP) treatments in the HPDE cell line**……..……..……35**

Figure 3.2: IC_{50} values of a) NVP-AEW541 and b) Picropodophyllotoxin (PPP) treatments in the PANC-1 cell line**……..36**

Figure 3.3: IC_{50} values of a) NVP-AEW541 and b) Picropodophyllotoxin (PPP) treatments in the Mia PaCa-2 cell line**……..……..……37**

Figure 3.4: IC_{50} values of a) NVP-AEW541 and b) Picropodophyllotoxin (PPP) treatments in the CF PAC-1 cell line**…….38**

Figure 3.5: Photomicrographs of HPDE cells showing morphological changes when exposed to different treatment groups a) untreated, b) DMSO, c) BSA, d) IGF-1, e) NVP-AEW541 and f) Picropodophyllotoxin after 72 hours**……40**

Figure 3.6: Photomicrographs showing morphological changes of PANC-1 cells when exposed to different treatment groups a) untreated, b) DMSO, c) BSA, d) IGF-1, e) NVP-AEW541 and f) Picropodophyllotoxin after 72 hours**……...…….41**

Figure 3.7: Photomicrographs showing morphological changes to Mia PaCa-2 cells when exposed to different treatments a) Untreated, b) DMSO, c) BSA, d) IGF-1, e) NVP-AEW541 and f) Picropodophyllotoxin after 72 hours**….……...……..…..42**

Figure 3.8: Photomicrographs of changes in morphology to CF PAC-1 cells when exposed to different treatments a) Untreated, b) DMSO, c) BSA, d) IGF-1, e) NVP-AEW541 and f) Picropodophyllotoxin after 72 hours**……43**

Figure 3.9: WST-1 proliferation in PDAC cell line following 72-hour treatment with IGF-1R modulators**……..…….…….45**

Figure 3.10: A comparison of proliferation in the untreated control, DMSO and BSA diluent controls, IGF-1, NVP-AEW541 and Picropodophyllotoxin treatment groups across all PDAC cell lines after 72 hours of treatment**……..……..46**

Figure 3.11: Survival and recovery of PDAC cell lines following 72 hours treatment with the DMSO and BSA diluent controls, IGF-1, NVP-AEW541 and Picropodophyllotoxin (PPP)**…….47**

Figure 3.12: Quantification of colony formation following treatment with the DMSO and BSA diluent controls, IGF-1, NVP-AEW541 and Picropodophyllotoxin for 72 hours**……..……..50**

Figure 3.13: Comparison of number of colonies formed in HPDE, PANC-1, Mia PaCa-2 and CF PAC-1 cell lines**……...……..51**

Figure 3.14: Photomicrographs of HPDE cells showing migration of the cells in the presence of effect of DMSO, BSA, IGF-1, NVP-AEW541 and Picropodophyllotoxin**…..…….55**

Figure 3.15: Photomicrographs of PANC-1 cells showing migration of the cells in the presence of DMSO, BSA, IGF-1, NVP-AEW541 and Picropodophyllotoxin**……..…….…….56**

Figure 3.16: Photomicrographs of Mia PaCa-2 cells showing migration of the cells in the presence of DMSO, BSA, IGF-1, NVP-AEW541 and Picropodophyllotoxin**…...……57**

Figure 3.17: Photomicrographs of CF PAC-1 cells showing migration of the cells in the presence of DMSO, BSA, IGF-1, NVP-AEW541 and Picropodophyllotoxin**……...……58**

Figure 3.18: Normalized percentage area difference for a) HPDE, b) PANC-1, Mia PaCa-2 and CF PAC-1 cells**……..59**

Figure 3.19: Relative gene expression of genes involved in proliferation, survival, migration, and apoptosis in the HPDE cell line**……...……..……67**

Figure 3.20: Relative gene expression of genes involved in proliferation, survival, migration, and apoptosis in PANC-1 cells**….……..……..67**

Figure 3.21: Relative gene expression of genes involved in proliferation, survival, migration, and apoptosis in Mia PaCa-2 cells**……...……68**

Figure 3.22: Relative gene expression of genes involved in proliferation, survival, migration, and apoptosis in the CF PAC-1 cells**……69**

Figure 3.23: Hierarchical clustering of relative gene expression in a) HPDE, b) PANC-1, c) Mia PaCa-2 and d) CF PAC-1 cells**……...……..70**

Figure 3.24: Protein expression in Mia PaCa-2 cells**.……...……71**

LIST OF TABLES

CHAPTER 1: INTRODUCTION

Table 1.1. Pancreatic tumours and associated histological features. Adapted from Maitra and Hruban, 2008**……..……2**

Table 1.2 The TNM classification of pancreatic cancer**…….5**

CHAPTER 2: METHODOLOGY

Table 2.1 Seeding densities of each PDAC cell line in 96-well plates**……..…21**

Table 2.2 Primer sequences and descriptions of the transcriptionally regulated genes chosen in this study**……...27**

Table 2.3 Thermal cycler conditions for cDNA synthesis**……29**

Table 2.4 Conditions used for qRT-PCR using the PikoReal® Real-Time instrument**……..…..29**

Table 2.5 Primary antibodies used to target proteins involved in the IGF-1R pathway**……33**

CHAPTER 3: RESULTS

Table 3.1 Comparison of different IC_{50} values as determined by experimentation vs manufacturer's guidelines and literature**……..…….33**

Table 3.2 Working concentrations of modulators used in experiments**……...39**

Table 3.3 The relative expression of BAX/BCL2**…….……..66**

ABBREVIATIONS, ACRONYMS AND SYMBOLS

μg	micro grams
μl	micro litres
μM	micro molar
μm	micrometres
CO_2	carbon dioxide
μM	micromolar
3D	three dimensional
4PL	four-parameter logistic
AJCC	American Joint Committee on Cancer
ANOVA	analysis of variance analysis
ATP	Adenosine triphosphate
BAD	BCL2 associated agonist of cell death
BAX	BCL2- associated X protein
BCA	bicinchoninic acid
BCL2	B-cell lymphoma
BCL-Xl	B-cell lymphoma-extra large
BRPC	borderline resectable pancreatic cancer
BSA	Bovine Serum Albumin
CAMs	cell adhesion molecules
cDNA	complementary deoxyribose nucleic acid
CT	computerized tomography
dH_2O	distilled water
DMEM	Dulbecco's modified eagle medium

DMSO	dimethyl sulfoxide
DNA	deoxyribose nucleic acid
ECS	electro coupling solution
EDTA	ethylenediametetraacetic acid
EGF	epidermal growth factor
EGFR	epidermal growth factor receptor
ELISA	enzyme-linked immunosorbent assay
EMT	epithelial-to-mesenchymal transition
ERK	extracellular-signal-regulated kinase
FBS	foetal bovine serum
FGF	fibroblast growth factor
FOXO	forkhead transcription factors
GSK3	glycogen synthase kinase 3
HER2	human epidermal receptor
HIF-1	hypoxia-inducible factor 1
HPDE	Human Pancreatic Ductal Epithelial Cell
HRP	horseradish peroxidase
IC_{50}	half inhibitory concentration
IDT	Integrated DNA Technologies
IGF	insulin-like growth factor
IGF-1	insulin-like growth factor 1
IGF-1R	IGF-1 receptor
IGF-2	insulin-like growth factor 2
IGFBPs	IGF binding proteins
IGFR	insulin-like growth factor receptor

IgG	immunoglobulin G
IL-3	interleukin-3
IPMN	Intraductal papillary mucinous neoplasms
IRS-1	insulin receptor substrate-1
KSFM	keratinocyte serum free medium
mA	milli- amperes
MAPK	mitogen activated protein kinase
MCN	Mucinous cystic neoplasms
ml	millilitres
mm	millimetres
mM	millimolar
MMPs	matrix metalloproteinases
MRI	Magnetic resonance imaging
mTOR	mechanistic target of rapamycin
NK	natural killer
nm	nano meters
NSCLC	non-small cell lung cancer
ºC	degrees Celsius
PanIN	Pancreatic intraepithelial neoplasia
PanIN1	Pancreatic intraepithelial neoplasia one
PanIN2	Pancreatic intraepithelial neoplasia two
PanIN3	Pancreatic intraepithelial neoplasia three
PBS	phosphate buffered saline
PCR	polymerase chain reaction
PDAC	Pancreatic Ductal Adenocarcinoma

PDGF	platelet-derived growth factor
PI3K	phosphatidylinositol-3 kinase
PI3KCA	phosphatidylinositol-3 kinase C isoform A
PPP	Picropodophyllotoxin
PS	phosphatidylserine
PVDF	Polyvinylidene difluoride
qRT-PCR	quantitative real-time polymerase chain reaction
RB	retinoblastoma
RIPA	radioimmunoprecipitation
RT	room temperature
RTKs	receptor tyrosine kinases
TGF-α	transforming growth factor-alpha
TGF-β	transforming growth factor-beta
TKIs	Tyrosine kinase inhibitors
TMB	3.3',5,5'-Tetramethylbenzidine
TME	Tumour microenvironment
TNM	tumour node metastasis
TP53	Tumour protein 53
USA	United States of America
V	volts
VEGF	vascular endothelial growth factor
w/v	weight/volume
WHO	World Health organization
WST-1	water-soluble tetrazolium salts-1
x g	centrifugal force

Zeb1	zinc finger E-box binding homeobox
α	alpha
β	beta
β-ME	β-mercapoethanol

CHAPTER 1: INTRODUCTION

1.1. Pancreatic Ductal Adenocarcinoma: Overview

Pancreatic ductal adenocarcinoma (PDAC) is becoming one of the world's most lethal forms of cancer. Regardless of treatment it has an overall 5-year survival rate of less than 5 % and a median survival of 6 months (Ghaneh *et al.*, 2008; Kamisawa *et al.,* 2016; Adamska *et al.*, 2017). PDAC accounts for more than 80 % of all pancreatic cancers, with mortalities caused by the disease being almost equal to the incidence each year (Kamisawa *et al.*, 2016; Torres & Grippo, 2018). Globally, PDAC accounts for approximately 7 % of cancer-related mortalities and in the United States of America (USA) it ranks as the fourth leading cause of cancer-related deaths (WHO, 2014). The true incidence of the disease is not known in South Africa as it is under-reported, however it ranks 11th in terms of mortality. While between 1993 and 2013, mortalities caused by the disease within the South African population appears to have increased by approximately 75.7 %, with the female black population being more severely affected having increased by 86.1 % (WHO, 2014). As of 2020, there was a 97.44 % mortality of new PDAC cases in Southern Africa (Globocan, 2020). While this increase in cases and mortalities are staggering, the apparent increase in numbers is largely influenced by improved reporting systems in Southern Africa. The poor prognosis associated with PDAC is attributed to its mostly asymptomatic nature and lack of specific biomarkers in the early stages of the disease, thus most cases are diagnosed at an advanced stage where metastasis has already occurred (Mihaljevic *et al.*, 2009; Michl & Gress, 2013).

A family history of chronic pancreatitis and pancreatic cancer are important risk factors for the disease where approximately 10 % of affected patients have a family history of prior pancreatic complications (Ilic & Ilic, 2016; Tang *et al.*, 2017). Other risk factors include cigarette smoking, obesity, diabetes mellitus and high-fat diets. The disease was also found to be more common with increasing age, in the male sex and more prominent in the African ethnic groups (Ilic & Ilic, 2016; Law *et al.*, 2020).

1.1.1. Biology

Pancreatic cancer, despite its relatively low incidence is fast becoming one of the most lethal and devastating malignancies. It represents the archetype of all metastatic and aggressive malignancies. These tumours show therapeutic resistance to a variety of targeted biological agents, cytotoxic chemotherapies and radiotherapy (Rajabpour *et al.*, 2017; Biancur & Kimmelman, 2018). The lack of effective therapy options and late diagnosis makes the

disease one of the most lethal malignancies, worldwide (Maitra & Hruban, 2008; Michl & Gress, 2013).

Pancreatic tumours are often divided into two subtypes, exocrine and endocrine tumours. The exocrine tumours originate in the enzyme-producing acinar pancreatic cells; while the endocrine tumours arise from the hormone-secreting cells of the pancreas (**Figure 1.1**) (Hruban *et al.*, 2000; Moore *et al.*, 2001; Nandy & Mukhopadhyay, 2011). A further classification of pancreatic cancers are shown in **Table 1.1.**

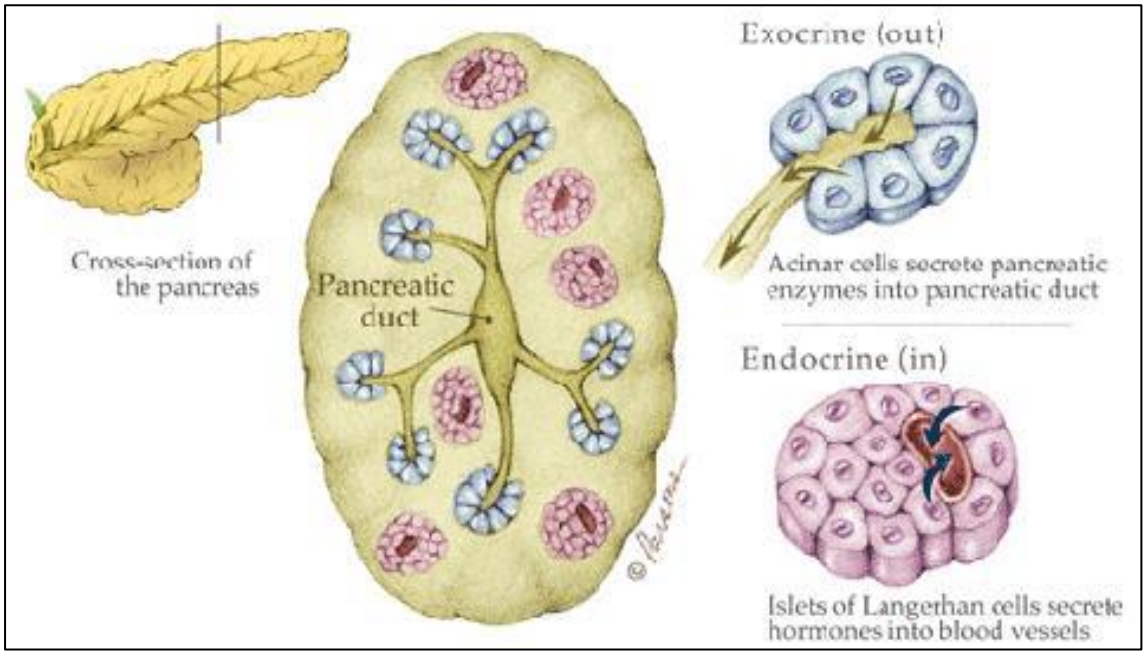

Figure 1.1: A cross-section of the pancreas. The pancreas is composed of exocrine and endocrine glands that contain cells which secrete enzymes into the pancreatic duct and hormones into blood vessels, respectively. Schematic shows the location of these cells in relation to the pancreatic duct (Hruban *et al.*, 2000).

Table 1.1. Pancreatic tumours and associated histological features

Pancreatic Neoplasm	**Histological Features**
Ductal adenocarcinoma	Ductal morphology, desmoplasia
a) Medullary carcinoma	Poorly differentiated, intratumoural lymphocytes
b) Colloid (mucinous noncystic) carcinoma	Mucin pools
Acinar cell carcinoma	Presence of zymogen granules
Pancreatoblastoma	Multilineage differentiation, squamous nests
Solid pseudopapillary neoplasm	Pseudo papillar, solid and cystic areas, hyaline globules
Serous cystadenoma	Multicellular cysts, glycogen-rich epithelium
Pancreatic endocrine tumours	Hormone production

Table adapted from Maitra & Hruban, 2008.

Before metastasis to organs such as the lungs and liver, PDAC commonly originates in the head of the pancreas and then infiltrates into the surrounding tissues such as the spleen, lymphatics and peritoneal cavity (Hezel *et al.,* 2006; Yachida & Iacobuzio-Donahue, 2008).

The most predominant subtype of PDAC demonstrates a glandular pattern with duct-like structures and a variation in cellular atypia (Hezel *et al.,* 2006). The less common subtypes of PDAC include tumours with a colloid, adenosquamous and sarcomatoid histological structure. PDAC evolves through three recognized precursor lesions such as pancreatic intraepithelial neoplasias (PanIN), intraductal papillary mucinous neoplasms (IPMN) or mucinous cystic neoplasms (MCN) (Singh & Maitra, 2007; Vincent *et al.,* 2011).

Of these precursor lesions, PanIN are the most common neoplastic precursor to invasive PDAC. These lesions follow a stepwise progression to PDAC which is graded through three stages: PanIN1, PanIN2 and PanIN3. PanIN1 are considered low-grade, correlated with increasing age and present with the columnar, mucinous epithelial differentiation of ductal cells. PanIN2 and PanIN3 are more advanced lesion grades and present with increased architectural disorganization and nuclear atypia that are usually detected adjacent to established carcinomas (Hezel *et al.,* 2006; Singh & Maitra, 2007; Vincent *et al.,* 2011) (**Figure 1.2.**). PanIN2 and PanIN3 lesions ultimately transform into PDAC with evidence of invasion beyond the basement membrane (Hezel *et al.,* 2006).

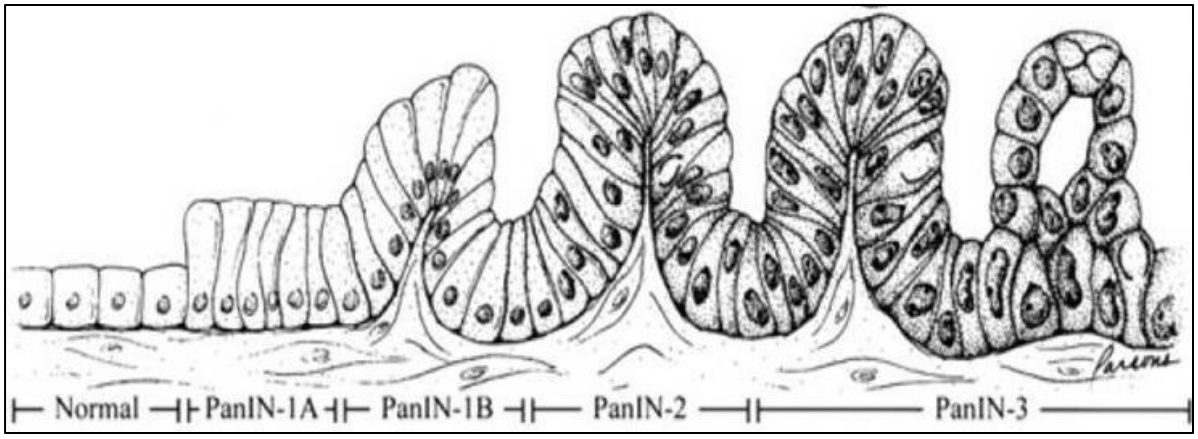

Figure 1.2: The development of normal pancreatic cells to a tumour. Image shows the progression of PDAC from precursor lesions. Adapted from Hezel *et al.,* 2006.

1.1.2. Symptoms

The presenting symptoms of PDAC is dependent on the stage of the disease and the location of the tumour within the gland. Early stages of the disease is usually "clinically silent", thus the disease only becomes apparent after local invasion or metastasis to distant organs (Vincent *et al.,* 2011). The most common symptoms of PDAC include abdominal or mid-back pain, jaundice, diarrhoea, nausea, and weight loss. The weight loss often arises from maldigestion from pancreatic ductal obstruction, cachexia, and anorexia. Chronic pancreatitis is also sometimes associated with pancreatic-duct obstruction. Deep and superficial venous thromboembolisms are associated with malignancy of the disease (Vincent *et al.,* 2011).

Tumours that are located at the head and the body of the pancreas present with jaundice, abdominal or back pain. Other less common symptoms include diabetes mellitus which occurs in approximately 25 % of affected individuals and an impaired glucose tolerance or state of hyperglycaemia that has been reported in 40 % of PDAC cases (Chari *et al.,* 2008; Pannala *et al.,* 2008).

1.1.3. Detection and staging

The best initial diagnostic test for PDAC follows the tri-phasic pancreatic-protocol computerized tomography (CT), this procedure can reliably detect locally advanced and metastatic tumours. These scans are also used for disease staging and provides a 3-dimensional reconstruction of tumours which provides about 80 % accuracy for the prediction of resectability (Vincent *et al.,* 2011; Cooperman *et al.,* 2018; Torres & Grippo, 2018). Another commonly used procedure for the detection of PDAC is the use of endoscopic ultrasounds, and magnetic resonance imaging (MRI) is used for staging in patients who cannot tolerate the intravenous contrast for CT (Vincent *et al.,* 2011; Cooperman *et al.,* 2018).

The disease is classified and staged using the American Joint Committee on Cancer (AJCC) tumour node metastasis (TNM) system, whereby the size of the primary tumour, regional lymph nodes and distant metastasis are assessed (Edge & Compton, 2010). The tumours are divided into stages, each with its own treatment and prognosis; Stage 1a and 1b: localised, resectable; Stage 2a and 2b: locally advanced, borderline resectable, Stage 3: regional lymph node metastasis, unresectable and Stage 4: distant metastasis (**Table 1.2**).

Table 1.2 The TNM classification of pancreatic cancer

AJCC Pancreas Cancer TNM classification

T (Tumour size)	N (lymph Node status)	M (Metastasis)
Tx-Unable to assess primary tumour	Nx-Unable to assess regional lymph nodes	M0- No distant metastasis
T0-No evidence for primary tumour	N0-No regional lymph node metastasis	M1-Distant metastasis
Tis- Carcinoma in situ	N1-Regional lymph node metastasis	
T1-Tumour limited to pancreas and <2cm in size		
T2-Tumour limited to pancreas and >2cm in size		
T3-Tumour extends beyond the pancreas		
T4-Tumour extends beyond the pancreas with the involvement of celiac axis and or superior mesenteric artery (unresectable)		

AJCC Pancreas Cancer staging

Stage	T status	N status	M status
0	Tis	N0	M0
IA	T1	N0	M0
IB	T2	N0	M0
IIA	T3	N0	M0
IIB	T1	N1	M0
	T2	N1	M0
	T3	N1	M0
III	T4	Any N	M0
IV	Any T	Any N	M0

Adapted from Edge & Compton, 2010.

1.1.4. Treatment of PDAC

Due to the high degree of tumour and tumour microenvironment (TME) heterogeneity, signalling cascade plasticity and genetic diversity, drug delivery and effective targeting proves a major challenge for the treatment of PDAC (Sciver *et al.*, 2018). Treatment of PDAC includes surgery, chemotherapy, radiotherapy, and palliative treatment. These treatment options are dependent on the stage of the disease and is selected accordingly (Kamisawa *et al.*, 2016).

1.1.4.1.Surgery

The choice of surgical technique is based on the following factors: tumour size and location, patient's wellbeing, and metastasis of the tumour (Torres & Grippo, 2018; Attard *et al.*, 2019). Pancreaticoduodenectomy, also called a Whipple procedure, is the most common surgical procedure performed for the removal of tumours found in the head of pancreas. A distal pancreatomy is performed when the tumour is located at the body and/or tail of the

pancreas; and a total pancreatectomy is performed when the tumour affects the entirety of the pancreas (Mihaljevic *et al.,* 2009; Torres & Grippo, 2018).

Patients with resectable tumours who undergo a surgical resection have been shown to have an overall survival up to 7 years (Mihaljevic *et al.,* 2009; Torres & Grippo, 2018). However, local recurrence (>20 %) and distant metastasis (>70 %) after surgery is common, consequently there is a need for adjuvant therapy which currently consists of chemotherapy with or without radiation (Song *et al.,* 2016).

1.1.4.2. Adjuvant therapy after resection

Adjuvant therapy is recommended for patients who have recovered from pancreatic resection, usually 1-2 months after surgery. Common adjuvant therapies administered include fluorouracil-based chemoradiation and gemcitabine. Clinical trials have concluded that the administration of these therapies following surgery has increased survival time when compared to surgery alone; with a median overall survival of 22.8 versus 20.2 months (Grützmann *et al.,* 2004; Singh & Maitra, 2007). Other adjuvant therapies administered after surgery include erlotinib, cisplatin, docetaxel and capecitabine (Vincent *et al.,* 2011). There is a significantly better survival rate for patients who present with locally advanced PDAC, with a median survival rate of 9-15 months compared to 3-6 months in patients with metastatic disease (Vincent *et al.,* 2011).

1.1.4.3. Treatment of metastatic disease

Since treatment of PDAC is dependent on the stage of the cancer, approximately 80 % of PDAC patients can only be offered chemotherapy due to the late clinical diagnosis and the advanced stage of the disease (Song *et al.,* 2016; Torres & Grippo, 2018).

Gemcitabine and cisplatin are the most common first line chemotherapies used in PDAC treatment. Other widely used chemotherapeutic agents include 5- Fluorouracil and Folfirinox (Adamska *et al.,* 2017). These chemotherapies induce a partial response in some cases and can alleviate symptoms in patients with advanced tumours (Rothenburg *et al.,* 1996; Burris *et al.,* 1997; Storniolo *et al.,* 1999; Vincent *et al.,* 2011). However chemo-resistance is common to Gemcitabine treatment alone or in combination with other chemotherapeutics (Michl & Gress, 2013; Song *et al.,* 2016; Adamska *et al.,* 2017). Hence the discovery of novel anti-PDAC therapies and reliable molecular tools for treatment selection in PDAC are needed.

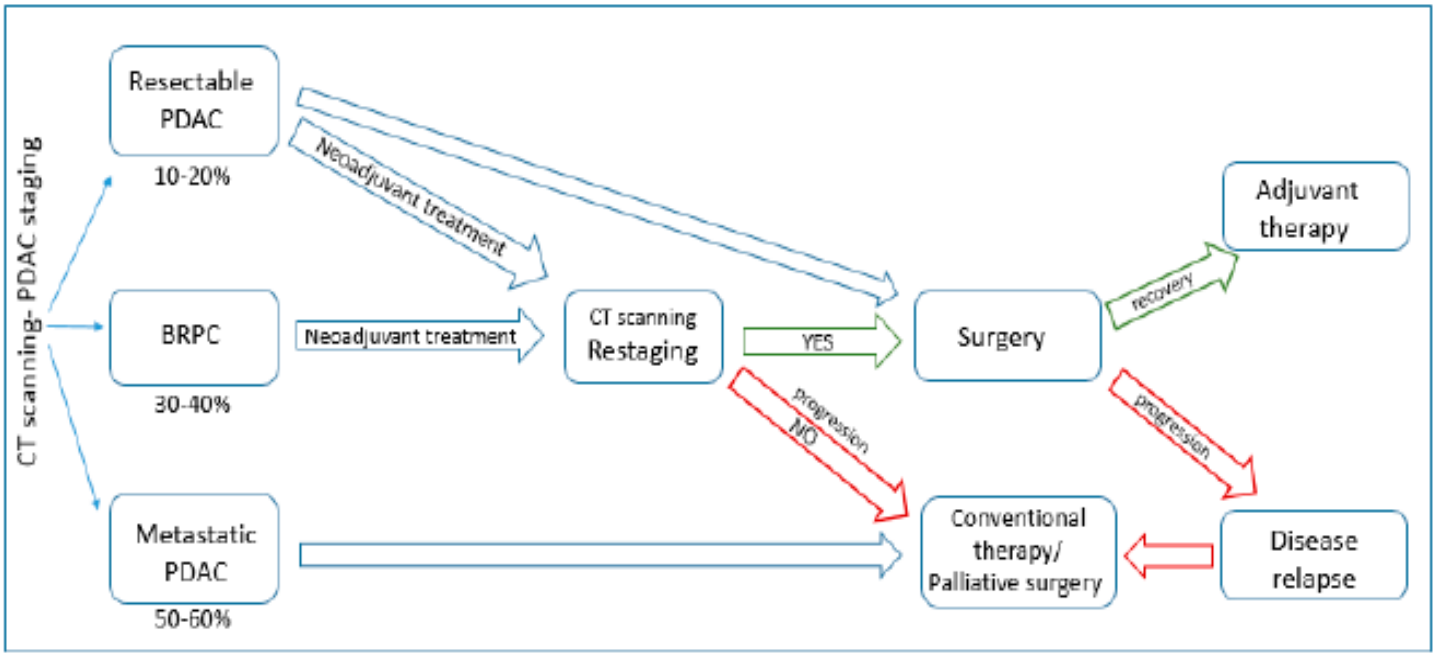

Figure 1.3. Therapeutic options of the different stages of PDAC. Flow chart summarizing the different treatment strategies for PDAC cases (Adamska *et al.*, 2017)**.** CT: computerized topography, BRPC: Borderline resectable pancreatic cancer.

1.2. Hallmarks of Cancer

For a tumour to survive, certain 'hallmarks' need to be achieved. These hallmarks of cancer were first published in the year 2000 by Hanahan and Weinberg, however due to the advancements made in malignant diseases, these hallmarks have since been amended. The cancer hallmarks provide an organizational framework of the cellular properties that are undergone during the phenotypic transformation of cancerous cells. This further provides a scaffold for which conventional therapy is targeted to prevent these cellular and phenotypic alterations from occurring.

1.2.1. Sustaining Proliferative Signalling

The proliferation of normal cells rely on the presence of mitogenic growth signals for their progression from a quiescent to an active proliferative state (Hanahan *et al.*, 2000). These growth signals provide the stimulus for the progression of cells through the cell cycle to undergo mitosis. This is a highly regulated signal transduction process which involves the signal binding to extracellular cell surface receptor and the proliferative signal being translated intracellularly. Tumorigenic cells possess the ability to stimulate autocrine proliferative signalling by producing its own growth stimuli to allow for the cancerous cells

to progress without restriction (Hanahan *et al.*, 2000; Hanahan & Weinberg 2011). Cancerous cells also rely on cell-cell contact mechanisms for paracrine signalling with neighbouring malignant cells, this further enhances the progression and survival of malignancies. Other mechanisms involve the manipulation of the tumour microenvironment and disruption of negative-feedback mechanisms that attenuate proliferative signalling (Hanahan *et al.,* 2000; Hanahan & Weinberg 2011).

In PDAC, there is an over-expression of several growth factor receptor pathways such as the epidermal growth factor (EGF) receptor and transforming growth factor-alpha (TGF-α). The overexpression of EGF has been reported in over 80 % of all PDAC cases and is associated with an aggressive phenotype and poor prognosis (Welsch *et al.,* 2007; Baxevanos & Fountzilas, 2017). The progression of PDAC is also promoted by other growth factors belonging to the insulin-like growth factor (IGF) receptor system, which are overexpressed in over 60 % of all PDAC cases, and the fibroblast growth factor (FGF) receptor families (Welsch *et al.,* 2007).

1.2.2. Evading growth suppressors

In normal tissues, multiple anti-proliferative signals exist to maintain homeostasis. These anti-proliferative signals may inhibit proliferation by forcing cells out of the proliferative cycle into the quiescent state (Alberts *et al.,* 2015). Alternatively, cells are forced into a post-mitotic state that disables its proliferative potential (i.e. in cells which are fully differentiated) (Hanahan *et al.,* 2000). This is usually achieved through the transforming growth factor-beta (TGF-β) cascade, which is a negative regulator of cellular proliferation (Welsch *et al.,* 2007). Cancer cells evade these mechanisms through the presence of oncogenes which allow for the disruption of regulatory processes in the cell cycle that inhibit the uncontrolled proliferation of cells. Although TGF-β isoforms are overexpressed in PDAC, a mutation to the *Smad4* gene make the cancer cells insensitive to this anti-growth signal transmission (Welsch *et al.,* 2007).

1.2.3. Enabling infinite replicative potential

A limit exists to the number of times non-cancerous cells can divide before senescence; this is known as the *Hayflick limit*. In mammalian cells the Hayflick limit is at about 60-70 replicative cycles (Shay & Wright, 2000). Cancerous cells avoid senescence and achieve immortalization by disrupting retinoblastoma (RB)-associated and tumour protein 53 (TP53) tumour suppressor. While senescence in normal cells is associated with the progressive shortening of telomeres on the chromosomes of cells, the telomeres in tumour cells remain

intact. Telomerase is an enzyme that is associated with maintenance of telomeres, and increased telomerase expression in pancreatic juices has been associated with PDAC (Welsch *et al.,* 2007).

1.2.4. Genome instability and mutation

Due to cancer being a micro-evolutionary process, the presence of mutations in the cancer genome introduces heterogeneity or 'variation' to the tumour cell population (Collisson & Maitra, 2017). The evolutionary process of *Natural Selection* favours populations with variation or heterogeneity and thus allows for that population's survival. Cancerous cells arise through the accumulation of mutations that in a normal cell's genome, this allows for genome instability and introducing heterogeneity within the cell microenvironment (Raphael et al. 2017). According to the process of natural selection, this variability in the gene pool is favoured thereby promoting tumour survival and progression. In PDAC, several gene mutations have been reported, with over 60 % of PDAC cases reporting mutations in *k-ras, Smad4* and *TP53* genes (Raphael *et al.,* 2017).

1.2.5. Angiogenesis

Angiogenesis refers to the development of new blood vessels. In normal tissues, blood vessels are a source of nutrient transport and delivery to ensure cell survival. For tumour cells to grow, a tumour must recruit a network of new blood vessels. This is regulated by the balance of pro- and anti-angiogenic molecules. In cancer, the establishment of new blood vessels is not only essential for tumour growth, but it has also been implicated in the initial progression from a pre-malignant lesion to a fully invasive cancer (Alberts *et al.,* 2015; Feitelson *et al.,* 2015).

A positive correlation has been observed between blood vessel density and the progression of PDAC. Moreover, the hypoxic conditions in the PDAC microenvironment further enhance vascular endothelial growth factor (VEGF)-mediated angiogenesis (Welsch *et al.,* 2007).

1.2.6. Inflammation and immune evasion

Most solid malignancies trigger an intrinsic inflammatory response which aids in the pro-tumorigenic microenvironment. The infiltration of immune cells such as lymphocytes, macrophages and neutrophils are associated with an inflammatory response. While the influx of immune cells is expected to initiate the process of immune surveillance and the elimination of malignant cells, the high influx of immune cells secrete several growth stimuli such as chemokines, cytokines and growth factors which further promotes tumour survival (Hanahan & Weinberg, 2011; Artacho-cordón *et al.,* 2012).

Other immune cells such as natural killer (NK) cells and dendritic cells may also be found in the stroma of tumours, however they are unable to exert their tumour-killing functions due to the release of signalling molecules by the tumour. One such molecule is TGF-β which may contribute to the immune cell's altered phenotype (Artacho-cordón *et al.,* 2012; Balkwill & Hagemann, 2012). This may be a key factor in cancer metastasis and disease progression.

The insulin-like growth factor (IGF) axis, which consists of insulin-like growth factors 1 and 2 (IGF-1, IGF-2), IGF binding proteins (IGFBPs) and IGFBP-related proteins are known to be associated in the inflammatory process. In PDAC, elevated levels of inflammatory proteins such as interleukins are strongly associated with IGF-1 levels. The pro-inflammatory cytokines increase the hepatic production of IGFBP-1 to cause an increase in IGF-1. This, in turn, stimulates the production of cytokines by monocytes and macrophages in the tumour microenvironment (Wlodarczyk *et al.,* 2018).

1.2.7. Metabolic rewiring

Cancer cells can reprogram their glucose production activity from aerobic to anaerobic conditions, thereby favouring glycolysis over subsequent energy pathways. Thus, less pyruvate being dispatched to the oxygen-consuming mitochondria. The hypoxic environment of tumours causes the stabilization of the hypoxia-inducible factor-1 (HIF-1) transcription factor, this leads to the cancerous cells overcoming nutrient and oxygen deprivation. This metabolic switch to glycolytic energy production has been implicated in the activation of autophagy (Eskelinen, 2011; Frentzel *et al.,* 2017).

Autophagy is a catabolic process which can act between cell survival and cell death mechanism, depending on the needs of the cell (Gozuacik & Kimchi, 2004; Sharma *et al.,* 2014). High levels of autophagic cell survival have been observed in PDAC. The increased autophagic flux is thought to be associated with the high expression of HIF-1 and the metabolic rewiring that occurs due to HIF-1 expression (Yang *et al.,* 2011; Valle *et al.,* 2018).

1.2.8. Invasion and metastasis

Metastasis refers to the ability of malignant cells to secede from the primary tissue site and invade adjacent tissues to establish new colonies. For this to occur, cancer cells need to acquire migratory and invasive properties which involves loss of many of its epithelial characteristics to mesenchymal traits. This is known as epithelial-to-mesenchymal transition (EMT) (Houg & Bijlsma 2018; Valle *et al.,* 2018). This process involves transcription factors such as Snail, Slug, zinc finger E-box binding homeobox 1 (Zeb1) and Twist. Alterations in

several proteins belonging to the cell-cell adhesion molecules (CAMs), extracellular proteases and cadherin and integrin families have been implicated in the EMT induction of cells (Houg & Bijlsma 2018; Valle *et al.*, 2018). To allow for invasion into the nearby stroma degradation of matrix components by matrix metalloproteinases (MMPs) are necessary (Welsch *et al.*, 2007).These molecular alterations are further aided by chemokines and signalling molecules secreted in the tumour microenvironment, inflammation, angiogenesis and platelet activity (Meikle *et al.*, 2017; Houg & Bijlsma 2018; Valle *et al.*, 2018).

The switch from E-cadherin to N-cadherin is an essential feature that has been observed in the epithelial tumour progression. Furthermore, IGF-1 receptor (IGF-1R) signalling has been implicated in EMT-mediated tumour metastasis and drug resistance (Li *et al.*, 2017). In PDAC, a reduced expression of E-cadherin has been correlated with its dedifferentiation to a mesenchymal-like phenotype (Welsch *et al.*, 2007).

1.2.9. Evasion of apoptosis

Apoptosis is a form of programmed cell death that is highly regulated with several triggers and pathways. This mechanism of cell death is essential in maintaining homeostasis. For conservation of homeostasis, the apoptotic programme is antagonized by survival factors including IGF-1, IGF-2 and interleukin-3 (IL-3) (Hanahan *et al.*, 2000; Welsch *et al.*, 2007; Hanahan & Weinberg 2011).

Resistance to apoptosis in PDAC is a result of various disturbances to apoptotic machinery. Studies have found that PDAC cells are resistant to pro-apoptotic signals, as well as the upregulation of anti-apoptotic proteins belonging to the Bcl-2 family (Welsch *et al.*, 2007).

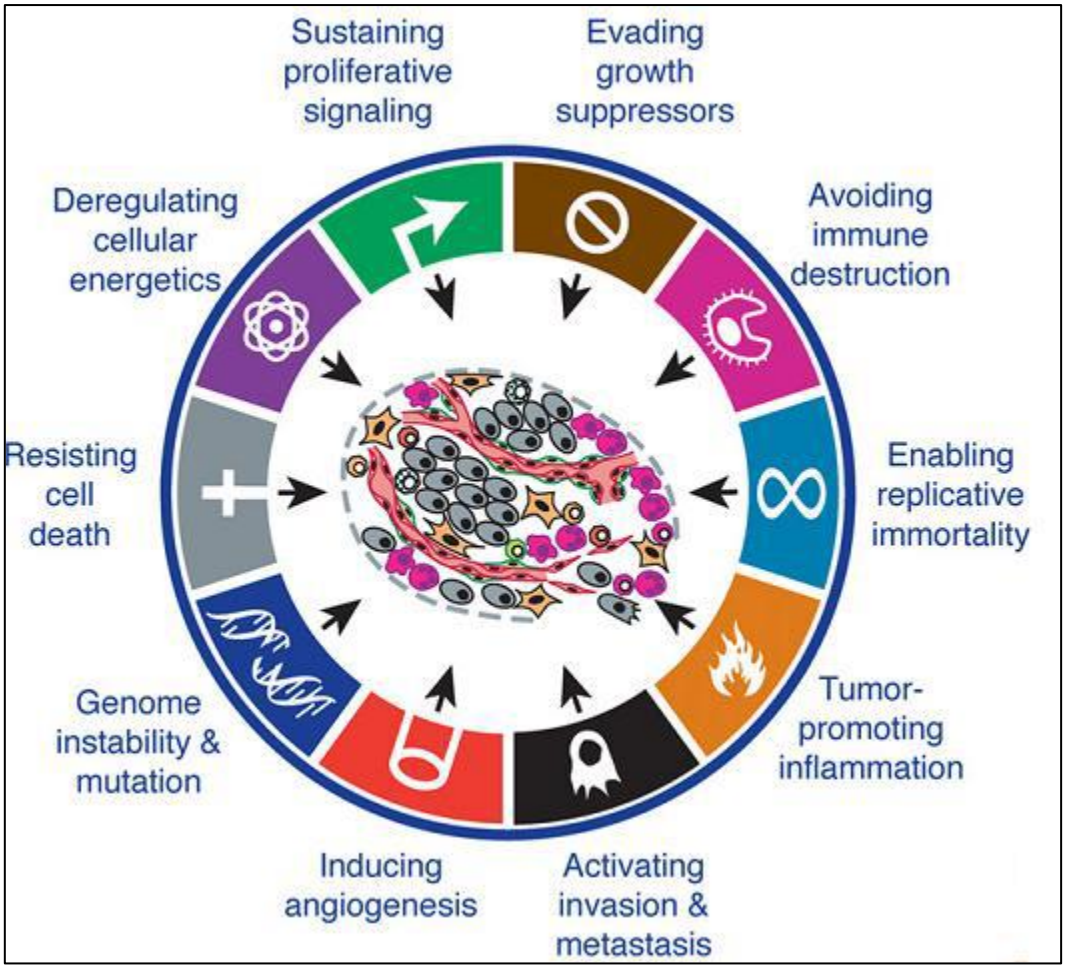

Figure 1.4: The Hallmarks of Cancer as described by Hanahan *et al.*, 2011. A summary of the cancer hallmarks and enabling characteristics that allow for tumour progression.

1.3. Signal Transduction

A constant communication exists between cells and their environment to maintain homeostasis in important biological processes such as cell proliferation, differentiation, cell motility, survival, and apoptosis. Cells are highly sensitive to changes in the internal and external microenvironment, thus the communication network is highly regulated (Bianco *et al.*, 2006; Alberts *et al.*, 2015). Signals are typically acquired through direct communication between cells by cell adhesion molecules (CAMs) and an indirect communication network through signals that are transmitted by ligand-activated cell-surface receptor tyrosine kinases (RTKs) and non-receptor tyrosine kinases. These signalling molecules include growth factors, hormones, neurotransmitters, chemokines, and cytokines which activate secondary messengers in the cell's cytoplasm. This enables the cells to amplify and integrate the signal to solicit a cellular response (Alberts *et al.*, 2015; Feitelson *et al.*, 2015). Overall, this process

is referred to as signal transduction. Signal transduction relies on the complex network and association of molecules to form signalling pathways.

1.3.1. Signalling pathways in PDAC

Due to the poor prognosis of PDAC and lack of effective treatment regimes, research focus has shifted to the characterisation of molecular alterations that contribute to the disease progression. Similar to other cancers, dysregulation exists in the growth factors and growth factor receptors which play a pivotal role in the pathogenesis and aggressiveness of PDAC (Oliveira-Cunha *et al.*, 2011).

1.3.1.1. Epidermal Growth Factor Receptor (EGFR) pathway

The epidermal growth factor receptor (EGFR) is a receptor tyrosine kinase of the human epidermal receptor (HER2/ERB-B) family that is activated following the binding of peptide growth factors such as EGF and TGF-α (Nandy & Mukhopadhyay, 2011; Oliveira-Cunha, Newman & Siriwardena, 2011). The binding of ligands to EGFR results in homo- or heterodimerization of the receptor, this results in a phosphorylation cascade to recruit signalling molecules. The EGFR family forms part of a complex signal transduction network, where the binding of peptide growth factors allows for the activation of downstream signalling cascades to promote cellular proliferation, angiogenesis and cell migration (Yarden, 2001; Oliveira-Cunha *et al.*, 2011). EGFR signalling indirectly activates the phosphatidylinositol-3 kinase (PI3K) pathway through its interaction with the downstream Ras/mitogen activated protein kinase (MAPK) signalling cascade (Bianco *et al.*, 2006; Oliveira-Cunha *et al.*, 2011; Nandy & Mukhopadhyay, 2011).

In several epithelial tumours, including pancreatic, breast and non-small cell lung cancer (NSCLC), the EGFR pathway is aberrantly activated (Oliveira-Cunha *et al.*, 2011). In PDAC, over 80 % of all cases are associated with EGFR is overexpression or have acquired gain-of-function mutations which allow for the manipulation and over-stimulation of downstream signalling. The overexpression of EGFR and its ligands suggests an opportunity to impede pancreatic tumour growth through the disruption of the autocrine loop of mitogenic signalling contributing to the pathogenesis of pancreatic neoplasia (Baxevanos & Fountzilas, 2017). EGFR over-expression is often associated with PDAC aggressiveness.

Several therapeutic agents such as specific antibodies, flavonoid antioxidants and low molecular weight EGFR-specific tyrosine kinase inhibitors have been designed to disrupt the EGFR signalling pathway (Oliveira-Cunha *et al.*, 2011; Yewale *et al.*, 2013). Tyrosine kinase inhibitors (TKIs) are the most common therapy used to treat cancers harbouring the EGFR

mutation or aberrant activation of EGFR. In cancers such as NSCLC, inhibition of this pathway has proven to be beneficial in increasing overall patient survival, however, inhibition of EGFR in pancreatic cancer has not been as successful (Marchetti *et al.,* 2005; Arnold *et al.,* 2006; Moore *et al.,* 2007; Hu *et al.,* 2016).

Clinical trials showed that a combination of EGFR targeted therapy and Gemcitabine increased sensitivity of the tumours to therapy, albeit not significantly (Moore *et al.,* 2007). This suggests a major role of the EGFR signalling pathway in the growth and progression of the disease. Moreover, *in vitro* studies have showed the role of EGFR in promoting cellular proliferation, evasion of apoptosis and in the induction of autophagic cell survival mechanisms (Oliveira-Cunha *et al.,* 2011; Nijkamp *et al.,* 2013; Park *et al.,* 2015). However, in clinical trials, inhibition of the EGFR signalling pathway has not been successful in increasing overall patient survival. Thereby suggesting that the tumour microenvironment and other signalling pathways may act as a bypass cell survival pathway *in vivo*.

The aetiology of resistance to TKIs can be attributed to the aberrated activation of bypass signalling pathways, secondary mutations and abnormal downstream pathways that exist in patients with PDAC.

1.3.1.2. Insulin-like Growth Factor Receptor (IGFR) pathway

During carcinogenesis, the presence of more than one growth factor would be expected to potentiate growth, thus multiple mitogenic signalling pathways are upregulated in cancerous cells. Therefore, the combination of multiple targeted therapies would be expected to improve overall patient survival than the use of one therapy alone. In pancreatic cancer, several dysregulated cytokine and protein profiles were found to act independently of the EGFR pathway, several of which directly or indirectly interacts with the insulin-like growth factor (IGF) pathway. Moreover, growth factors, including EGF and platelet-derived growth factor (PDGF), are known to increase levels of circulating insulin-like growth factors. Previous studies using NSCLC and breast cancer cells, have suggested that an abnormality in the insulin-like growth factor receptor (IGFR) pathway may represent a novel mechanism of resistance to anti-EGFR therapy, whereby researchers have found an association between tumour cells treated with EGFR-TKIs, and an increased activation of IGF-1 receptor (IGF-1R) signalling (Yewale *et al.,* 2013; Huang & Fu, 2015).

The IGF-1R is a type 2 tyrosine kinase receptor, found as a heterotetramer and consisting of two-alpha and two beta-subunits. Unlike other growth factor pathways, IGF-1R activity is

highly regulated and dependent on ligand binding where overexpression of the receptor itself is not sufficient to result in receptor activation (Moschos & Mantzoros, 2002; Barbieri *et al.*, 2003; Heidegger *et al.*, 2011). Therefore, clinical data analysing IGF-1R expression alone may be insufficient to draw conclusions on the activity of the signalling cascade found downstream of the receptor.

The intrinsic tyrosine kinase of the cytoplasmic domain of IGF-1R is activated by the conformational change in receptor subunits caused by ligand-binding. The role of the IGF-1R signalling cascade involves the interplay between the downstream Ras/MAPK cascade which promotes cell growth and proliferation (Casa *et al.*, 2008; Nandy & Mukhopadhyay 2011; Trajkovic-Arsic *et al.*, 2013). Additionally, the IGF-1 pathway can provide resistance to apoptotic processes through the activation of the PI3K and Akt cascades. PI3K/Akt signalling can promote cell survival through the phosphorylation and inactivation of the pro-apoptotic protein B-cell lymphoma associated agonist of death (BAD) (Cejas *et al.*, 2003; Casa *et al.*, 2008). In addition, IGF signalling has been shown to promote cell motility through PI3K, MAPK and extracellular-signal-regulated kinase (ERK) signalling (Casa *et al.*, 2008; Trajkovic-Arsic *et al.*, 2013). Thus, overexpression of the IGF-1R signalling pathway in cancers contribute to tumour survival and progression.

Overexpression of IGF-1 and IGF-1R has been reported in pancreatic cancer cell lines and in cancerous human pancreatic tissues (Hakam *et al.*, 2003). While elevated levels of IGF-1 has been implicated in tumour progression in breast, colon and prostate cancers, its role in PDAC is not completely understood (Nandy & Mukhopadhyay, 2011; Skandalis *et al.*, 2014; Wlodarczyk *et al.*, 2018).

Clinical trials using a combination of Gemcitabine and IGF-1R blocking antibodies on PDAC patients have shown an increase in overall patient survival (McCaffery *et al.*, 2013; Abdel-Wahab *et al.*, 2018).

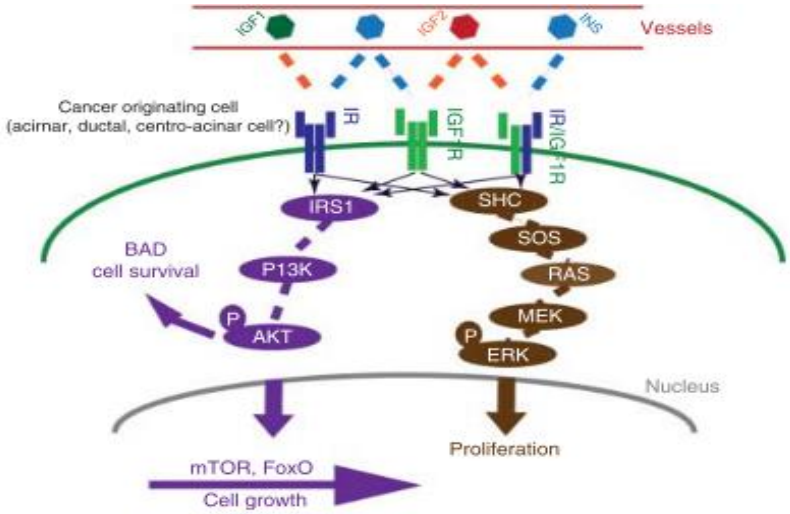

Figure 1.5: The interaction of IGF-1R and its major downstream signalling cascades. (Wlodarczyk *et al.*, 2018)**.**

1.3.1.3.Potential crosstalk between the EGFR and IGF-1R pathways in PDAC

A crosstalk between the EGFR and IGF-1R signalling pathways have been reported in several cancers, where the crosstalk can involve components that are common between both pathways, as well as positive and negative feedback loops. The interaction between the EGFR and IGF-1R pathways occurs in the cross-interaction between several downstream molecules which eventually converge into the Ras/Raf/MAPK and PI3K/Akt cascades.

IGF-1R signalling is considered an important mechanism of resistance to anti-EGFR therapy in several tumours including NSCLC and breast tumours (Renoir *et al.*, 2013; Huang & Fu, 2015). Resistance to EGFR is due to the activation of the PI3K/Akt signalling cascade by IGF-1R signalling in these tumours. The role of IGF-1R signalling as a mechanism of resistance to anti-EGFR therapies has not been thoroughly explored in PDAC. While it is understood that IGF-1R and IGF-1 is overexpressed in some PDAC cases, the role of this signalling cascade in PDAC is not completely understood.

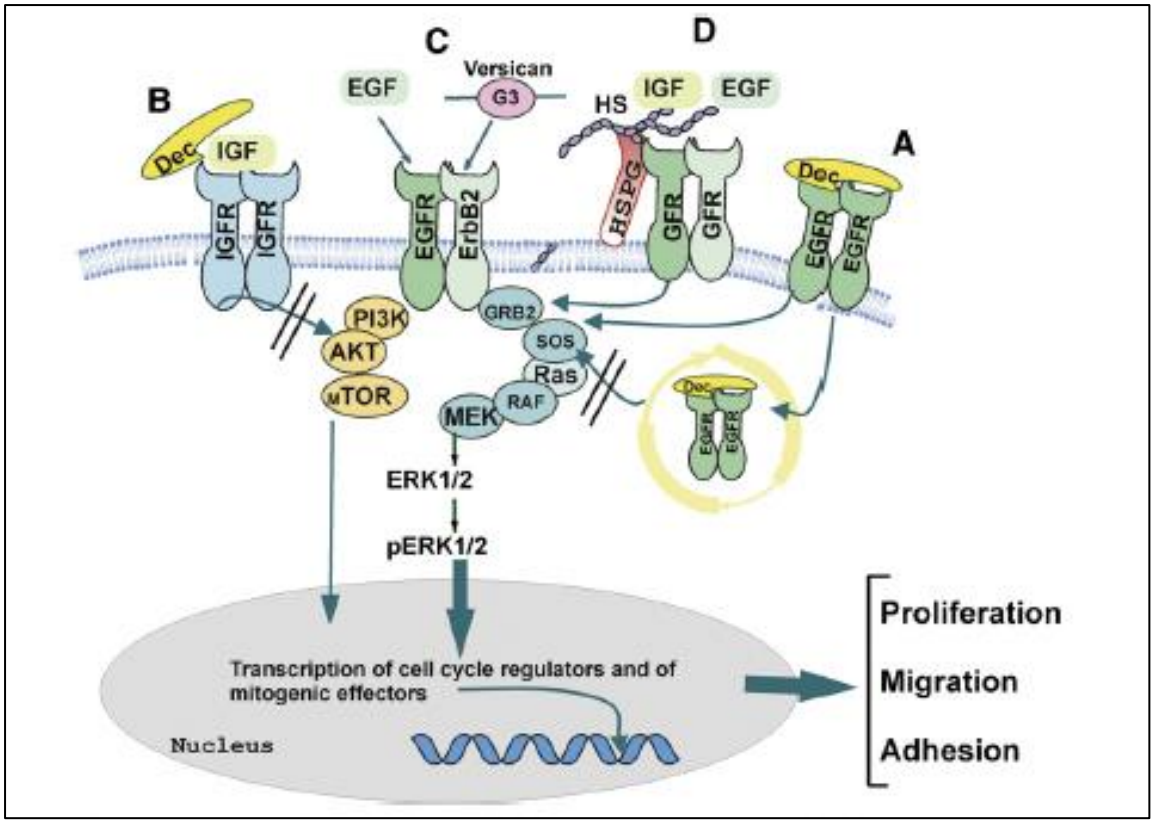

Figure 1.6: The role of EGFR and IGFR in cancer progression. The crosstalk of EGFR and IGFR via downstream signalling cascades occurs primarily through the PI3K/Akt signalling (Skandalis *et al.,* 2014)**.**

1.4. Study Rationale

Some genetic alterations in common mitogenic pathways have been clinically investigated in PDAC patients using chemical inhibitors and antibodies (Maitra & Hruban, 2008; Mihaljevic *et al.*, 2009; Torres & Grippo, 2018). Clinical trials aimed at using combination therapy aimed at inhibition of the EGFR and IGFR pathways with chemotherapy found that groups treated with IGFR inhibitors in addition to EGFR inhibitors resulted in no change in patient progression-free survival when compared to patients treated with a combination of EGFR inhibitors and chemotherapy (Abdel-wahab *et al.*, 2018). However, combination therapy with the IGFR inhibitor resulted in an improvement in overall-patient survival, thereby suggesting a role for the IGFR pathway in contributing to PDAC progression. A possible explanation for the poor outcome in several clinical trials may be attributed to the genetic and epigenetic heterogeneity which exists in all tumours, whereby an as yet to be discovered resistance mechanism may be attributed to the molecular interactions within individuals. Additionally, the role of the IGF-1R pathway in PDAC tumours is not completely understood. Thus, there is a need for further preclinical research.

Despite perceived improvements in chemotherapeutic and biological agent strategies, the prognosis of advanced PDAC remains dismal (Hanna & Greenhalf, 2017; Torres & Grippo, 2018). To develop new therapeutic strategies for PDAC, the identification of molecular markers to individualise therapy for PDAC patients is required. However, in PDAC there is insufficient data to adequately describe the molecular characterization, phenotype and specific biomarkers that exist within different stages of the disease. Thus, the investigation of the IGF-1R signalling pathway and its downstream targets in PDAC cells representing different disease stages may be beneficial in understanding the mechanisms of resistance and provide data for developing novel, multi-targeting drug therapies.

1.5. Aim:

To characterise the expression of the IGF-1R signalling pathway in an *in vitro* model representing different stages of PDAC tumorigenesis.

1.6. Objectives:

1) To culture pancreatic derived cell lines from both early and metastatic stages of PDAC and compare this to normal pancreatic ductal cells.
2) To determine the baseline phenotypic characteristics of the different PDAC cell lines which are representative of the different stages of the disease, using proliferation, migration, and apoptosis assays.
3) To investigate the phenotypic changes associated with the different PDAC cell lines after treatment with IGF-1R inhibitors. The proliferative, migratory, and apoptotic responses of the PDAC cells were assessed using WST-1 assay, wound-healing assay and an Annexin V ELISA, respectively.

CHAPTER 2: METHODOLOGY

2.1 Cell lines and cell maintenance

2.1.1. Cell lines

The following cell lines were used within this study:

- *Human Pancreatic Ductal Epithelial Cell (HPDE):* An adherent human epithelial cell line derived from a non-diseased pancreatic duct. HPDE cells were described as having an 'almost normal' genotype and phenotype (Liu *et al.,* 2019). As such this cell line was used as a control cell line, representing normal pancreatic ductal cells.
- *PANC-1:* An adherent human epithelial cell line derived from the head of a pancreatic ductal tumour of a 56-year-old Caucasian male. This cell line has a doubling time of 52-hours and has a mixed population of epithelial and mesenchymal cells. PANC-1 cells have a K-Ras mutation at codon 12 Asp and is known to express EMT marker Vimentin (Moore *et al.,* 2001; Sipos *et al.,* 2003). This cell line is representative of an early stage of PDAC.
- *Mia PaCa-2:* An adherent PDAC cell line that was derived from the poorly differentiated tumour of a 65-year-old Caucasian male and has mesenchymal-like morphology. The doubling time of Mia PaCa-2 cells ranges between 18-48 hours (Sipos *et al.,* 2003; Wong, 2015). A K-Ras mutation in codon 12 Cys has been reported (Moore *et al.,* 2001; Sipos *et al.,* 2003). This cell line represents an intermediate stage of PDAC.
- *CF PAC*-1: An adherent, well-differentiated human epithelial PDAC cell line derived from the metastatic tumour of a 26-year-old Caucasian male. This cell line has a K-Ras mutation at codon 12 Val (Moore *et al.,* 2001). It represents a metastatic stage of PDAC.

2.1.2. Cell culture and cell maintenance

- HPDE cells were grown in keratinocyte serum free medium (KSFM) supplemented with bovine pituitary extract and epidermal growth factor (EGF) (Thermo Scientific, MA, USA, 17005075) and 1 % penicillin/ streptomycin (v/v) (Sigma-Aldrich, St Louis Missouri, USA, P4458).
- PANC-1 cells were grown in Dulbecco's modified eagle medium (DMEM) (Sigma-Aldrich, BE12-604F), 10 % foetal bovine serum (FBS) (Thermo Scientific, 10493106), and 1 % penicillin/streptomycin (v/v).

- Mia PaCa-2 cells were grown in DMEM, 10 % FBS, 5 % horse serum (Celtic, S091G-500) and 1 % penicillin/streptomycin.
- CF PAC-1 cells were cultured in Iscove's modified Dulbecco's medium (Lonza, LO190-500) supplemented with 10 % FBS and 1 % penicillin/streptomycin.

All cell lines were cultured under aseptic conditions, under an ESCO Airstream® Gen 2 Laminar Flow unit. The cells were maintained in a HERAcell 150i humidified incubator (Thermo Scientific, 02451) at a temperature of 37 °C and 5 % CO_2 until they reached a confluency of 70-90 %.

Cells were routinely subcultured when the cells reached a confluency of 70-90 %, cells were detached using 0.25 % Trypsin- 0.53 mM ethylenediametetraacetic acid (EDTA) (Thermo Scientific, 25200072) for 5-10 minutes. Matched volumes of the appropriate growth medium were added to each culture flask to neutralize the reaction. The resulting cell-media suspension was centrifuged in a Rotafix 32A centrifuge (Labotech, South Africa) for 5 minutes and the cell pellet was aspirated in 1 ml fresh media. Cells were then split in a 1:2 ratio.

Cells that were not to be used for immediate experimentation were resuspended in cryopreservation medium – 60 % FBS, 30 % growth medium and 10 % dimethyl sulfoxide (DMSO) (Sigma-Aldrich, 186500) and stored at -80 °C or in liquid nitrogen.

2.1.3 Modulation of IGF-1R signalling

IGF-1R signalling was modulated using Recombinant Human IGF-1/IGF-1 (R&D systems. 291-G1), NVP-AEW541 (Sigma-Aldrich, SML1973-5mg) and Picropodophyllotoxin (PPP) (Sigma-Aldrich, T9576-1mg). IGF-1 was used as a stimulatory compound of IGF-1R, and NVP-AEW541 and Picropodophyllotoxin were both used as inhibitors of IGF-1R. The optimal concentration for each cell line and inhibitors was calculated using IC_{50}. The IGF-1 concentration was chosen based on manufacturer's guidelines, and a standard concentration was maintained across all cell lines.

2.1.3.1. NVP-AEW541

The receptor tyrosine kinase (RTK) inhibitor, NVP-AEW541 is a highly sensitised IGF-1R kinase inhibitor that can differentiate and selectively bind to IGF-1R and not the insulin receptor (García-Echeverría *et al.,* 2004). NVP-AEW541 is classified a pyrrolopyrimidine derivative and an adenosine triphosphate (ATP) receptor antagonist. Therefore, the NVP-

AEW541 drug inhibits the activity of the IGF-1R by blocking the binding of the associated ATP molecules, thereby inhibiting the efficacy of the IGF-1R.

In an *in vivo* mouse model of pancreatic cancer, it was shown that NVP-AEW541 disrupted signal transduction involved in IGF/IGF-1R signalling, leading to a decrease in tumour cell growth and decreased migratory ability of the pancreatic cancer cells (Wong *et al.*, 2014; Blasco *et al.*, 2019).

2.1.3.2. Picropodophyllotoxin (PPP)

Picropodophyllotoxin is a cyclolignan that inhibits the phosphorylation of the IGF-1R tyrosine. Picropodophyllotoxin functions in a non-ATP antagonistic manner. It is known to mediate anticancer functions as well as induce G_2-M cell cycle arrest even in IGF-1R deficient cells (Linder *et al.*, 2007). It inhibits tumour growth rates through the activation of apoptosis in these cells. It is commonly used in *in vitro* studies of melanomas, breast cancer and leukaemia, where it was shown that the inhibitor preferentially affects the PI3K/Akt signalling cascade downstream of the IGF-1R (Teicher 2003; Vasilcanu *et al.*, 2004).

In pancreatic cancer, it was found that Picropodophyllotoxin significantly inhibits proliferation, and motility in the PANC-1 and Mia PaCa-2 cell lines (Tomizawa *et al.*, 2010)

2.1.3.3. Drug preparation

IGF-1 was initially dissolved in 1 ml of 0.1 % bovine serum albumin (BSA) (Appendix B). The NVP-AEW541 and Picropodophyllotoxin inhibitors were initially dissolved in 5 ml and 4 ml of DMSO, respectively. To obtain the desired IC_{50} concentrations, the inhibitors were further diluted in the specified growth medium for each cell line. The final concentration of DMSO in working solution was 0.03 % and BSA was 0.01 %. As such, the concentrations used for the DMSO and BSA diluent controls were 0.03 % and 0.01% respectively.

2.2. IC_{50}

Different concentrations of NVP-AEW541 and PPP were tested in each cell line to determine the IC_{50} values.

The HPDE, PANC-1, Mia PaCa-2 and CF PAC-1 cells were cultured under normal cell culture conditions. Once the cells reached 50 % confluency, the cells were washed twice with phosphate buffered saline (PBS) and treated with 200 µl of each drug solution. Concentrations of NVP-AEW541 were tested between 0.2 µM to 5 µM, and Picropodophyllotoxin concentrations were tested at a range of between 1 µM-5 µM. The PDAC cultures were incubated for a further 72 hours. After the 72-hour incubation cells were

trypsinized and the number of viable cells in each well were counted using a TC20™ Automated Cell Counter (BioRad, Hercules, California, USA, 145-0101).

2.2.1. Analysis

A comparison was made on the different ways to deduce IC_{50} values. Therefore, the data obtained was plotted as line graphs on Microsoft excel, and the concentrations extrapolated from the graphs. Alternatively, the raw IC_{50} data concentrations were log transformed and the percentage cell viability was unchanged. Graphs were plotted using the log transformed concentrations (x-axis) and percentage cell viability (y-axis) on GraphPad Prism V4.3. The software automatically generates $LogIC_{50}$ and IC_{50} values using the four-parameter logarithm (4PL) method. Additionally, IC_{50} values were obtained from literature and from manufacturer's information for a thorough comparison of the IC_{50} values.

2.3. Assessment of cell proliferation

Cell proliferation and viability is often measured by means of colorimetric assays. These assays can be used to measure cell proliferation in response to growth factors, cytokines, mitogens, and cytotoxic compounds such as anti-cancer therapies and signalling pathway modulators.

2.3.1. Water Soluble Tetrazolium Salts (WST)-1 Assay

The WST-1 cell proliferation kit (Sigma-Aldrich, 5015944001) was used. The assay is based on the cleavage of the water-soluble tetrazolium salt to formazan by cellular mitochondrial dehydrogenases. As the number of proliferating cells increases, the mitochondrial dehydrogenase activity is increased which increases the amount of formazan dye formed. Thus, the amount of formazan dye formed is directly proportional to proliferating cells.

Table 2.1 Seeding densities of each PDAC cell line in 96-well plates

Cell line	**Seeding Density**
HPDE	5×10^4 cells/well
PANC-1	2.5×10^4 cells/well
Mia Paca-2	2.5×10^4 cells/well
CF PAC-1	2.5×10^4 cells/well

Cells were cultured under normal culture conditions. The cells were seeded in 96-well plates at seeding densities described in **Table 2.1.** The seeding densities were optimized depending on the growth rate of the cell lines, so that following 24 hours the cells reached at least 50 % confluency to allow for treatment of the cells. The cells were incubated for 24 hours in a humidified incubator to allow for attachment of the cells to the plate surface. The cells were washed twice with PBS and treated with 100 µl of either DMSO, BSA, IGF-1, NVP-AEW541 or Picropodophyllotoxin diluted in the normal growth medium, for the respective cell lines, and incubated for 72 hours under standard cell culture conditions.

At hour 70 of incubation, 10 µl of the WST-1/ electrocoupling solution (ECS) was added to each well. The cells with the WST-1 solution were incubated for a further 2 hours before absorbance could be measured.

2.3.1.2. Analysis

The absorbance of the treated and untreated samples was measured using a BioTek 800TS microtiter plate reader with Gen5 software at a wavelength of 420 nm with a reference wavelength of 620 nm. Data was sorted in Microsoft Excel 2016. Graphs were generated using GraphPad Prism Version 4.1.3.

2.4. Clonogenic Assay

The clonogenic assay, also known as a colony formation assay, is used as a cell survival assay that is based on the ability of a single cell in a population to grow into a colony. The assay is used to test every cell in an *in vitro* population for its ability to undergo unlimited cell division (Franken *et al.*, 2006).

2.4.1. Crystal Violet Staining

Cells were treated with the pathway modulators for 72 hours, thereafter cells were washed twice in PBS and trypsinized for 5 minutes. Cells were plated in 6-well plates and were seeded at densities of 10 000 cells/well for each cell line.

The appropriate growth medium was added to each well and the cells were incubated at 37 °C and 5 % CO_2 in a humidified incubator for a period of 7-14 days or until the untreated cell control formed colonies of at least ~50 cells per colony. Cells were washed twice with PBS and fixed using ice-cold 100 % methanol for 20 minutes. Thereafter, the cell colonies were stained using 0.5 % crystal violet (w/v) and incubated at room temperature for 2 hours. The crystal violet stain was washed off in tap water and the plates were air-dried at room temperature for a few days before imaging.

2.4.2. Imaging and Analysis

Cells were imaged using the G-box image analyser using GeneSens software. The number of colonies were counted manually. The graphs were generated using GraphPad Prism version 8.4.3.

2.5. Migration Assay

A scratch or wound-healing assay is often used in *in vitro* studies to investigate the effects of biological or therapeutic factors on the migration of cells (Conant *et al.*, 2010). A scratch assay can be used to monitor the effect of a drug-treatment or biological agent on cell motility or cell proliferation. Wound-healing assays can also be used to assess molecular activities such as cell signalling, inflammatory response and tissue remodelling, all of which are important in tumour progression (Conant *et al.*, 2010).

2.5.1. Scratch Assay

The HPDE, PANC-1, Mia PaCa-2, and CF PAC-1 PDAC cell lines were seeded at a standard concentration of 100 000 cells/well in 6-well culture plates. The cultures were incubated at 37 ºC in a 5 % CO_2 in air humidified incubator until they had reached 100 % confluence, approximately 7-10 days following seeding.

On reaching confluence, the wells were washed twice with PBS to reduce cell membrane adhesion (Büth *et al.*, 2007). The PBS was aspirated, and the surface of the culture wells were scratched at right angles using a 1000 µl pipette tip. The wells were washed again to remove all the dislodged cells. Thereafter, 2 ml of IGF-1 treated medium, NVP-AEW541 treated medium, Picropodophyllotoxin treated medium, untreated control medium or the DMSO or BSA vehicle control medium were added into the respective wells of the culture plates. The cells were incubated at 37 ºC in a 5 % CO_2 in a humidified incubator with images taken at 24-hour intervals for the entire 72-hour incubation period. The time immediately after scratching was designated as “0-hour”.

2.5.2. Imaging and Analysis

Images were taken at each experimental time point using an inverted phase contrast Olympus IX35 microscope with an attached digital camera. At each time point, t (0, 24, 48 and 72 hours) the area of the wound was measured using the area measurement tool in the ImageJ software. The area of the inflicted wound was measured in 3 independent experiments. In addition, the area of each image was measured three times to eliminate the chances of intra-observer error. For each cell line, the average area measured was used to calculate the percentage migration at each experimental time point using the 0-hour as the reference point.

2.6. Quantitative real-time Polymerase Chain Reaction (qRT-PCR)

Polymerase chain reaction (PCR) is a technique used in molecular biology which allows for the amplification of specific sequences in a DNA or a complementary DNA (cDNA) template. While conventional PCR quantifies expression of the amplified product at the end of the reaction, real-time quantitative PCR measures the PCR product at the exponential-amplification phase of each cycle. This allows for more precision when determining the initial quantity of a target or gene. The quantification of the amplified product is attained using fluorescent dyes and real-time PCR instruments that measure the fluorescence while the sample is being amplified.

2.7.1. Primer design

Primers are short complementary sequences of nucleotides which bind to a specific region of DNA to be amplified in PCR. Primers were designed and synthesized using the PrimerQuest Tool on the Integrated DNA Technologies (IDT) website (https://eu.idtdna.com/Primerquest/Home/Index) and the primer design and conditions were checked using the Oligo Analysis Tool on the Eurofins genomics website (https://www.eurofinsgenomics.eu/en/dna-rna-oligonucleotides/oligo-tools/oligo-analysis-tool/). The genes were selected on the basis that they are known to be transcriptionally regulated genes.

The target gene names, descriptions and sequences of the primers that were used are detailed in **Table 2.2.**

Table 2.2 Primer sequences and descriptions of the transcriptionally regulated genes chosen in this study

Gene Name	Description	Forward Sequence	Reverse Sequence
IGF1R		5'-ATT CCA GCA GTC CCA GTT ATG-3'	5'-CTG CTT AGC CCA GGA AAT GA-3'
MYC	Cell cycle progression, apoptosis and cellular transformation.	5'-CTG TAG CCA CGC AGA TAA TAC A-3'	5'-CAG CAC ATT AGA CCC AGA TGA A-3'
PI3KCA	Survival	5'-CAG CAG CCT TCA ACA AAG ATG-3'	5'- CCA GCA CAG GAC AGT GTA AA-3'
AKT3	Survival, autophagy	5'-TCT GCA AGT GGA CGA GAA TAA G-3'	5'-AGA GCT AGG ACT GGT GAT GT-3'
FOX01	regulates different processes such as apoptosis and autophagy	5'-TGG GCA GGA AAG TGA TGT ATA G-3'	5'-TGC AGT ACG CAT AGT TCA GTA G-3'
SNAI1	Migration	5'-CAG CTA TTT CAG CCT CCT GTT-3'	5'-CCG ACA AGT GAC AGC CAT TA-3'
VIM	Migration	5'-GAT TCA CTC CCT CTG GTT GAT AC-3'	5'-GTC ATC GTG ATG CTG AGA AGT-3'
BCL2	Anti-apoptotic	5'-GGC CAG GGT CAG AGT TAA ATA G-3'	5'-GGA GGT TCT CAG ATG TTC TTC TC-3'
BAX	Pro-apoptotic	5'-TTC CTT ACG TGT CTG ATC AAT CC-3'	5'-GGG CAG AAG GCA CTA ATC AA-3'
RPLPO	Reference Gene	5'-GCT GAT CCA TCT GCC TTT GT-3'	5'-TCT TCC TTG GCT TCA ACC TTA G-3'

2.7.2. RNA extraction

RNA was extracted from cultures using the Qiagen RNeasy Mini Kit. Cells were trypsinized following a 72-hour treatment period and centrifuged at 25 200 x g for 5 minutes and resuspended in 350 µl Buffer RLT with 1:100 β-mercapoethanol (β-ME). Thereafter, 350 µl of 70 % ethanol was added to the lysate and was mixed gently by pipetting. This Buffer RLT and ethanol suspension of the sample (700 µl) was transferred to a RNeasy Mini spin column placed in a 2 ml collection tube and centrifuged for 15 seconds at 8000 x g. The flow-through was discarded and 350 µl of the Buffer RW1 was added to the RNeasy spin column. This was centrifuged for 15 seconds at 8000 x g and the flow-through discarded. On column DNase digestion was performed by adding 10 µl of DNase I incubation mix (**Appendix B**) to the column membrane and left at room temperature for 15 minutes. Buffer RW1 was added again to the column, centrifuged for 15 seconds at 8000 x g and the flow-through discarded. Then, 500 µl Buffer RPE was added to the column and centrifuged for 5 seconds at 8000 x g and the flow-through discarded. Another 500 µl Buffer RPE was added to the spin column and centrifuged for 2 minutes at 8000 x g. The RNA was eluted by placing the RNeasy spin-column in an unused 1.5 ml collection tube and 30 µl RNase-free water was added to the column. And the column was centrifuged for 1 minute at 8000 x g.

The concentration of the total RNA in the samples was measured using the Nanodrop Spectrophotometer (**Appendix C, 9.3**).

2.7.3 cDNA synthesis

cDNA was synthesised using the High-Capacity cDNA Reverse Transcription Kit (Applied Biosystems, California, USA). A total concentration of 100 ng/ µl of RNA was used for experimentation, therefore, RNA concentrations were adjusted accordingly and diluted in RNase-free water. A 2X Reverse Transcription Master Mix was made on ice using 2.0 µl 10X RT Buffer, 0.8 µl 25X dNTP Mix (100 mM), 2.0 µl 10X RT Random primers, 1.0 µl MultiScribe Reverse Transcriptase and 4.2 µl Nuclease-free H_2O. A 1:1 ratio of the 2X RT master mix and RNA sample (at a concentration of 100 ng/µl) were added to a 0.2 ml Eppendorf tube and mixed by pipetting. The samples were briefly spun in a centrifuge tube to eliminate any air bubbles. A non-reverse transcribed control was used as a control to ensure no DNA contamination of the samples had occurred. This is a highly sensitive way to determine the presence of genomic DNA contamination and negates the use of agarose gels and waste of precious RNA sample. The samples were placed in a MJ Mini Personal Thermal Cycler (Biorad, California, USA) at the following conditions:

Table 2.3 Thermal cycler conditions for cDNA synthesis

	Step 1	**Step 2**	**Step 3**	**Step 4**
Temperature (°C)	25	37	85	4
Time	10 min	120 min	1 min	∞

The samples were stored at 4 °C for use for qPCR the following day or at -20 °C until use.

2.7.4. Quantitative Real-Time Polymerase Chain Reaction (qRT-PCR)

The experiments were performed using the following protocol:

A 2.5 µl 1:20 cDNA dilution in RNase-free H_2O was added to a qRT-PCR master mix containing 5 µl SYBR (iTaq™ Universal SYBR® Green Supermix), 2.2 µl H_20, 0.2 µl forward primer (10 µM) and 0.2 µl reverse primer (10 µM). This solution was pipetted in duplicate into the wells of a white 96-well Piko® PCR Plate (Thermo Scientific™) and the plate sealed with the Adhesive Sealing Film (Thermo Scientific™). The qRT-PCR was completed using the PikoReal® Real-Time instrument programmed conditions specified in **Table 2.4.**

Table 2.4 Conditions used for qRT-PCR using the PikoReal® Real-Time instrument:

		40 cycles			Melt Curve	
	Step 1	Step 2	Step 3	Step 4	Step 5	Step 6
Temperature (°C)	95	95	60	60	60, 95 (0.2 °C increase)	20
Time	10 min	15 sec	1 min	30 sec	1 sec hold	10 sec

2.7.5. Analysis

The gene expression data was averaged for each gene and standard deviations calculated. Thereafter the data was analysed using the $2^{-\Delta\Delta Cq}$ method as outlined by the stipulated MIQE

guidelines. The data was then log transformed to normalize the data, so that the data were then expressed as the fold-change relative to the untreated control of each cell line.

These data were then transferred to the GraphPad Prism 8.4.3 software and where bar graphs and heatmaps were generated to show a comparison of gene expression across all the cell lines and treatment groups.

2.8. Western Blot Analysis

Western blotting or immunoblotting is a technique commonly used for the identification and quantification of a specific protein in a complex protein solution. The technique allows for the indirect detection of proteins immobilized on a nitrocellulose or a Polyvinylidene difluoride (PVDF) membrane (Wu *et al.,* 2014).

2.8.1. Total protein extraction

Cells were harvested by trypsinization and pelleted by centrifugation and the pellet washed in PBS. The cell pellet was lysed in radioimmunoprecipitation (RIPA) buffer (**Appendix B**) and incubated on ice for 20 minutes (with vortexing at 5 minute intervals). The lysate was centrifuged (Eppendorf 5402 centrifuge, 4 °C, 20 minutes) and the supernatant stored at –20 °C until required.

2.8.2. Protein Quantification

The concentration of the extracted proteins was determined using the Micro BCA™ Assay Kit (Thermo Scientific™, Massachusetts, USA) according to the following protocol:

Ten microliters of the bicinchoninic acid (BCA) protein standards (125, 250, 500, 750, 1000 and 2000 μg/ml) and unknown protein samples were individually incubated with 10 μl the Micro BCA working reagent (25 parts Micro BCA reagent MA, 24 parts Micro BCA reagent MB and 1 part Micro BCA reagent MC) for 1 hour at 37 °C.

2.8.2.1. Analysis

The absorbance of the standards and unknown samples were measured using a microplate reader at a wavelength of 562 nm. The concentrations of the protein samples were determined using extrapolation from the standard curve (**Appendix C**, **9.4**).

2.8.3. Dot Blot

Dot blots were done to determine the optimal concentrations of primary and secondary antibodies that were used in the Western Blot Analysis.

Briefly, the polvinylidene difluoride (PVDF) membrane was prepared by laying it on the surface of 100 % methanol for 15 seconds, to allow for the membrane to uniformly change

from opaque to semi-transparent. The membrane was then soaked in dH_2O for 2 minutes, and thereafter placed in 1X transfer buffer **(Appendix B**) for 5 minutes. A stack was prepared as follows:

Figure 2.1: Experimental set-up for spotting of samples in a dot blot.

When the membrane was wet enough to absorb the sample, but not too wet that the sample spread across the membrane, approximately 10 µg of the protein sample was spotted on to the membrane. After the sample was adsorbed, the membrane was allowed to dry at room temperature. Once dry, the membrane was blocked in 5 % BSA on a shaker at room temperature for 1 hour. The membrane was then incubated in the primary antibody (**Table 2.5.**) for 1 hour at room temperature with gentle agitation. The membrane was then washed 3 times for 10 minutes each with PBS-Tween. Thereafter, the membrane was incubated with the secondary antibody for 1 hour at room temperature on a shaker. Once more, the membrane was washed 3 times for 10 minutes with PBS-Tween.

The expression of the protein of interest was detected using the SuperSignal® West Pico Chemiluminescent Substrate (Thermo Scientific™, Massachusetts, USA) mixed in a 1:1 ratio. Images of the resultant bands were captured using the G-box Imager with GeneSens software.

2.8.4. Electrophoresis

2.5.4.1. Sodium Dodecyl Sulphate Polyacrylamide Gel Electrophoresis (SDS-PAGE) to Resolve Proteins

10 µg of protein was mixed with 6 X loading dye and incubated at 90 °C for 5 minutes. Following this, the protein samples were electrophoresed at 60 mA for ~2 hours or until the dye front reached ~1 cm from the bottom of the gel.

2.5.4.2. Transfer of Proteins from Resolved Gel to a Polyvinylidene difluoride (PVDF) Membrane

The resolved gel, 0.2 µm PVDF membrane (activated in 100 % methanol) and filter paper were pre-soaked in cold transfer buffer for 5 minutes at room temperature (RT). The gel was placed above the PVDF membrane and sandwiched between filter paper with the gel facing

the cathode (**Figure 2.2.**). The sandwich was placed in the transfer tank filled with cold transfer buffer and a voltage of 10 V was applied overnight at 4 °C.

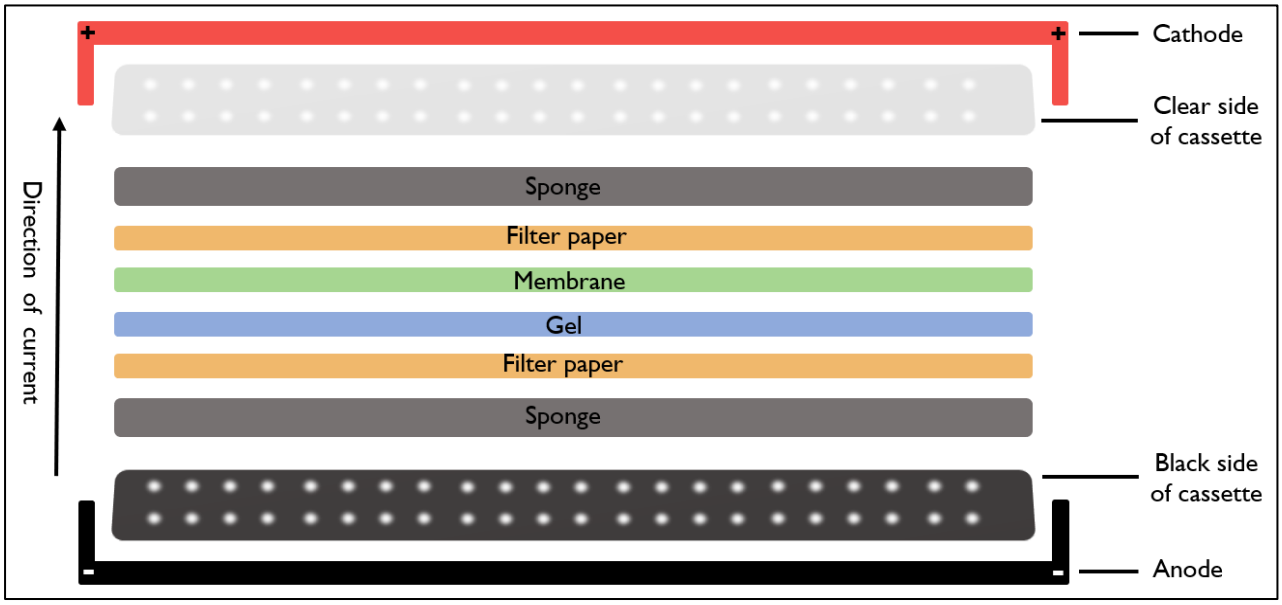

Figure 2.2: Schematic demonstrating the assembly of western blotting equipment for protein transfer. Protein blotting involves the use of a cassette in which a stack of sponges, filter paper, gel and PVDF membrane is stacked.

2.8.4.3. Detection and Analysis

After transfer, the PVDF membrane (now containing the proteins transferred from the gel) was removed from the sandwich and blocked in 5 % BSA in PBS-Tween for 1 hour at RT with gentle shaking. Following blocking, the membrane was incubated with the appropriate primary antibody (**Table 2.5**) (diluted in 5 % BSA in PBS-Tween) overnight at 4 °C with gentle shaking. The membrane was washed 3 times (10 minutes each) in PBS-Tween at RT with gentle shaking. Thereafter, the membrane was incubated with the appropriate secondary antibody (diluted in 5 % BSA in PBS-Tween) for 1 hour at RT with gentle shaking. The membrane was washed 3 times (10 minutes each) in PBS-Tween at RT with gentle shaking.

The expression of the protein of interest was detected using the SuperSignal® West Pico Chemiluminescent Substrate (Thermo Scientific™) mixed in a 1:1 ratio. Images of the resultant bands were captured using the G-box Imager with GeneSens software. The ImageJ analysis program was used to quantify the resulting band intensities.

Table 2.5 Primary antibodies used to target proteins involved in the IGF-1R pathway.

Protein of Interest	Primary Antibody	Rationale for Protein Chosen	Catalogue no.
p-IGF-1R Beta	Phospho-IGF-1 Receptor β (Tyr1135) (DA7A8) Rabbit mAb	Since the NVP-AEW541 and Picropodophyllotoxin block the phosphorylation of the IGF-1R, expression of the phosphorylated protein was included to determine efficacy of these inhibitors in each cell line.	CST3024S
IGF-1R	IGF-1 Receptor β Antibody	To determine baseline protein expression levels of the IGF-1R in PDAC cells.	CST3027S
mTOR	mTOR (Ser2448) (D9C2) Rabbit mAb	mTOR is a protein found downstream of Akt and is an important regulator of proliferation (Hassan *et al.*, 2013).	CST9239S
Akt	Akt Rabbit mAb	A downstream signalling pathway of IGF-1R. It has been suggested that elevated levels of Akt may contribute to the aggressiveness of late stage and/or metastatic tumours and is consistently activated in PDAC (Altomare & Testa, 2005).	CST4491S
BAD	BAD Antibody	BAD is a protein that is involved in apoptosis, when phosphorylated BAD acts as an anti-apoptotic signal in its dephosphorylated isoform (She *et al.*, 2005).	CST2939S

Histone H3 (CST4499S) was used as a control for Western Blot analyses.

Anti-rabbit IgG horse-radish peroxidase (HRP)-linked antibodies was used as the secondary antibody for all targets. All antibodies were purchased from Cell Signaling Technology (Masssachusetts, USA).

2.9. Statistical Analysis

The Statistica Software (TIBCO Inc., Texas) was used for the analysis of all statistical data. A Shapiro-Wilk normality test was performed to determine whether the data is parametrically or non-parametrically distributed. Thereafter, the respective analysis of variance analysis (ANOVA) or Kruskal-Wallis test were used, with the relevant Tukey or Dunn's non-parametric comparison post-hoc adjustments to determine the differences that exists within each group. Student t-tests were used to compare the differences between two treatment groups within a cell line. P-values of <0.05 were considered significant.

CHAPTER 3: RESULTS

3.1. IC_{50}

The fifty percent inhibitory concentrations (IC_{50} values) were determined for the NVP-AEW541 and Picropodophyllotoxin (PPP) IGF-1R inhibitors for the HPDE, PANC-1, Mia PaCa-2 and CF PAC-1 cell lines by constructing dose-response curves from the WST-1 assay. These values were obtained by treating the PDAC cells to ranging concentrations of NVP-AEW541 from between 0.2 µM to 5 µM, and Picropodophyllotoxin concentrations ranging from 1 µM to 5 µM. A comparison was made between dose-response curves generated using Microsoft excel using raw data and using the four-parameter logarithmic (4PL) function on GraphPad Prism (V8.4.3.). Inhibitory concentrations obtained from articles and manufacturer's instructions were also compared to the IC_{50} values obtained from the Microsoft excel and GraphPad Prism dose-response curves. Dose-response curves are shown in **Figures 3.1., 3.2., 3.3**., and **3.4**, with the comparison of the IC_{50} values shown in **Table 3.1**.

Table 3.1: Comparison of different IC_{50} values as determined by experimentation vs manufacturer's guidelines and literature.

		Concentration (µM)				
Cell Line	**Treatment**	**Graphical**	**GraphPad**	**As per manufacturer**	**Literature**	**Reference**
HPDE	NVP-AEW541	2.3	2.178	0.86-5	n/a	
	PICROPODOPHYLLOTOXIN	0.75	0.8650	0.05 - 15	n/a	
PANC-1	NVP-AEW541	3.8	3.057	0.86-5	2.5	Wong (2015)
	PICROPODOPHYLLOTOXIN	3.99	3.96	0.05 - 15	n/a	
Mia PaCa-2	NVP-AEW541	2.47	2.052	0.86-5	2.0	Ioannou *et al.*, (2013)
	PICROPODOPHYLLOTOXIN	1.93	1.493	0.05 - 15	n/a	
CF PAC-1	NVP-AEW541	2.59	2.907	0.86-5	3.9	Wong, (2015)
	PICROPODOPHYLLOTOXIN	1.99	2.162	0.05 - 15	n/a	

3.1.1. HPDE

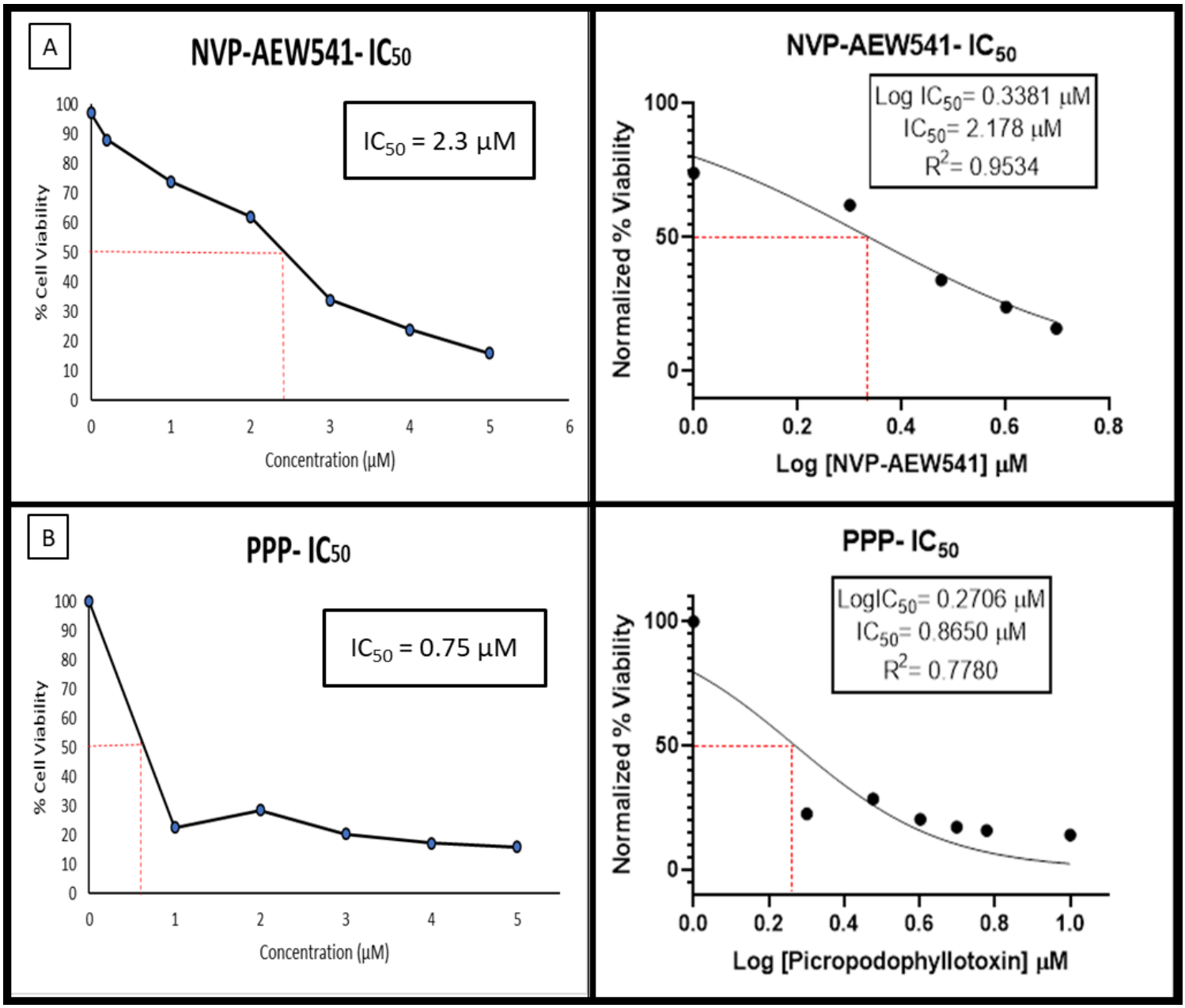

Figure 3.1: IC_{50} values of a) NVP-AEW541 and b) Picropodophyllotoxin (PPP) treatments in the HPDE cell line. The HPDE cells were treated with concentrations of NVP-AEW541 ranging from 0.2 µM to 5 µM, and Picropodophyllotoxin concentrations ranging from 1 µM to 5 µM. Each point represents the mean percentage cell viability obtained from three independent experiments. A comparison was made between IC_{50} values obtained from graphs generated on Microsoft excel (left) and logarithmic transformed IC_{50} values obtained from statistical software GraphPad Prism. Similar graphical IC_{50} values were obtained for the NVP-AEW541 inhibitor using both curves. The curve generated for PPP showed a drastic decline in cell viability for concentrations exceeding 1 µM.

3.1.2. PANC-1

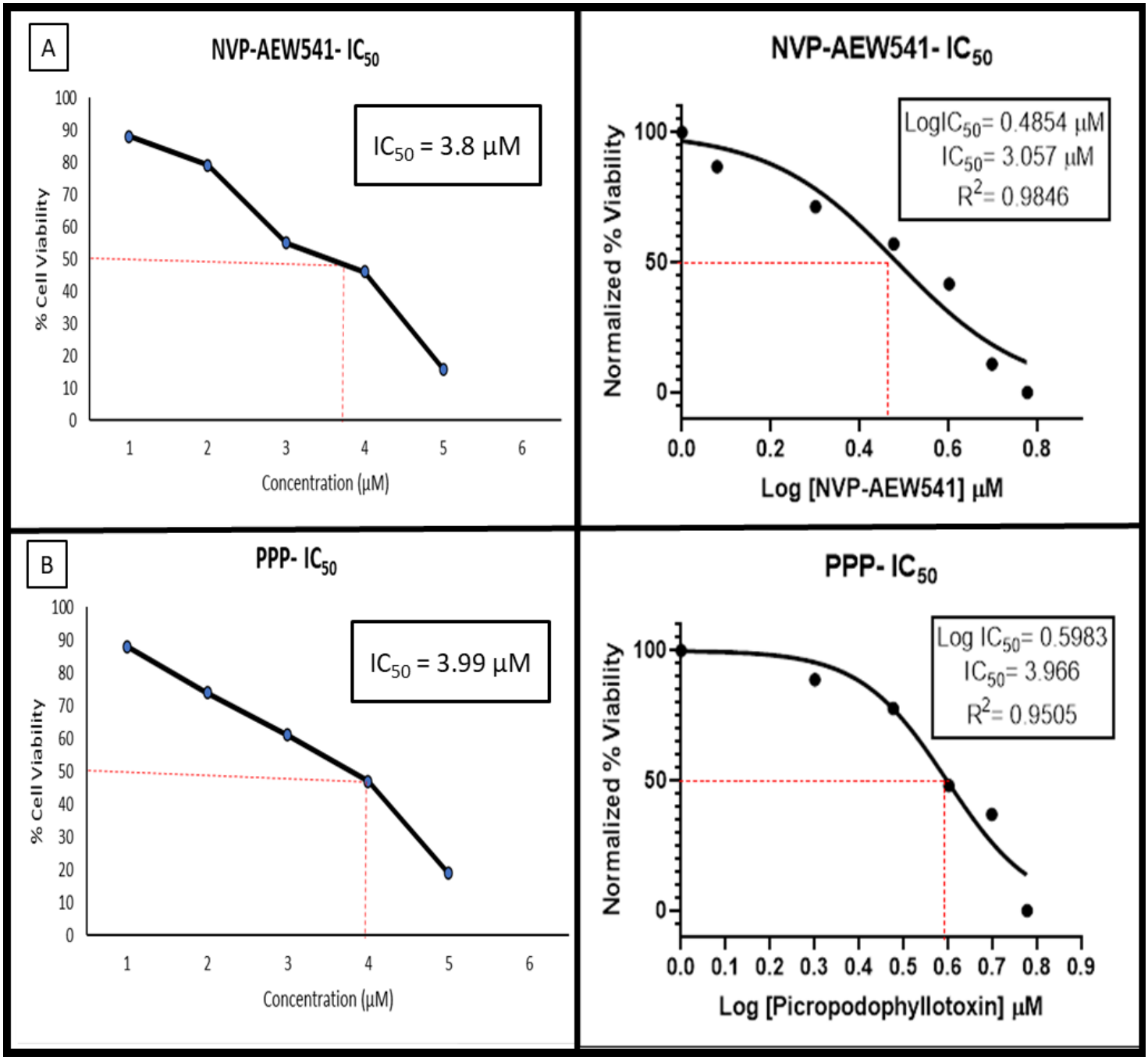

Figure 3.2: IC_{50} values of a) NVP-AEW541 and b) Picropodophyllotoxin (PPP) treatments in the PANC-1 cell line. PANC-1 cells were treated with concentrations of NVP-AEW541 ranging from 0.2 µM to 5 µM, and Picropodophyllotoxin concentrations ranging from 1 µM to 5 µM. Each point represents the mean percentage cell viability obtained from three independent experiments. A comparison was made between IC_{50} values obtained from graphs generated on Microsoft excel (left) and logarithmic transformed IC_{50} values obtained from statistical software GraphPad Prism.

3.1.3. Mia PaCa-2

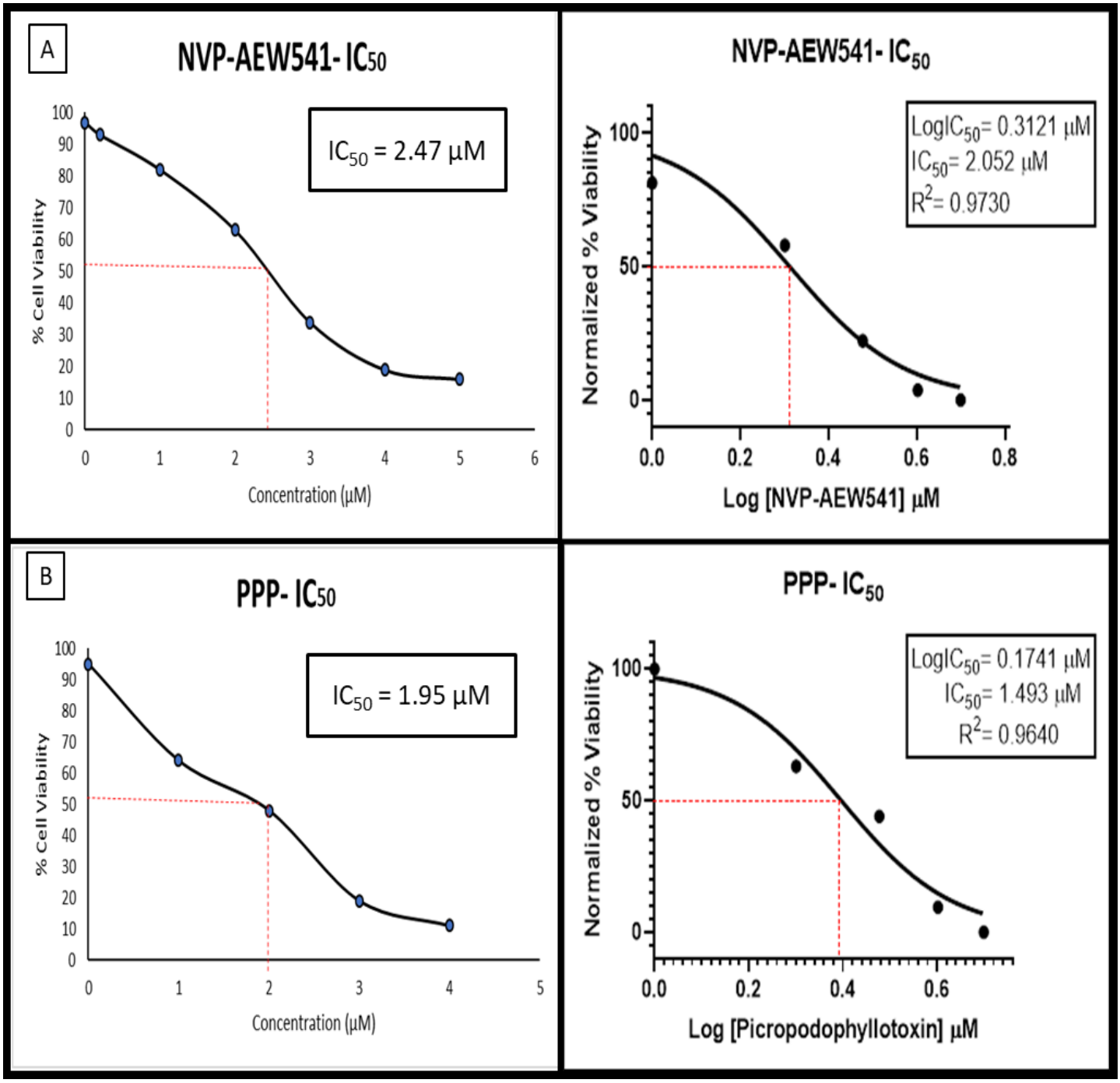

Figure 3.3: IC_{50} values of a) NVP-AEW541 and b) Picropodophyllotoxin (PPP) treatments in the Mia PaCa-2 cell line. Mia PaCa-2 cells were treated with concentrations of NVP-AEW541 ranging from 0.2 µM to 5 µM, and Picropodophyllotoxin concentrations ranging from 1 µM to 5 µM. Each point represents the mean percentage cell viability obtained from three independent experiments. A comparison was made between IC_{50} values obtained from graphs generated on Microsoft excel (left) and logarithmic transformed IC_{50} values obtained from statistical software GraphPad Prism.

3.1.4. CF PAC-1

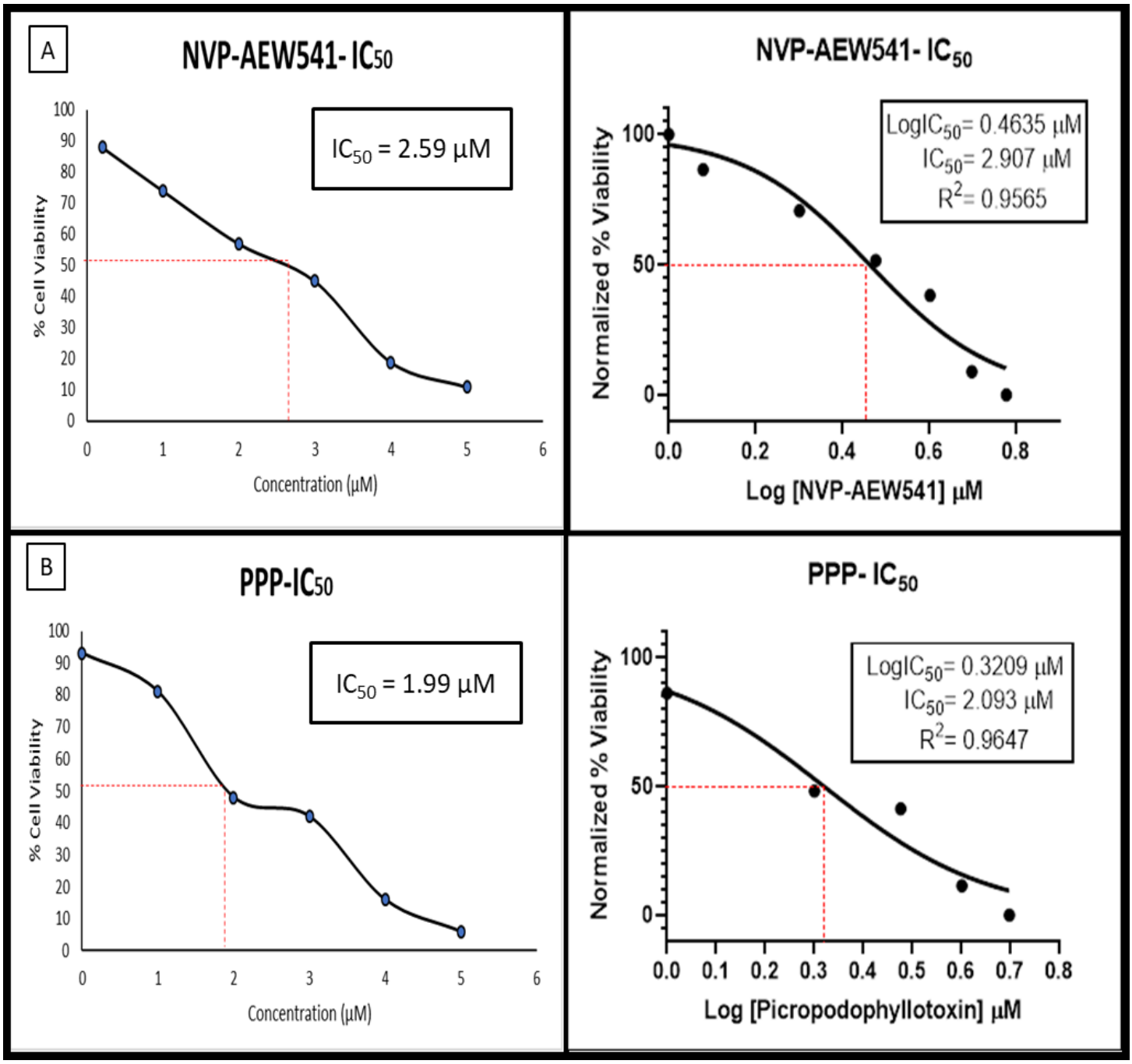

Figure 3.4: IC_{50} values of a) NVP-AEW541 and b) Picropodophyllotoxin (PPP) treatments in the CF PAC-1 cell line. CF PAC-1 cells were treated with concentrations of NVP-AEW541 ranging from 0.2 µM to 5 µM, and Picropodophyllotoxin concentrations ranging from 1 µM to 5 µM. Each point represents the mean percentage cell viability obtained from three independent experiments. A comparison was made between IC_{50} values obtained from graphs generated on Microsoft excel (left) and logarithmic transformed IC_{50} values obtained from statistical software GraphPad Prism.

The optimal concentration of IGF-1 for stimulation of cell growth was determined using the Trypan Blue Exclusion method. The concentration of IGF-1 was kept constant throughout all cell lines to determine the role of IGF-1 in the different stages of PDAC. A concentration of 4 ng/ml was used for IGF-1 treatment across all cell lines.

Table 3.2: Working concentrations of modulators used in experiments.

	IGF-1	NVP-AEW541 (μM)	PICROPODOPHYLLOTOXIN (μM)
HPDE	4ng/ml	2.5	0.65
PANC-1		2.7	4
Mia PaCa-2		2.5	2
CF PAC-1		2.6	3

HPDE cells appeared to be more sensitive to the Picropodophyllotoxin inhibitor compared to the NVP-AEW541 inhibitor, this is indicated by the lower IC_{50} value obtained. Interestingly, the PANC-1 cells were not as sensitive as the other PDAC cell lines, having the highest concentration of NVP-AEW541 at 2.7 μM, and Picropodophyllotoxin treatment with a concentration of 4 μM being the most effective in reducing cell viability to 50 %. While the graphical IC_{50} values of NVP-AEW541 in the PANC-1 cell line exceeded 3 μM, the use of these concentrations in following experimentation yielded a cell viability of less than 50 %, therefore, as a result a concentration of 2.7 μM was used that was obtained from literature.

3.2. Morphology

The PDAC cells were grown in 6-well plates and treated with IGF-1, NVP-AEW541 and Picropodophyllotoxin (PPP). DMSO and BSA were used as diluent controls. The PDAC cells were viewed following the 72-hour treatment using an Olympus IX35 microscope at a magnification of 100 X and the images were taken with the attached camera.

3.2.1. HPDE

The HPDE cell line is derived from normal pancreatic ductal cells. These cells form plaques as they become confluent and become a monolayer. These cells maintain its epithelial, ductal-like morphological characteristics. They are small and elongated cells, with a small

nucleus and an attenuated cytoplasm. As the cells become more confluent, some cells give rise to rosette-like formations. This rosette morphology is typically associated with duct formation (Soule *et al.*, 1973). DMSO treated HPDE cells were shrunken with a lack of clear cell boundaries. HPDE cells treated with the BSA diluent maintained some of its original cell morphology as displayed in **Figure 3.5**, however, the cells were more sparsely populated with stellate and pyramidal shaped cells. IGF-1 treated HPDE cells were sparsely arranged in the culture dish, with more elongated cells with oval-shaped nuclei. Cells treated with NVP-AEW541 no longer maintained its normal ductal-like morphology, these cells lacked clear cell boundaries, were oddly shaped, had the presence of blebbing and had a lot of cell debris. Picropodophyllotoxin treated HPDE cells, lacked clear cell boundaries, had a granulated cytoplasm and large nuclei. These cells displayed a form of cell death called secondary necrosis.

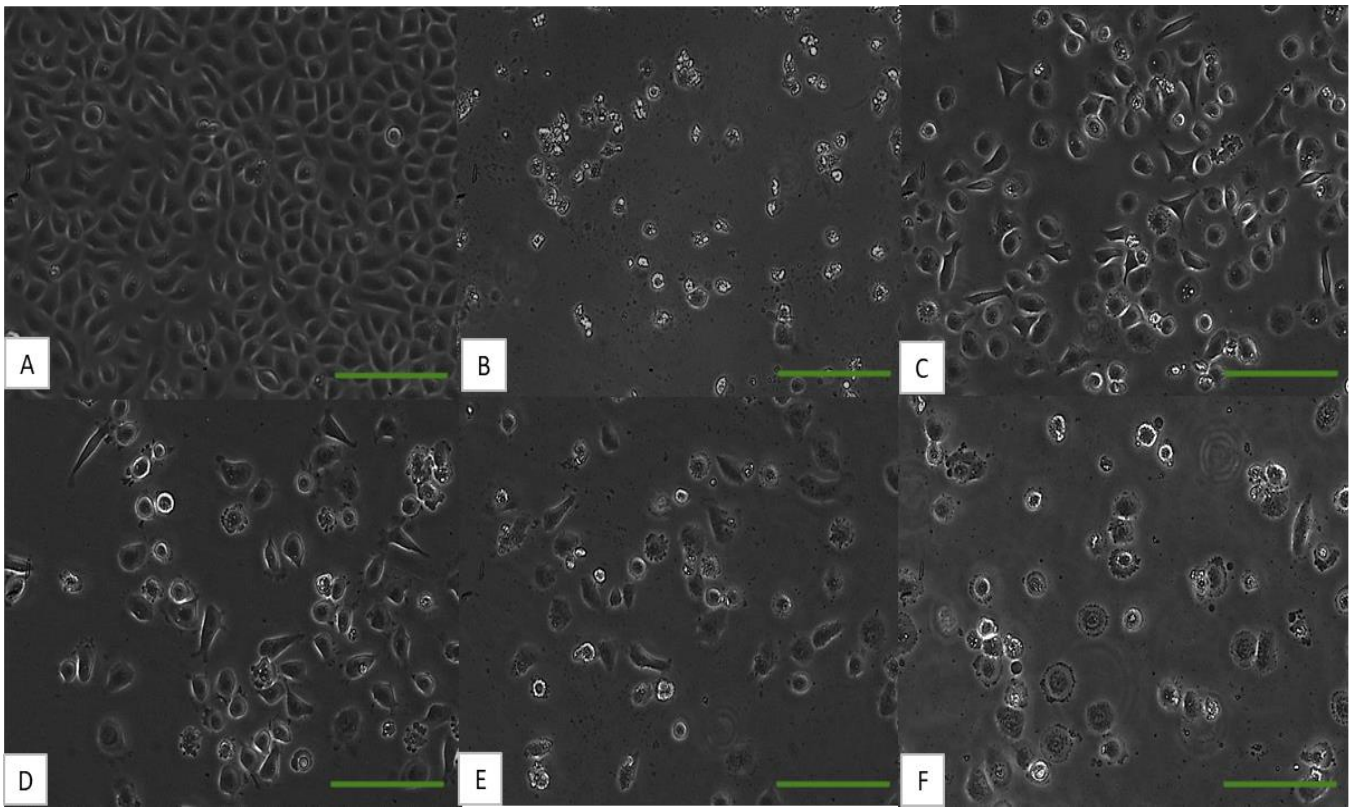

Figure 3.5: Photomicrographs of HPDE cells showing morphological changes when exposed to different treatment groups a) untreated, b) DMSO, c) BSA, d) IGF-1, e) NVP-AEW541 and f) Picropodophyllotoxin after 72 hours. Cells showed an epithelial cell morphology. HPDE cells were treated with 4 ng/ml of IGF-1, 2.5 µM of NVP-AEW541 and 0.65 µM of Picropodophyllotoxin. Magnification 100 X, scale bar: 10 µm.

3.2.2. PANC-1

Untreated PANC-1 cells had a stellate morphology with a centrally placed, round nucleus. DMSO-treated cells appeared more sparsely in the culture dish and were more rounded with a smaller, displaced nucleus. PANC-1 cells treated with the BSA diluent had a brick-like morphology and were more confluent when compared to untreated cells. IGF-1-treated cells were more densely populated in the culture dish and had a variety of shapes ranging from small, rounded cells, stellate-shaped cells, and elongated cells. PANC-1 cells that were treated with NVP-AEW541 were stellate shaped and had granular cell bodies, while cells treated with Picropodophyllotoxin were irregularly shaped, lacked clear cell boundaries and were granulated.

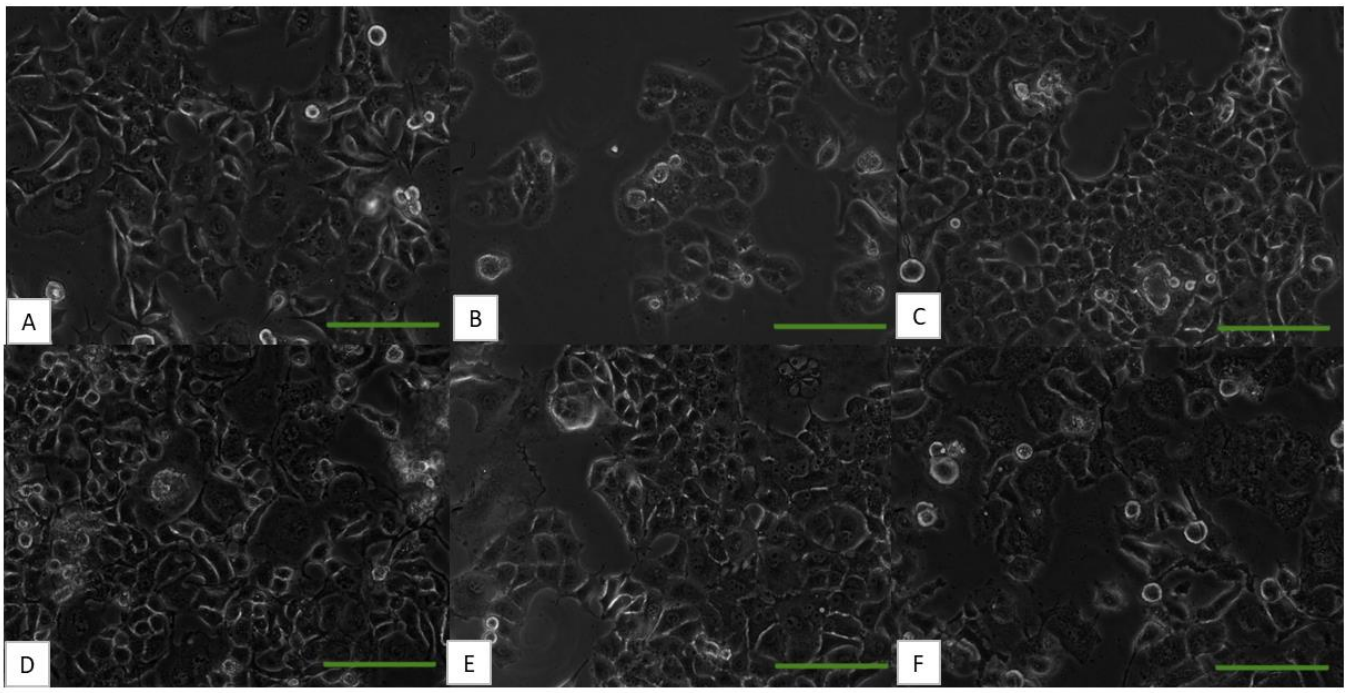

Figure 3.6: Photomicrographs showing morphological changes of PANC-1 cells when exposed to different treatment groups a) untreated, b) DMSO, c) BSA, d) IGF-1, e) NVP-AEW541 and f) Picropodophyllotoxin after 72 hours. PANC-1 cells were treated with 4 ng/ml of IGF-1, 2.7 μM of NVP-AEW541 and 4 μM of Picropodophyllotoxin. Magnification 100 X, scale bar: 10 μm.

3.2.3. Mia PaCa-2

Untreated Mia PaCa-2 cells are adherent and attach loosely to form clusters. The cells maintain an epithelial and mesenchymal cell morphology. Similar to HPDE cells, the Mia PaCa-2 cells are small, elongated and has a small centrally placed nucleus. Smaller, rounded cells were observed when treated with the DMSO diluent. These cultures also showed signs

of cell shrinkage and more condensed colony formations. BSA treated cells were shrunken and more rounded. IGF-1 treated cells became more elongated and spindle-shaped and showed the initial stages of plasma membrane blebbing. Mia PaCa-2 cultures treated with NVP-AEW541 had irregularly shaped, granular cell bodies and formed irregular dense cell colonies. Compared to the untreated control, Picropodophyllotoxin-treated cultures had a variety of cell shapes, with some spindle-shaped with the presence of blebbing, fibroblast-like cells and rounded granular cells.

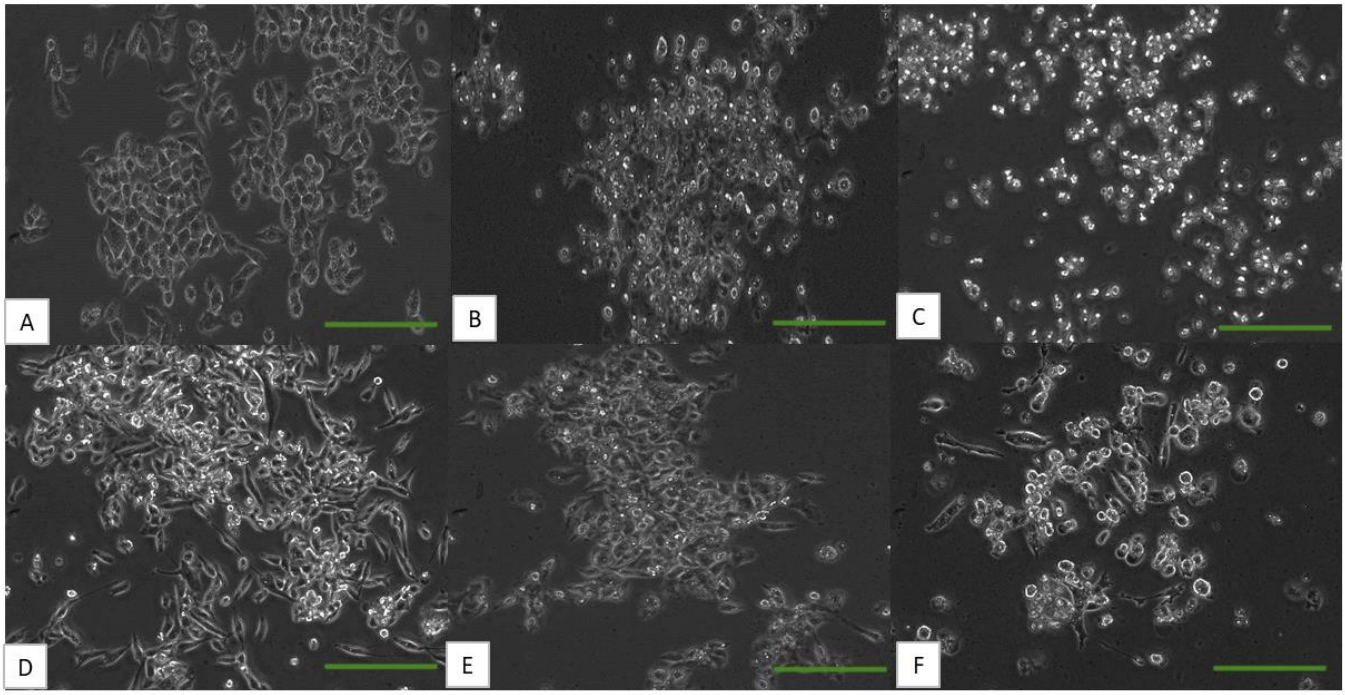

Figure 3.7: Photomicrographs showing morphological changes to Mia PaCa-2 cells when exposed to different treatments a) Untreated, b) DMSO, c) BSA, d) IGF-1, e) NVP-AEW541 and f) Picropodophyllotoxin after 72 hours. Mia PaCa-2 cells were treated with 4 ng/ml of IGF-1, 2.5 µM of NVP-AEW541 and 2 µM of Picropodophyllotoxin. Magnification 100 X, scale bar: 10 µm.

3.2.4. CF PAC-1

Untreated CF PAC-1 cultures had cells that were small, elongated and formed large cell colonies. Cells treated with the DMSO diluent resulted in rounding and subsequent lifting of cells from culturing dishes. BSA treated cultures had a similar appearance to that of untreated cells, with small, elongated cell bodies, however, unlike the untreated cultures, BSA treated cells showed granulation within the cell bodies. CF PAC-1 cultures treated with IGF-1 were characterised by the presence of irregularly shaped and granular cell bodies with displaced nuclei, the presence of blebbing was also observed in these cultures. NVP-AEW541 treated

cultures showed small cell colonies of irregularly shaped, granulated CF PAC-1 cells. Cultures that were treated with PPP presented with the loss of clear cell boundaries, granulation, and plasma membrane blebbing. Moreover, an increase in cell debris was observed across the IGF-1, NVP-AEW541 and PPP treated cultures.

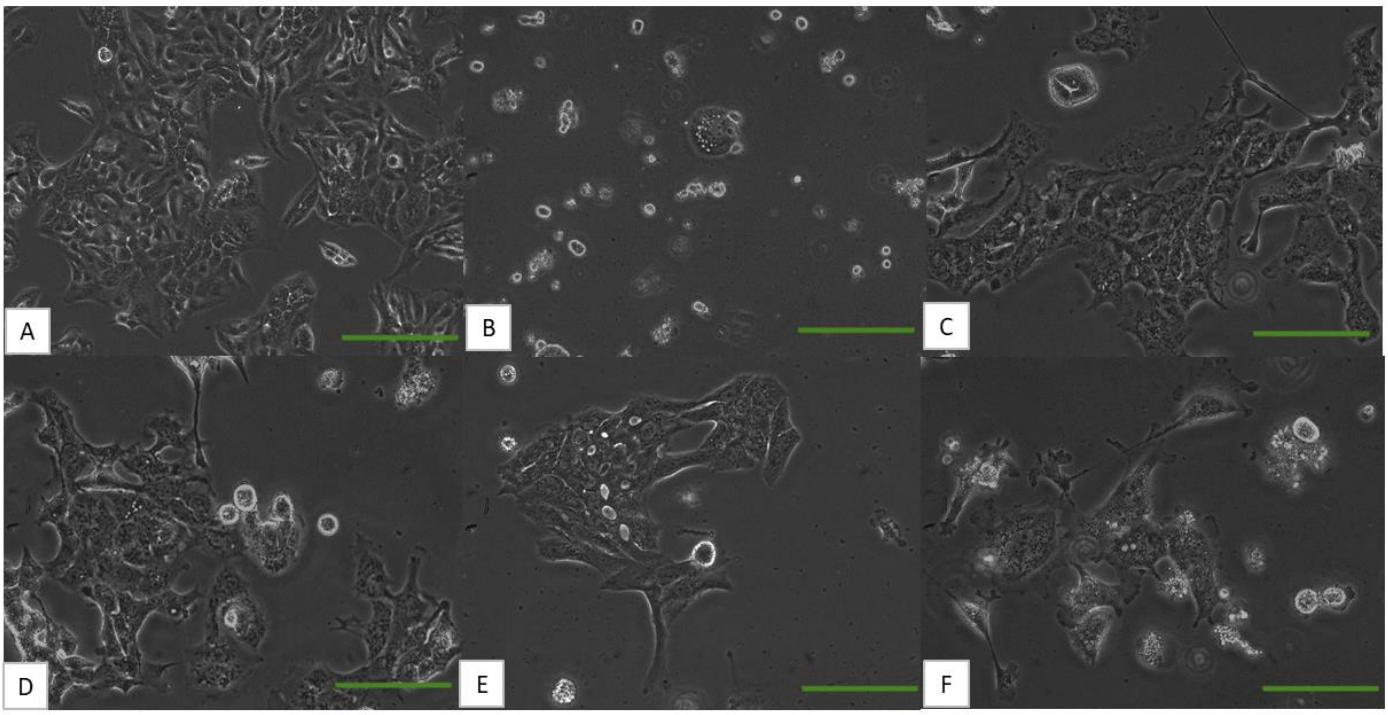

Figure 3.8: Photomicrographs of changes in morphology to CF PAC-1 cells when exposed to different treatments a) Untreated, b) DMSO, c) BSA, d) IGF-1, e) NVP-AEW541 and f) Picropodophyllotoxin after 72 hours. CF PAC-1 cells were treated with 4 ng/ml of IGF-1, 2.5 µM of NVP-AEW541 and 3 µM of Picropodophyllotoxin. Magnification 100 X, scale bar: 10 µm.

3.3. WST-1 Proliferation Assay

Proliferation data obtained from the WST-1 analysis showed that IGF-1R modulation affected the proliferation of PDAC cells, moreover, significant differences were seen within each cell line.

The HPDE cells showed significantly decreased levels of proliferation in the DMSO and BSA diluent treatment groups ($p<0.05$), while IGF-1 did not significantly increase the proliferation when compared to untreated control ($p>0.05$). Compared to untreated cells, the NVP-AEW541 and PPP inhibitors significantly decreased proliferation in the cell line ($p<0.05$), these treatment groups also significantly decreased proliferation compared to the IGF-1 treated cells ($p<0.05$). A comparison between the different treatment groups showed

that DMSO significantly decreased cell proliferation compared to all treatment groups ($p<0.05$). Picropodophyllotoxin treatment was also found to be more effective in decreasing cell proliferation in the HPDE cell line when compared to cells treated with NVP-AEW541 treatment groups ($p<0.05$).

PANC-1 cells had a varied proliferative response to all treatments ($p<0.05$), where all treatments groups were significantly different from the untreated control. IGF-1 treated PANC-1 cells exhibited a significantly greater level of proliferation when compared to all treatment groups ($p<0.05$). Cells treated with the NVP-AEW541inhibitor showed decreased proliferation compared to the untreated control but exhibited similar levels of proliferation as the DMSO and BSA diluents. Cells exposed to Picropodophyllotoxin showed significantly decreased proliferation compared to all treatments, including NVP-AEW541 ($p<0.05$). This indicates that Picropodophyllotoxin is more effective in decreasing cellular proliferation in PANC-1 cells.

Mia PaCa-2 cells had a similar level of cell proliferation induced in response to all drug treatments ($p>0.05$). Cellular proliferation in cells exposed to IGF-1 was significantly increased compared to the untreated control ($p<0.05$). Interestingly, Mia PaCa-2 cells had an increased level of proliferation when exposed to the NVP-AEW541 and Picropodophyllotoxin IGF-1R inhibitors when compared to the untreated and diluent controls, albeit not significantly ($p>0.05$).

CF PAC-1 cells showed varying levels of proliferation when exposed to the drug treatments ($p<0.05$). All treatments appeared to decrease the proliferative capacity of CF PAC-1 cells with a marked decrease in cell proliferation observed when comparing all treatment groups to the untreated control ($p<0.05$). DMSO had the severest effects on the CF PAC-1 cells with the lowest proliferation occurring in cells treated with this diluent. Cells treated with IGF-1 and BSA showed similar levels of proliferation, indicating that IGF-1 did not have a major impact on the proliferation of CF PAC-1 cells and that the levels of proliferation observed in cells treated with IGF-1 may not be due to the effects of IGF-1 itself, but may be the effects of the BSA diluent. Proliferation of CF PAC-1 cells treated with NVP-AEW541 and Picropodophyllotoxin were significantly decreased when compared to the untreated control ($p<0.05$), with Picropodophyllotoxin treatment being significantly more effective than NVP-AEW541 in decreasing cell proliferation.

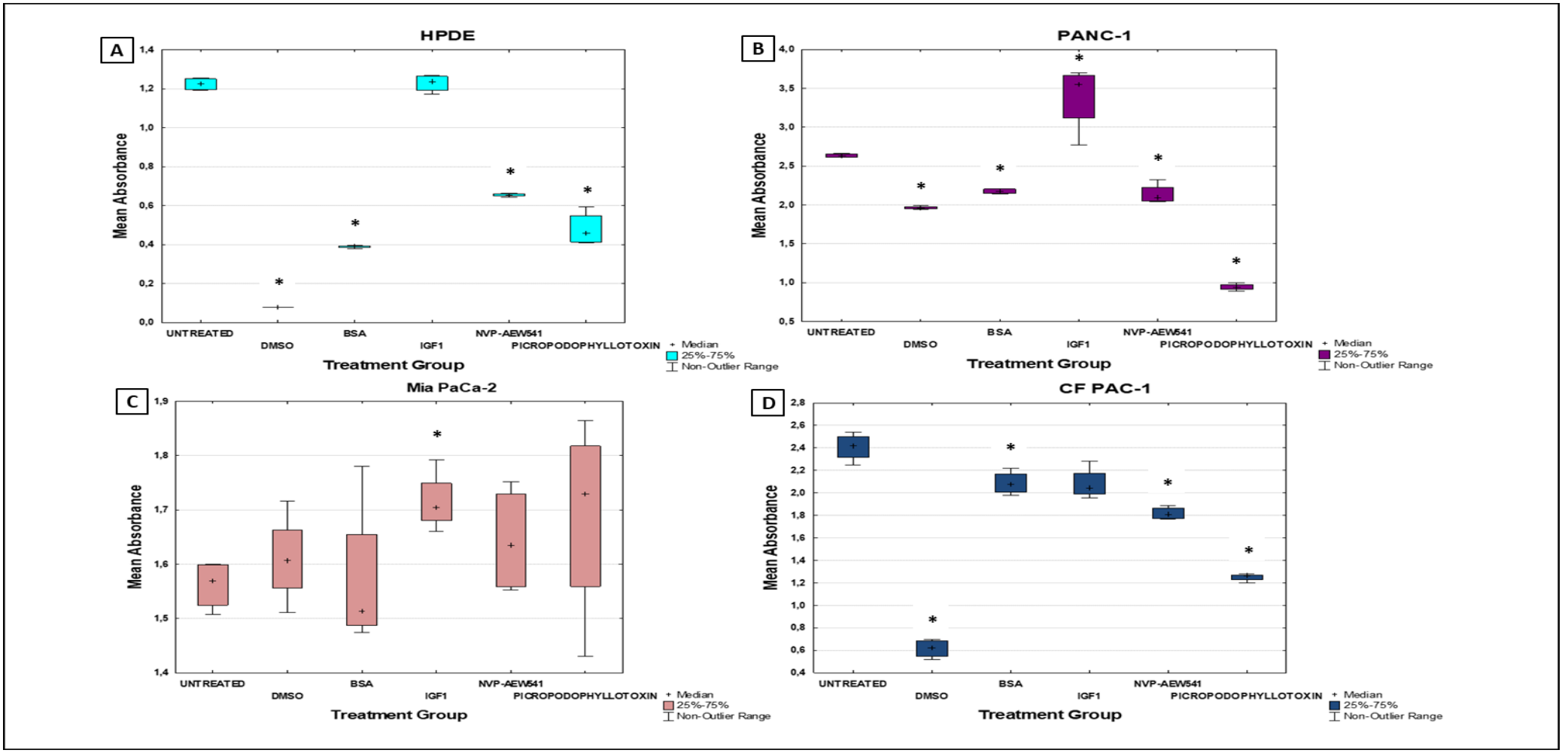

Figure 3.9: WST-1 proliferation in PDAC cell line following 72-hour treatment with IGF-1R modulators. Proliferation was significantly decreased in **a) HPDE, b) PANC-1** and **d) CF PAC**-1 cells treated with DMSO, BSA, NVP-AEW541 and Picropodophyllotoxin. IGF-1 treatment significantly increased proliferation in **b) PANC-1** and **c) Mia PaCa-2** cells. A non-parametric ANOVA test was done to determine the differences between treatment groups in each cell line, n=3. Each box plot represents the average lower and upper quartile percentages, and the whiskers represents the non-outlier range. *The mean absorbance is directly proportional to proliferative capacity within the cells.* Asterisk represents treatments that are significantly different from the untreated control. $P<0.05$.

A comparison between all PDAC cell lines showed that proliferation in the HPDE cell line across all treatment groups was significantly lower when compared to PANC-1, Mia PaCa-2 and CF PAC-1 cells. In addition, HPDE cells appeared to be the most sensitive cell line to the different treatments when compared to the other cell lines. The data shows that untreated PANC-1 cells were more proliferative than the other PDAC cells. CF PAC-1 cells had a higher proliferation rate across all treatment groups, apart from DMSO treated cells. Mia PaCa-2 proliferation was relatively unchanged across all treatment groups. The DMSO diluent significantly decreased cell proliferation in HPDE and CF PAC-1 cells. Only PANC-1 and Mia PaCa-2 cells increased in proliferation when exposed to IGF-1, while proliferation was not significantly affected in HPDE and CF PAC-1 cells exposed to IGF-1 for 72 hours. It was also observed that Picropodophyllotoxin was significantly more effective that NVP-AEW541 in decreasing cell proliferation in HPDE, PANC-1 and CF PAC-1 cells.

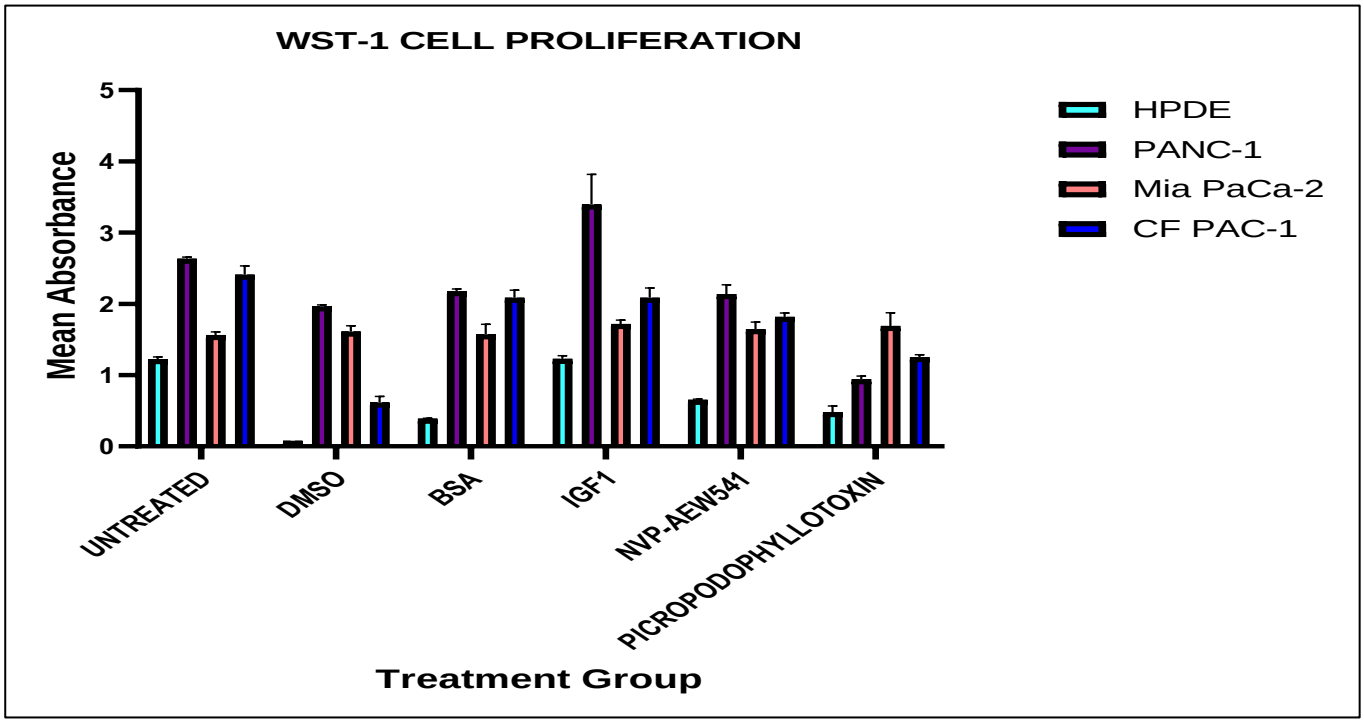

Figure 3.10: A comparison of proliferation in the untreated control, DMSO and BSA diluent controls, IGF-1, NVP-AEW541 and Picropodophyllotoxin treatment groups across all PDAC cell lines after 72 hours of treatment. Each bar represents the mean ± SEM values obtained from three independent experiments. The mean absorbance is directly proportional to proliferative capacity within the cells. Mia PaCa-2 cell proliferation remained relatively unchanged when treated with IGF-1R modulators.

3.4. Clonogenic Assays

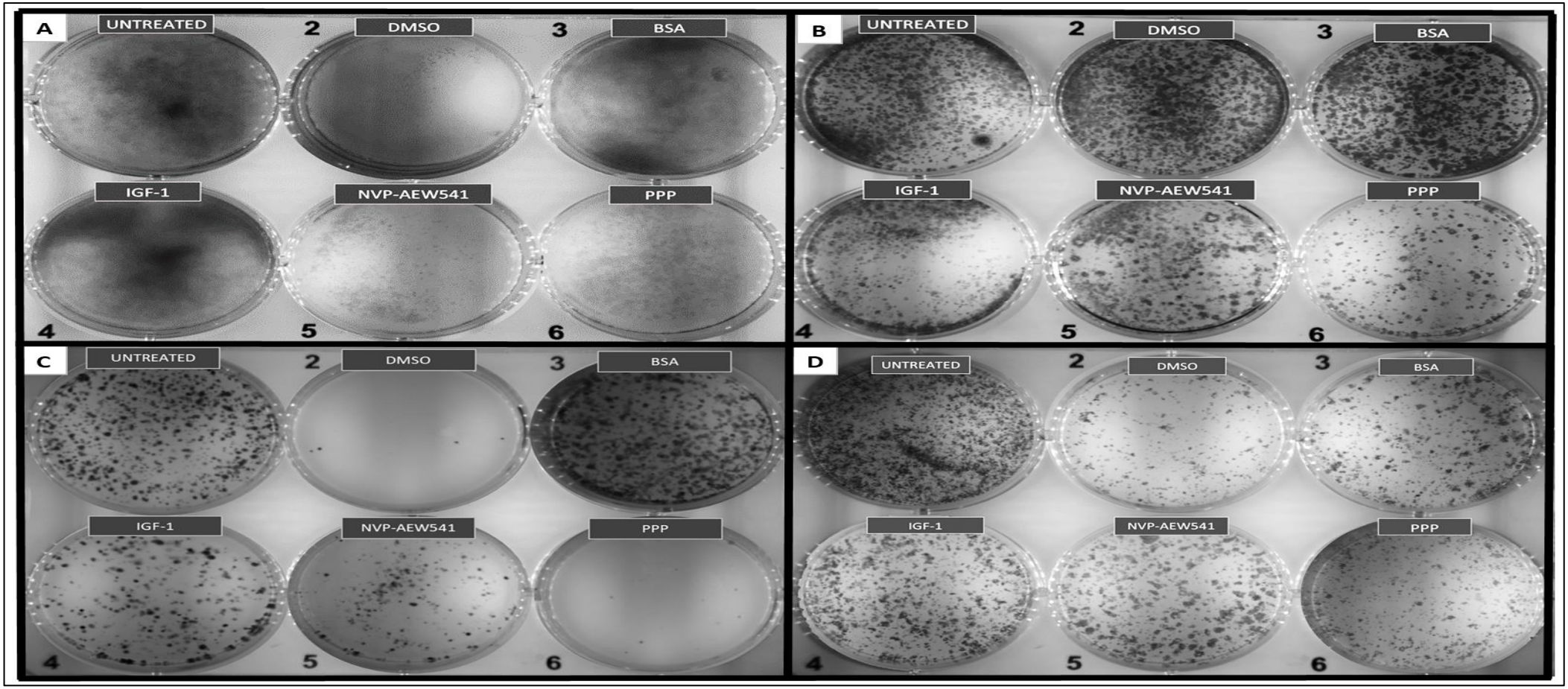

Figure 3.11: Survival and recovery of PDAC cell lines following 72 hours treatment with the DMSO and BSA diluent controls, IGF-1, NVP-AEW541 and Picropodophyllotoxin (PPP). Cells were re-plated in 6-well plates following treatment for 72 hours and were stained with 0.5 % crystal violet after 7-14 days. **a)** HPDE cells showed more confluent monolayers of cells than singular defined colonies across all treatment groups; **b)** PANC-1 cell colonies were more darkly stained due to the high density of cells in each colony, IGF-1 and PPP-treated cells had fewer colonies; **c)** Mia PaCa-2 cell colonies were more sparsely populated and had fewer colonies in DMSO and PPP treatment groups; **d)** CF PAC-1 cells showed a better recovery following the 72-hour treatment with all treatment groups, DMSO and PPP-treated cells showed significantly fewer colony formations.

Clonogenic assays were performed to show the ability of the cells to form colonies following 72-hour treatment. Cultures were exposed to DMSO and BSA diluents, and the IGF-1R modulators- IGF-1, NVP-AEW541 and Picropodophyllotoxin for 72-hours, and thereafter re-plated in 6-well plates in complete growth medium. Thus, showing cell survival by determining how well the cells 'recovered' from the IGF-1R modulation.

HPDE cells grew more confluently than the PANC-1, Mia PaCa-2, and CF PAC-1 cell lines, therefore, the lack of clearly defined colony staining of the different treatment groups within the HPDE cell line. This should be noted when considering the lower colony numbers reported in this cell line. Since the cell line was more confluent, there were fewer larger colonies that resulted from the fusion of smaller colonies. Therefore, the effectiveness of a clonogenic assay in determining the recovery and proliferation of cells depends on the characteristics of the cell line and is heavily dependent on the cell's doubling time. It was observed that HPDE cells had a doubling time of approximately 20 hours, and colony formation started 3 days after reseeding of treated cells. Cultures treated with DMSO resulted in no colonies formed. BSA, IGF-1 and NVP-AEW541 treatments had significantly lower colonies counted when compared to the untreated control ($p<0.05$). Interestingly, it was found that cells exposed to IGF-1 formed significantly fewer colonies compared to the NVP-AEW541 and Picropodophyllotoxin inhibitors. No differences were observed between NVP-AEW541 and Picropodophyllotoxin.

Crystal violet staining of PANC-1 cell colonies were darker as the colonies were more densely populated in each well. Moreover, PANC-1 cells showed the greatest variability in the number of colonies formed in cultures that were exposed to IGF-1, NVP-AEW541 and Picropodophyllotoxin (**Figure 3.12, B**). Cultures treated with DMSO and Picropodophyllotoxin had a significantly lower number of colonies counted when compared to the untreated control. Fewer colonies were also counted in IGF-1 and NVP-AEW541-treated cultures than the untreated control, albeit not significantly. No significant differences in colony counts were observed between IGF-1, NVP-AEW541 and Picropodophyllotoxin treated cultures in the PANC-1 cell line.

Colony formation in Mia PaCa-2 cells was significantly decreased in response to all treatment groups, with less than 20 colonies formed in Mia PaCa-2 cultures treated with DMSO and Picropodophyllotoxin. Interestingly, cells exposed to IGF-1 resulted in significantly fewer colonies. It is to be noted that Mia PaCa-2 cells were found to have a

doubling time of 15-20 hours, often resulting in the detachment of cells from the surface of the culture dish due to overcrowding. Therefore, it is not clear whether the reduced colony formation observed in cells exposed to IGF-1 is due to the treatment itself or overcrowding of the culture plate, resulting in detachment and subsequently fewer observable colonies formed. A comparison between the different treatment groups showed that IGF-1 treated cells formed significantly more colonies than cells exposed to NVP-AEW541 and Picropodophyllotoxin. Picropodophyllotoxin was more effective than NVP-AEW541 in reducing colony formation in Mia PaCa-2 cells.

Colony formation was significantly decreased in CF PAC-1 cells exposed to DMSO, IGF-1, NVP-AEW541 and Picropodophyllotoxin. Cultures exposed to the BSA diluent resulted in more colonies formed compared to the untreated control, albeit not significantly. Cells treated with the NVP-AEW541 inhibitor resulted in significantly more colonies formed compared to cells treated with IGF-1 and Picropodophyllotoxin. Picropodophyllotoxin significantly reduced colony formation compared to NVP-AEW541 ($p<0.05$).

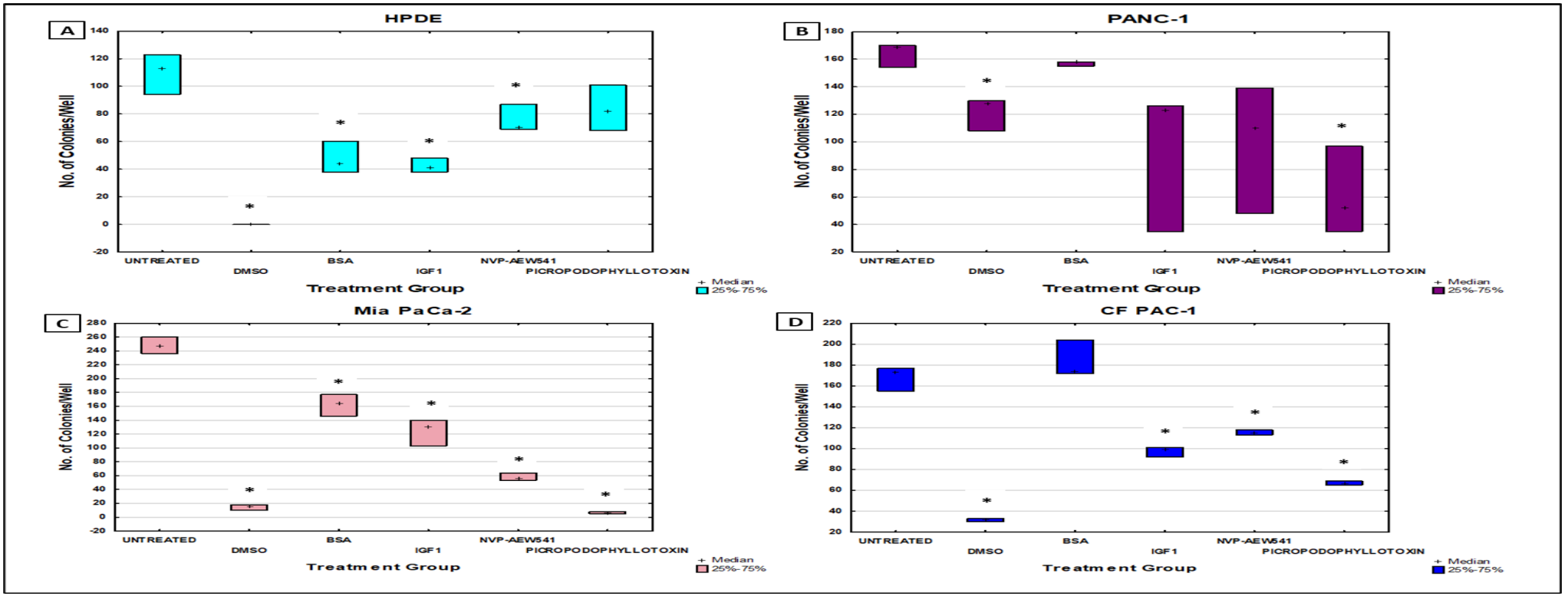

Figure 3.12: Quantification of colony formation following treatment with the DMSO and BSA diluent controls, IGF-1, NVP-AEW541 and Picropodophyllotoxin for 72 hours. Colonies were counted manually and only colonies of ~ 50 cells or more were counted. Box plots represents the mean upper and lower quartiles of the number of colonies counted from three independent experiments (n=3). A parametric t-test or non-parametric ANOVA test were performed to determine the differences between treatment groups in each cell line. **a)** There was no colony formation in DMSO-treated **HPDE cells** and colony formation was significantly reduced in all treatment groups except PPP-treated cells, with NVP-AEW541 and PPP treated cells having a significantly greater number of colonies than DMSO, BSA and IGF-1 treatment groups; **b) PANC-1** cell colonies were significantly decreased in DMSO, IGF-1, NVP-AEW541 and PPP treated cells; **c) Mia PaCa-2** colonies were significantly decreased in all treatment groups, with the least number of colonies being counted in PPP-treated cells; **d) CF PAC-1** colonies were significantly decreased in all treatment groups except BSA, and DMSO- and PPP-treated cells had the least colonies counted. Asterisks represent treatment groups that were significant compared to the untreated control. *Significance was set at $p<0.05$.*

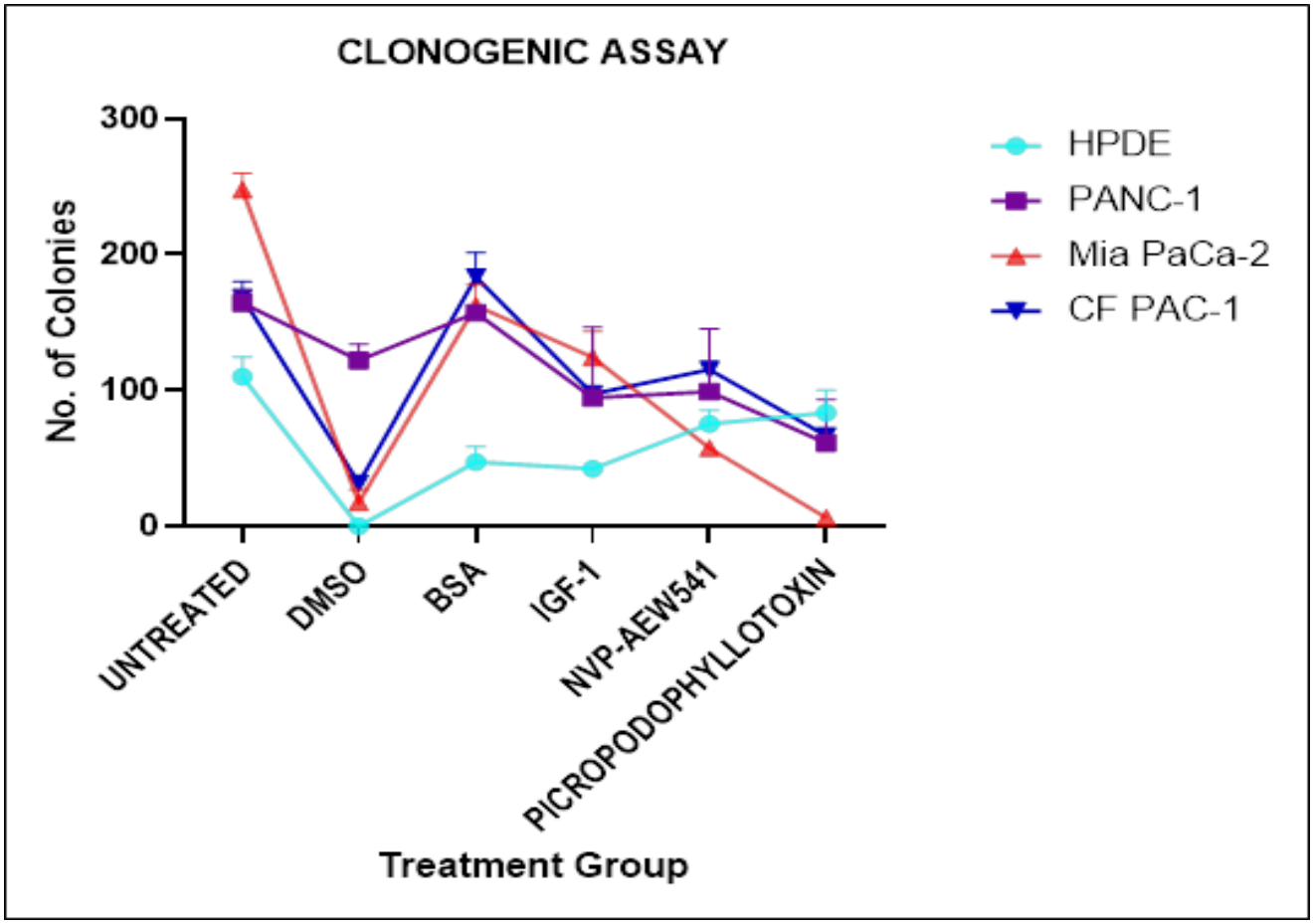

Figure 3.13: Comparison of number of colonies formed in HPDE, PANC-1, Mia PaCa-2 and CF PAC-1 cell lines. Each point represents the mean ± SEM number of colonies counted in three independent experiments. HPDE cells produced the fewest number of colonies in relation to the other PDAC cell lines.

A comparison of all cell lines showed that the HPDE cell line had relatively lower colony counts when compared to the other cell lines. Across all cell lines, the DMSO diluent control effectively prevented the formation of large colonies, while the BSA controls had significantly more colonies than DMSO-treated cells. Cells treated with NVP-AEW541 appeared to recover following treatment but did not form as many colonies as the BSA control and IGF-1 treated cells. Colony formation in the NVP-AEW541-treated cells was significantly increased compared to the Picropodophyllotoxin inhibitor. Picropodophyllotoxin treatment effectively decreased the number of colony formations in the Mia PaCa-2 and CF PAC-1 cell lines. However, the effect of Picropodophyllotoxin treatment on the Mia PaCa-2 cell line may be attributed to the effect of the DMSO diluent and not the active component of Picropodophyllotoxin itself, as seen by similar colony counts in DMSO and Picropodophyllotoxin treated cells.

3.5. Migration Assay

Throughout the duration of the 72-hour treatment period, migration of the cells was observed at 24-hour intervals by measuring the area between the wounded area. Cells were viewed under an Olympus IX35 microscope at 40 X magnification and captured images were processed using the LC Micro software. The area was measured at 0, 24, 48 and 72 hours. Migration data is shown as percentage area difference from the time of exposure to the treatment i.e., 'Hour 0'. A negative percentage area represents migration towards the closure of the scratch and a positive percentage area represents an increase in area of the wound.

3.5.1. HPDE

It was observed from the photomicrographs of HPDE cells (**Figure 3.14.**) that at Hour 24 of treatment more cells were dislodged and suspended in the growth medium of IGF-1 and NVP-AEW541 exposed cultures. This also occurred at Hour 48 of the DMSO and BSA diluents. Untreated, BSA and IGF-1 treated HPDE cells showed closure of the wound. A comparison of the percentage area difference between treatment groups (**Figure 3.18, A**) showed that the untreated control had the greatest closure of the area, IGF-1 treated cells had approximately 50 % wound closure, followed by the BSA diluent which showed less than 20 % area closure. While the percentage area difference first increased in cells that were treated with DMSO and NVP-AEW541, at the 72-hour endpoint there was no area difference when compared to the 0-hour reference point. Picropodophyllotoxin had no effect on the migration of HPDE cells throughout the 72-hour treatment period.

A comparison of the effects of the different treatment groups on the migration of cells when compared to the untreated control showed that all treatment groups decreased the migration of the HPDE cells. While IGF-1 and BSA treated cultures showed migration towards the closure of the wounded area, this was decreased compared to the untreated control. Although DMSO, NVP-AEW541 and Picropodophyllotoxin had a 0 % area difference compared to Hour 0 of treatment, these treatment groups were found to be 100 % effective in inhibiting the migration of HPDE cells compared to the untreated control, this without the disruption of cell confluency.

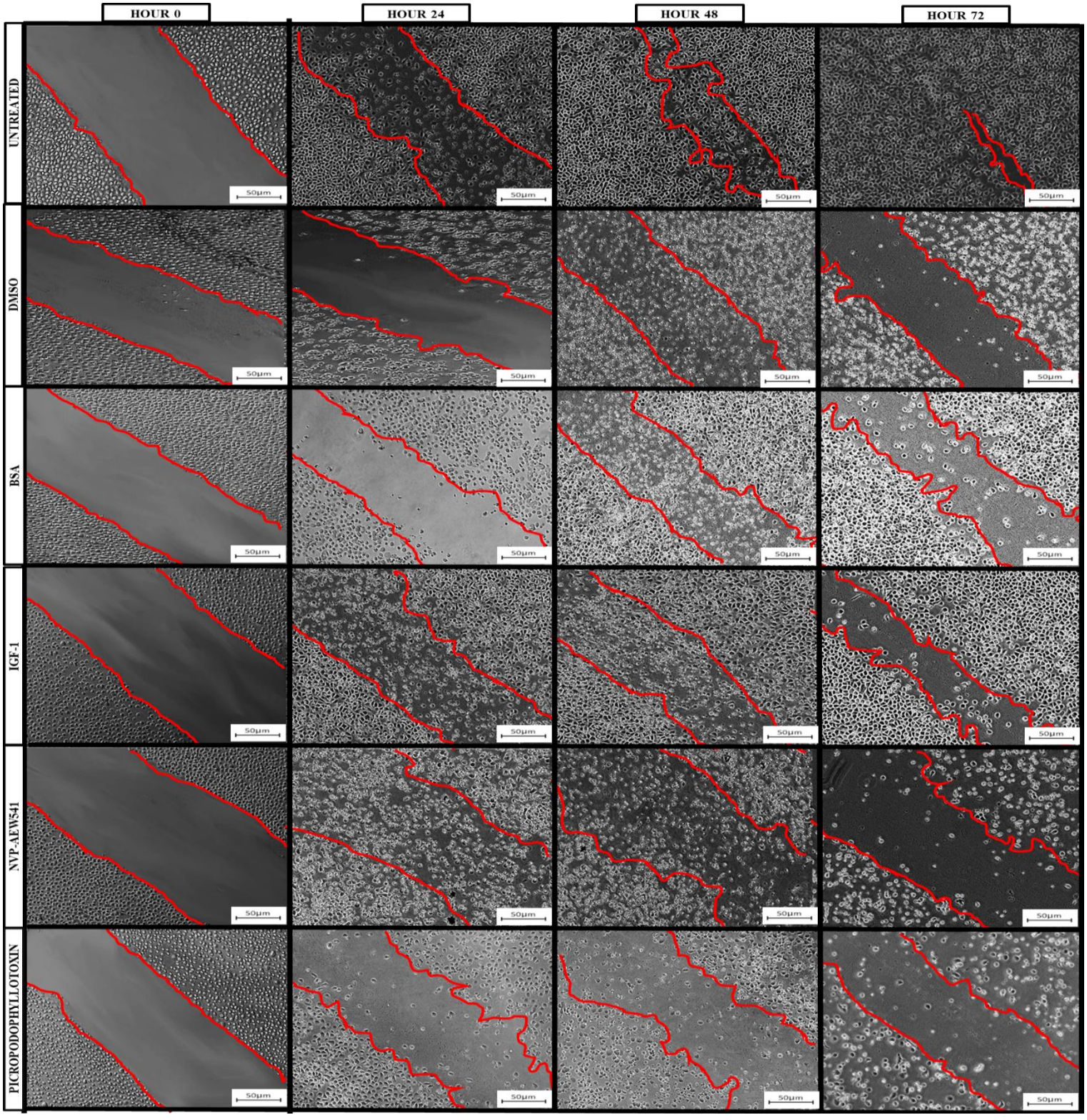

Figure 3.14: Photomicrographs of HPDE cells showing migration of the cells in the presence of effect of DMSO, BSA, IGF-1, NVP-AEW541 and Picropodophyllotoxin. The area between the scratch was measured at 0-, 24-, 48- and 72-hour time intervals. Untreated and IGF-1 treated cells showed the greatest migration towards closure of the wounded area, while the area of DMSO, NVP-AEW541 and Picropodophyllotoxin-treated cells remained relatively unchanged. Magnification 40 X and scale bar: 50 µm.

3.5.2. PANC-1

Compared to HPDE cells, fewer PANC-1 cells were found to be detached in all treatment groups. Photomicrographs of PANC-1 cells (**Figure 3.15**) and analysis of the percentage area difference (**Figure 3.18, B**) showed closure of the wounded area in cultures from the untreated control, IGF-1 and NVP-AEW541 treatment groups from 24 hours of being exposed to the treatment. At the 72-hour endpoint it was observed that cells treated with IGF-1 had the greatest area closure of approximately 60 %. Cultures treated with the BSA diluent and NVP-AEW541 had similar percentage area closure of 20-30 %. The DMSO diluent had no observable effect on the migration of PANC-1 cells compared to the initial time of exposure to DMSO. The Picropodophyllotoxin treatment appeared to decrease the migratory ability and affect the confluency of PANC-1 cells, showing an increase in area of the wound.

Compared to the untreated control, IGF-1 treated cultures increased the migration of the PANC-1 cells by 10 %. BSA and NVP-AEW541 treatment groups, while showing closure of the wounded area, decreased the migration of PANC-1 cells by approximately 30 % compared to the untreated control. Even though DMSO exposure to the cells had no observable effects on cell migration, when compared to the untreated control, DMSO treatment decreased the migration of PANC-1 cells by 60 %.

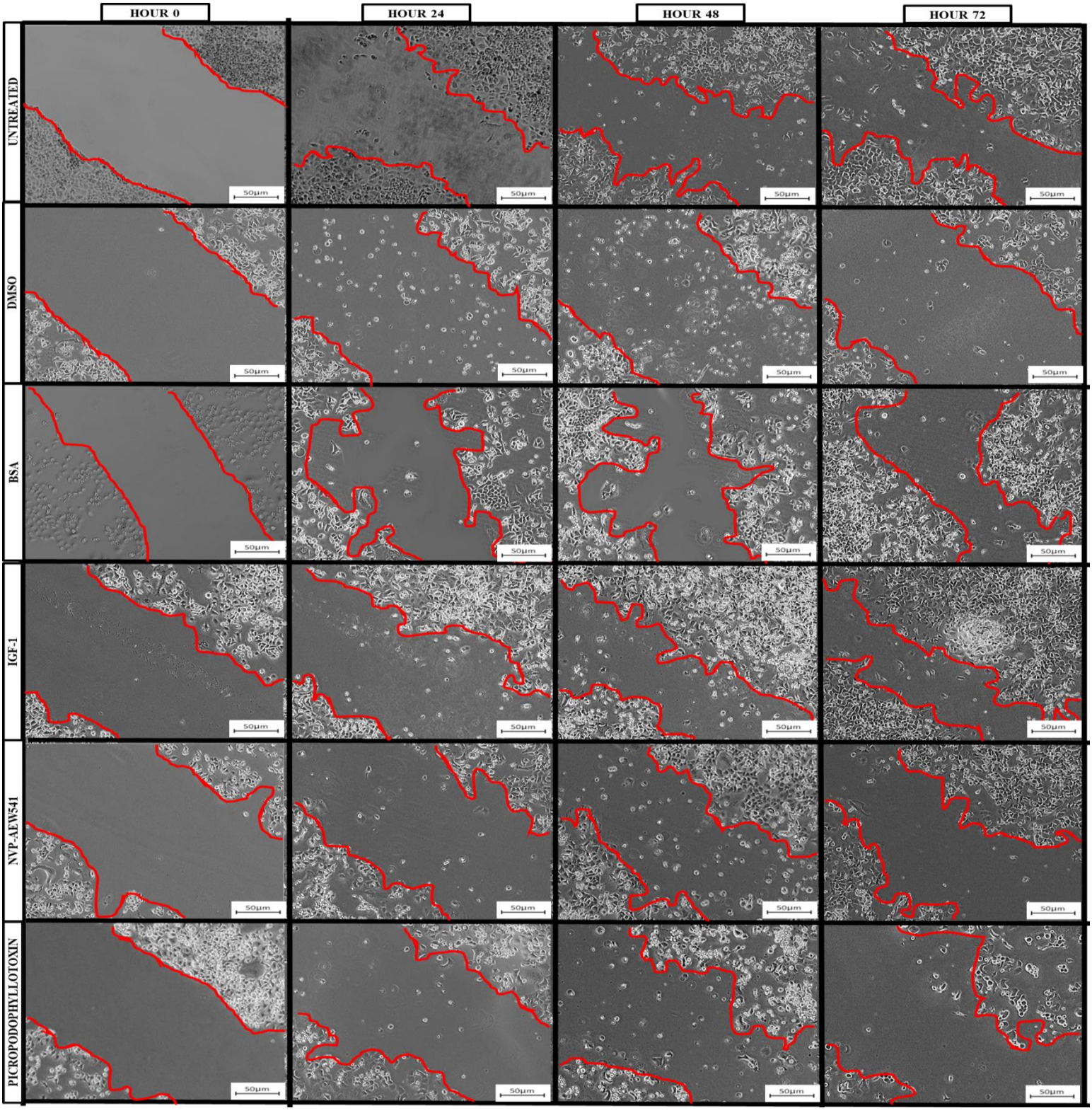

Figure 3.15: Photomicrographs of PANC-1 cells showing migration of the cells in the presence of DMSO, BSA, IGF-1, NVP-AEW541 and Picropodophyllotoxin. The area between the scratch was measured at 0-, 24-, 48- and 72-hour time intervals. The untreated control, BSA diluent and IGF-1 treated cells showed the largest closure of the wounded area at hour 72. The area of the wound increased in Picropodophyllotoxin treated cells. Magnification 40 X and scale bar: 50 µm.

3.5.3. Mia PaCa-2

The photomicrographs of Mia PaCa-2 cells (**Figure 3.16**) showed no observable changes to the wounded area for the untreated control, DMSO and BSA diluent controls, and IGF-1 treatment groups throughout the 72 hours. Mia PaCa-2 cultures that were exposed to NVP-AEW541 showed migration of the cells through wound closure from 48 hours of treatment. Picropodophyllotoxin treated cells showed further widening of the area from Hour 48 of treatment, with all the cells being completely dislodged at 72 hours. Percentage area difference analysis (**Figure 3.18, C**) showed that BSA, IGF-1 and NVP-AEW541 treatment groups appeared to have no major effects on the migration of the Mia PaCa-2 cells compared to the Hour 0 reference time point. The percentage area difference at 72 hours for the BSA, IGF-1 and NVP-AEW541 treatment groups were similar to untreated Mia PaCa-2 cells, with less than 20 % of the area being closed. There was no change in area in DMSO treated cells. Picropodophyllotoxin-treated cultures showed an area increase of 100 % in the initial scratch with the detachment of cells. It was found that BSA, IGF-1 and NVP-AEW541 treatment had no effect on the migration of Mia PaCa-2 cells compared to the untreated control, with DMSO slightly decreasing the migration of the cells compared to untreated cells.

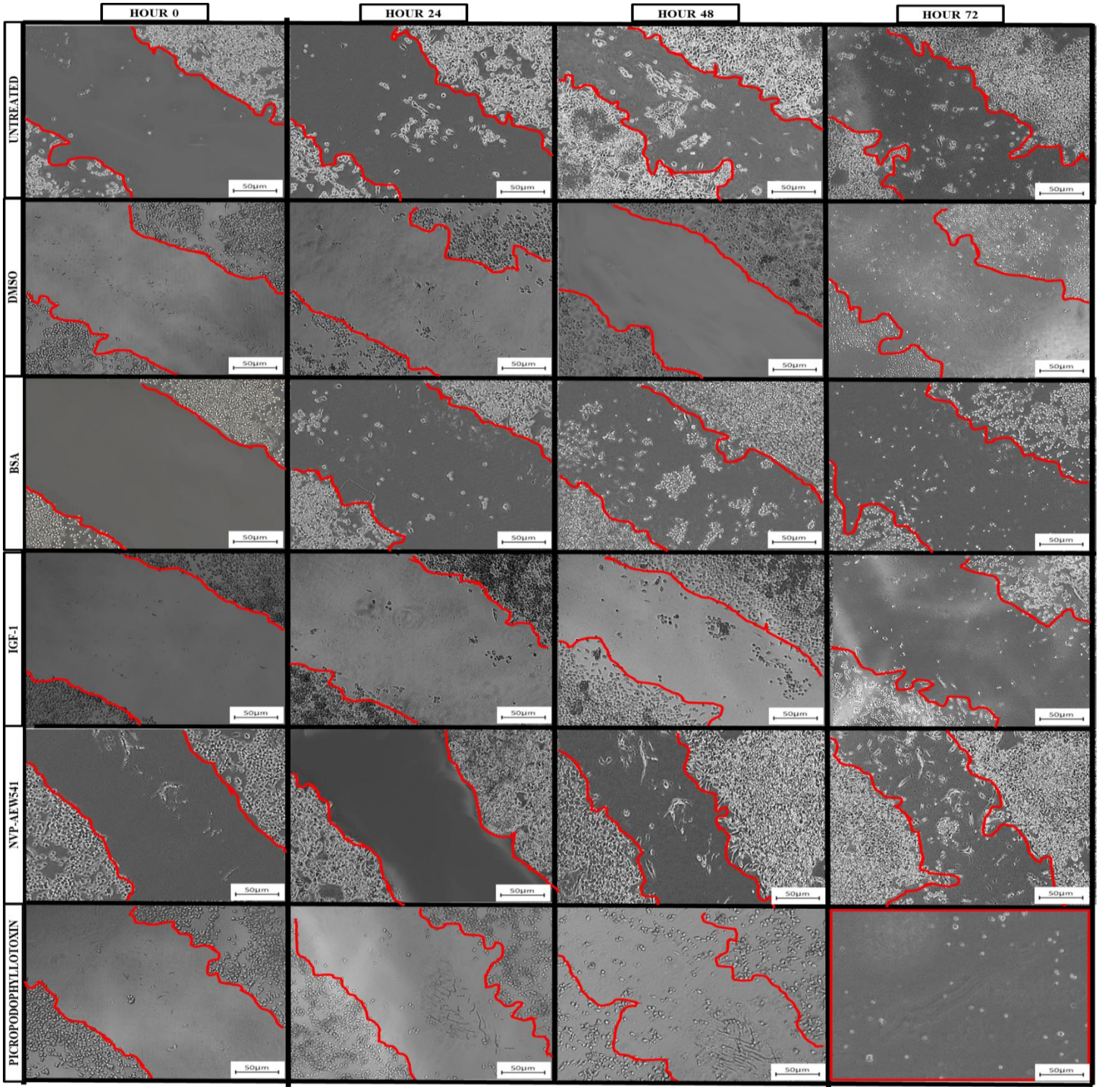

Figure 3.16: Photomicrographs of Mia PaCa-2 cells showing migration of the cells in the presence of DMSO, BSA, IGF-1, NVP-AEW541 and Picropodophyllotoxin. The area between the scratch was measured at 0-, 24-, 48- and 72-hour time intervals. The Mia PaCa-2 cell line showed the least migratory response to DMSO, BSA and IGF-1 exposure. NVP-AEW541 treatment promoted migration of cells towards closure of the wounded area. Picropodophyllotoxin had the greatest effect on the cells at 72 hours, with complete detachment of the cells in the area that was imaged. Magnification 40 X and scale bar: 50 µm.

3.5.4. CF PAC-1

Untreated CF PAC-1 cells, BSA and IGF-1 treated cells showed a uniform pattern of cellular migration in the closure of the wounded area (**Figure 3.17**). At 48 hours of exposure to DMSO, there was a lot of detached cells in the growth medium.

It was observed that IGF-1 and BSA treatments induced migration in the CF PAC-1 cells, as shown by the 50-60 % decrease of the wounded area (**Figure 3.18, C**). Moreover, these treated CF PAC-1 cultures showed greater migration than the untreated control. NVP-AEW541 treatment, while showing wound closure, showed decreased migration of the CF PAC-1 cells compared to the untreated control. DMSO treated cells showed that these cultures initially migrated towards closure of the wounded within the first 24 hours, however at 48 and 72 hours, the area of the wound increased. Picropodophyllotoxin appeared to have no observable effects on the migration of the CF PAC-1 cells throughout the 72-hour treatment period. However, when compared to the untreated control, the Picropodophyllotoxin treatment reduced the migratory ability of the CF PAC-1 cells by over 60 %.

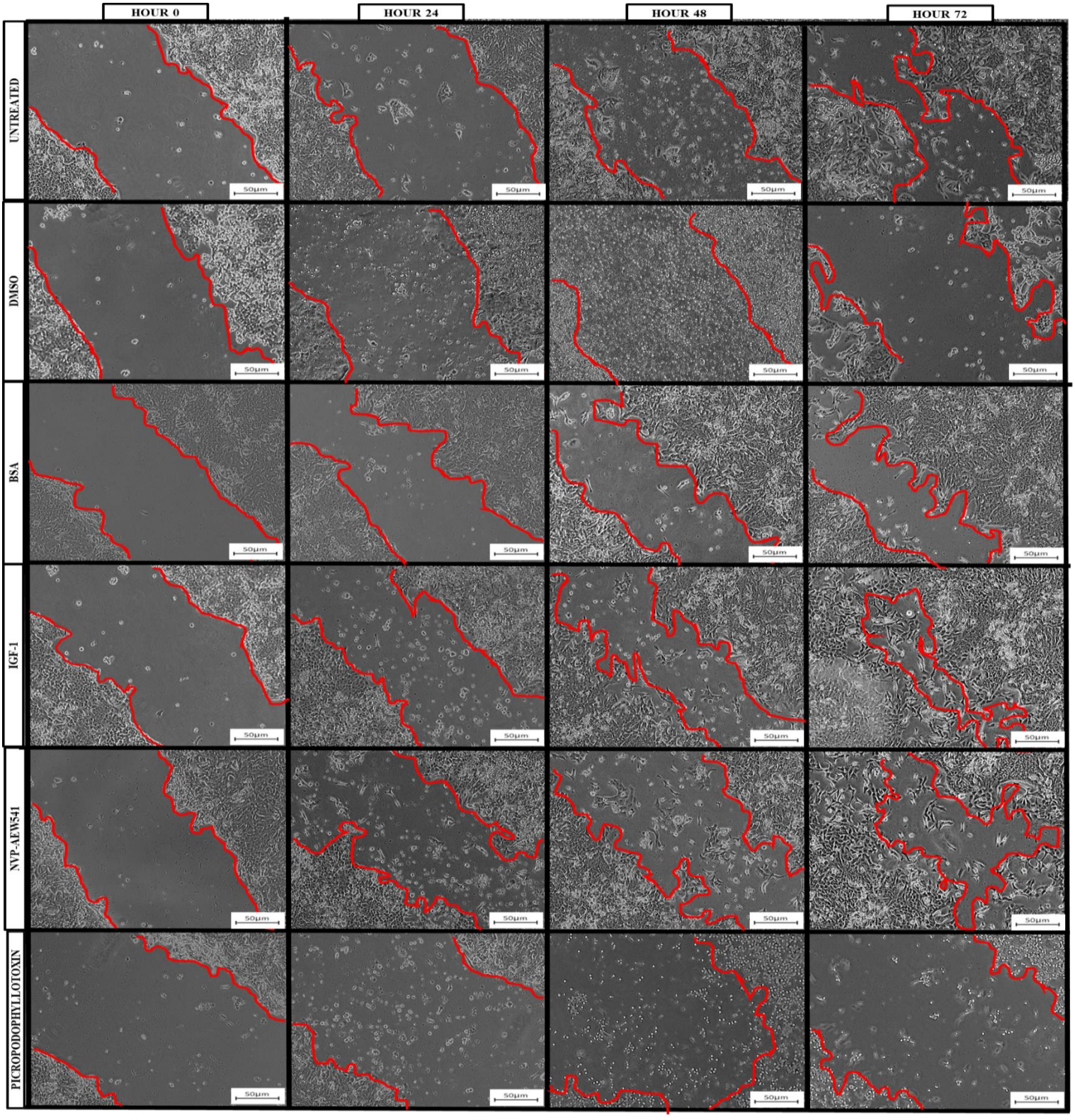

Figure 3.17: Photomicrographs of CF PAC-1 cells showing migration of the cells in the presence of DMSO, BSA, IGF-1, NVP-AEW541 and Picropodophyllotoxin. The area between the scratch was measured at 0-, 24-, 48- and 72-hour time intervals. Untreated, BSA, IGF-1 and NVP-AEW541- treated cells showed the greatest migration towards closure of the scratch. Magnification 40 X and scale bar: 50 µm.

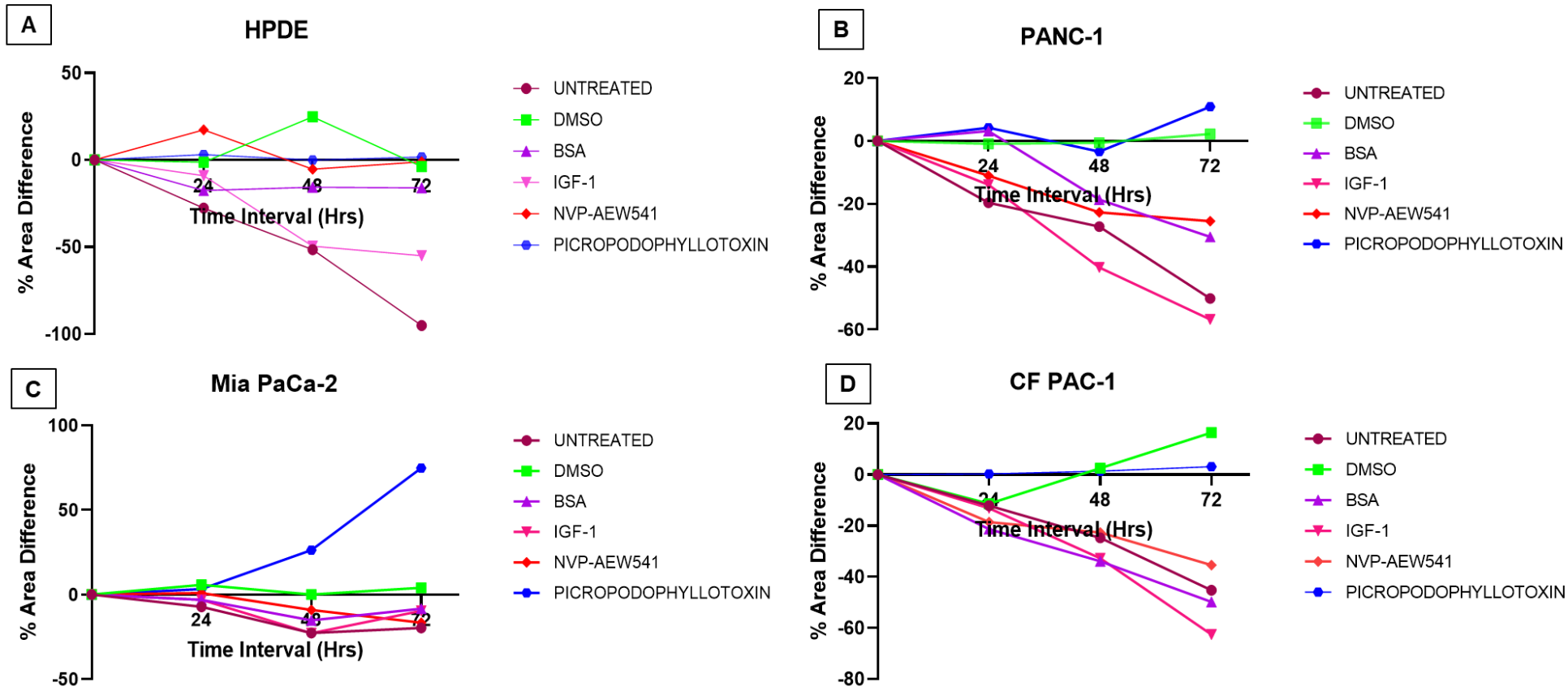

Figure 3.18: Normalized percentage area difference for a) HPDE, b) PANC-1, Mia PaCa-2 and CF PAC-1 cells. Each point represents the percentage area difference for the DMSO, BSA, IGF-1, NVP-AEW and Picropodophyllotoxin treatments at 0-, 24- 48- and 72-hour time intervals. The percentage is expressed as the area difference in the field of view at each time interval against the area difference at 0-hr time interval. n=3. The area in each field of view was measured three times to eliminate intra-observer error. Picropodophyllotoxin and DMSO treatments were found to be the most effective in inhibiting the migration of all PDAC cells. NVP-AEW541 treatment resulted in the closure of the wounded area in the PANC-1, Mia PaCa-2 and CF PAC-1 cell lines, but showed less migration than untreated controls of each cell line.

3.6. Quantitative Real Time PCR

Following treatment of the cells with the IGF-1R modulators and respective diluents, the mRNA expression levels of several genes involved in proliferation, survival, migration, and apoptosis was measured using qRT-PCR. The levels of expression were expressed relative to the gene expression of the untreated control in each cell line. A decrease in gene expression is shown as negative and an increased gene expression is represented by a positive value. Statistical analysis was performed to determine the differences between mRNA expression levels between treatment groups within the PDAC cell lines (**Appendix C, 9.4**).

3.6.1. HPDE

IGF-1R RNA expression levels were significantly decreased in HPDE cells treated with the DMSO and BSA diluents, IGF-1 and NVP-AEW541 modulators ($p<0.05$) (**Figure 3.19, A**). Expression of IGF-1R in HPDE cells exposed to Picropodophyllotoxin was not detected. DMSO significantly decreased IGF-1R mRNA expression levels compared to all other treatment groups ($p<0.05$) (**Appendix C, 9.4.1.3**). When compared to IGF-1 treatments, it was found that NVP-AEW541 treatment decreased IGF-1R mRNA, however this was not significant ($p=0.091$).

No expression of PI3KCA mRNA was detected in HPDE cells treated with the DMSO diluent. DMSO-treated HPDE cells showed a significantly downregulated expression of the AKT3, FOXO1A and MYC genes ($p<0.05$), all of which are involved in proliferation and cell survival (**Figure 3.19, B**). Expression levels of MYC mRNA was found to be lower than that of AKT3 and FOXO1A. Moreover, it was detected that HPDE cells exposed to DMSO had significantly decreased mRNA expression of the AKT3, FOXO1A and MYC genes compared to all other treatment groups within the cell line. HPDE cells treated with the BSA diluent showed significant downregulation of AKT3 and MYC mRNA expression ($p<0.05$). Cells that were exposed to IGF-1, NVP-AEW541 and Picropodophyllotoxin showed significantly upregulated expression of AKT3 and FOX01A genes ($p<0.05$), while the PI3KCA expression levels was significantly downregulated in the Picropodophyllotoxin treatment group ($p<0.05$). Moreover, PI3KCA mRNA expression was significantly decreased in Picropodophyllotoxin treated cells compared to other treatment groups ($p<0.05$).

The mRNA expression levels of the genes involve in migration, Vimentin (VIM) and Snail (SNAI1) are shown in **Figure 3.19, C**. VIM mRNA expression levels were decreased in DMSO, BSA and NVP-AEW541 treatment groups ($p<0.05$). No expression of SNAI1 was

detected in HPDE cells treated with DMSO and Picropodophyllotoxin. An increase in SNAI1 expression was detected in BSA and IGF-1 exposed HPDE cells ($p<0.05$).

The pro-apoptotic BAX gene expression was downregulated in both the DMSO and BSA diluents ($p<0.05$) (**Figure 3.19, D**). The anti-apoptotic BCL2 gene expression was upregulated in DMSO, IGF-1 and NVP-AEW541-treated HPDE cells ($p<0.05$). None of the apoptotic genes were detected in HPDE cells treated with Picropodophyllotoxin.

3.6.2. PANC-1

IGF-1R gene expression was upregulated in PANC-1 cells treated with all treatment groups ($p<0.05$) (**Figure 3.20, A**). The expression of IGF-1R in cells exposed to IGF-1 was significantly increased compared to BSA, NVP-AEW541 and Picropodophyllotoxin treatments ($p<0.05$). Similar expression levels of IGF-1R were detected in BSA, NVP-AEW541 and Picropodophyllotoxin exposed PANC-1 cells ($p<0.05$).

Overexpression of PI3KCA, AKT3, FOX01A and MYC was detected in PANC-1 cells that were treated with DMSO, IGF-1 and Picropodophyllotoxin ($p<0.05$) (**Figure 3.20, B**). These genes that are involved in proliferation and survival were downregulated in the BSA and NVP-AEW541 treatment groups. IGF-1 treated cells showed the highest upregulation of AKT3 compared to other treatment groups ($p<0.05$). It was observed that expression of the genes involved in proliferation and survival were all significantly upregulated in Picropodophyllotoxin treated PANC-1 cells compared to cells treated with the NVP-AEW541 inhibitor ($p<0.05$).

The PANC-1 cells that were treated with DMSO and Picropodophyllotoxin had overexpression of both, SNAI1 and VIM genes (**Figure 3.20, C**). These genes were both decreased in cells treated with BSA and NVP-AEW541, with SNAI1 downregulated expression being significant ($p<0.05$). IGF-1 treated cells showed downregulation of SNAI1 ($p>0.05$) and overexpression of VIM mRNA ($p<0.05$). Both, SNAI1 and VIM expression was significantly increased in cells treated with Picropodophyllotoxin compared to NVP-AEW541 ($p<0.05$).

An assessment of the expression levels of pro- and anti-apoptotic genes is shown in **Figure 3.20, D**. The anti-apoptotic BCL2 gene was upregulated in all treatment groups in the PANC1 cell line, with BAX, the pro-apoptotic gene being significantly downregulated in DMSO-treated cells and upregulated in the IGF-1 ($p<0.05$) and Picropodophyllotoxin ($p>0.05$) treatment groups. A comparison on the expression levels of BAX and BCL2

between the NVP-AEW541 and Picropodophyllotoxin inhibitors were not significant ($p>0.05$).

3.6.3. Mia PaCa-2

Figure 3.21, A shows IGF-1R mRNA expression levels of Mia PaCa-2 cells. IGF-1R expression was downregulated in all treatment groups ($p<0.05$), apart from cells treated with the NVP-AEW541, where downregulated expression of the gene was detected ($p<0.05$). Similar IGF-1R expression levels were detected in cells exposed to IGF-1 and its BSA diluent ($p<0.05$).

Expression levels of genes that are involved in cell proliferation and survival were minimally affected in the Mia PaCa-2 cell line (**Figure 3.21, B**). PI3KCA expression levels were significantly upregulated in BSA treated cells and downregulated in cells exposed to IGF-1 and NVP-AEW541 ($p<0.05$). AKT3 mRNA expression levels were significantly increased in cells treated with DMSO ($p<0.05$) and downregulated in NVP-AEW541 ($p<0.05$). FOXO1A expression was upregulated in cells that were exposed to BSA, IGF-1 and Picropodophyllotoxin ($p<0.05$), with expression being downregulated in NVP-AEW541 treated Mia PaCa-2 cells ($p<0.05$). A significant downregulation of MYC was detected in BSA and IGF-1 treated cells ($p<0.05$).

Mia PaCa-2 cells that were treated with DMSO, BSA, IGF-1 and Picropodophyllotoxin showed overexpression of the SNAI1 gene ($p<0.05$), while SNAI1 gene expression was downregulated in cells that were treated with NVP-AEW541 ($p<0.05$) (**Figure 3.21, C)**. The VIM gene was downregulated in DMSO, BSA, IGF-1 and Picropodophyllotoxin treated cells, with a significant decreased in expression in cells exposed to IGF-1.

Mia PaCa-2 cells that were treated with the DMSO diluent had minimal changes in BAX and BCL2 apoptotic gene expression levels (**Figure 3.21, D**). The pro-apoptotic gene, BAX expression levels were significantly upregulated in cells exposed to BSA ($p<0.05$). Whereas both BAX and BCL2 genes were downregulated in cells treated with IGF-1, NVP-AEW541 and Picropodophyllotoxin.

3.6.4. CF PAC-1

Expression levels of IGF-1R was significantly downregulated in all treatment groups in the CF PAC-1 cell line ($p<0.05$) (**Figure 3.22, A**). Cells exposed to IGF-1 had significantly downregulated IGF-1R expression levels compared to DMSO, BSA, NVP-AEW541 and Picropodophyllotoxin. BSA and NVP-AEW541 had similar expression levels of IGF-1R.

CF PAC-1 cells that were exposed to DMSO showed a significant upregulation of all genes involved in cell proliferation and survival (**Figure 3.22, B**). Cells that were treated with the BSA diluent had increased levels of PI3KCA and FOXO1A mRNA expression levels ($p<0.05$). Expression of MYC was significantly downregulated in BSA treated cells ($p<0.05$). No FOXO1A expression levels were detected in CF PAC-1 cells that were exposed to IGF-1. However, there was an increased expression levels of PI3KCA, AKT3 and MYC in IGF-1 treated cells. All 4 genes were upregulated in cells that were treated with NVP-AEW541, however MYC upregulation was not significant. FOXO1A was not detected in cells that were exposed to Picropodophyllotoxin. However, expression of PI3KCA, AKT and MYC were all downregulated in this treatment group.

SNAI1 gene expression was not detected in any treatment group of the CF PAC-1 cell line (**Figure 3.22, C**), including untreated cells. No expression of VIM gene was detected in cells treated with Picropodophyllotoxin, but the gene expression was overexpressed in DMSO, BSA, IGF-1 and NVP-AEW541 treatment groups.

The pro-apoptotic, BAX gene was overexpressed in DMSO, BSA and IGF-1 treated CF PAC-1 cells ($p<0.05$) and downregulated in cells treated with the NVP-AEW541 ($p>0.05$) and Picropodophyllotoxin ($p<0.05$) inhibitors. BCL2 gene expression was upregulated in the DMSO, BSA and NVP-AEW541 treatments, and decreased in Picropodophyllotoxin-treated cells. No BCL2 gene expression was detected in CF PAC-1 cells treated with IGF-1. While both BAX and BCL2 was upregulated in cells treated with the BSA diluent, equal levels of both genes was observed.

3..5. <u>BAX/BCL2</u>

The relative expression of BAX/BCL2 was calculated to determine whether a pro-apoptotic or anti-apoptotic environment was favoured across the treatment groups.

Table 3.3.: The relative expression of BAX/BCL2

Cell Line	Treatment Group	BAX/BCL2 expression (Log10)	
HPDE	DMSO	-4,91321*	Pro-apoptotic
	BSA	-13,6442*	Pro-apoptotic
	IGF-1	0,235372	Pro-apoptotic
	NVP-AEW541	0,105394	Pro-apoptotic
	Picropodophyllotoxin	n/a	n/a
PANC-1	DMSO	-0,2355*	Pro-apoptotic
	BSA	-0,14573	Pro-apoptotic
	IGF-1	0,249372*	Pro-apoptotic
	NVP-AEW541	0,150558	Pro-apoptotic
	Picropodophyllotoxin	1,833259	Anti-apoptotic
Mia PaCa-2	DMSO	-0,66938*	Neutral
	BSA	3,364896*	Anti-apoptotic
	IGF-1	0,877732*	Neutral
	NVP-AEW541	1,07659*	Neutral
	Picropodophyllotoxin	0,300323*	Anti-apoptotic
CF PAC-1	DMSO	0,432972*	Pro-apoptotic
	BSA	0,939811*	Pro-apoptotic
	IGF-1	n/a	Anti-apoptotic
	NVP-AEW541	-0,68627	Pro-apoptotic
	Picropodophyllotoxin	6,440193*	Pro-apoptotic

Asterisks indicate ratios that are significantly different from the untreated control for the respective cell line. n/a: Data not available due to both or either of the genes not being detected in the sample. The data was determined as being either pro-apoptotic or anti-apoptotic. Neutral refers to equal gene expression of BAX and BCL2, even though gene expression was increased or decreased. n=3.

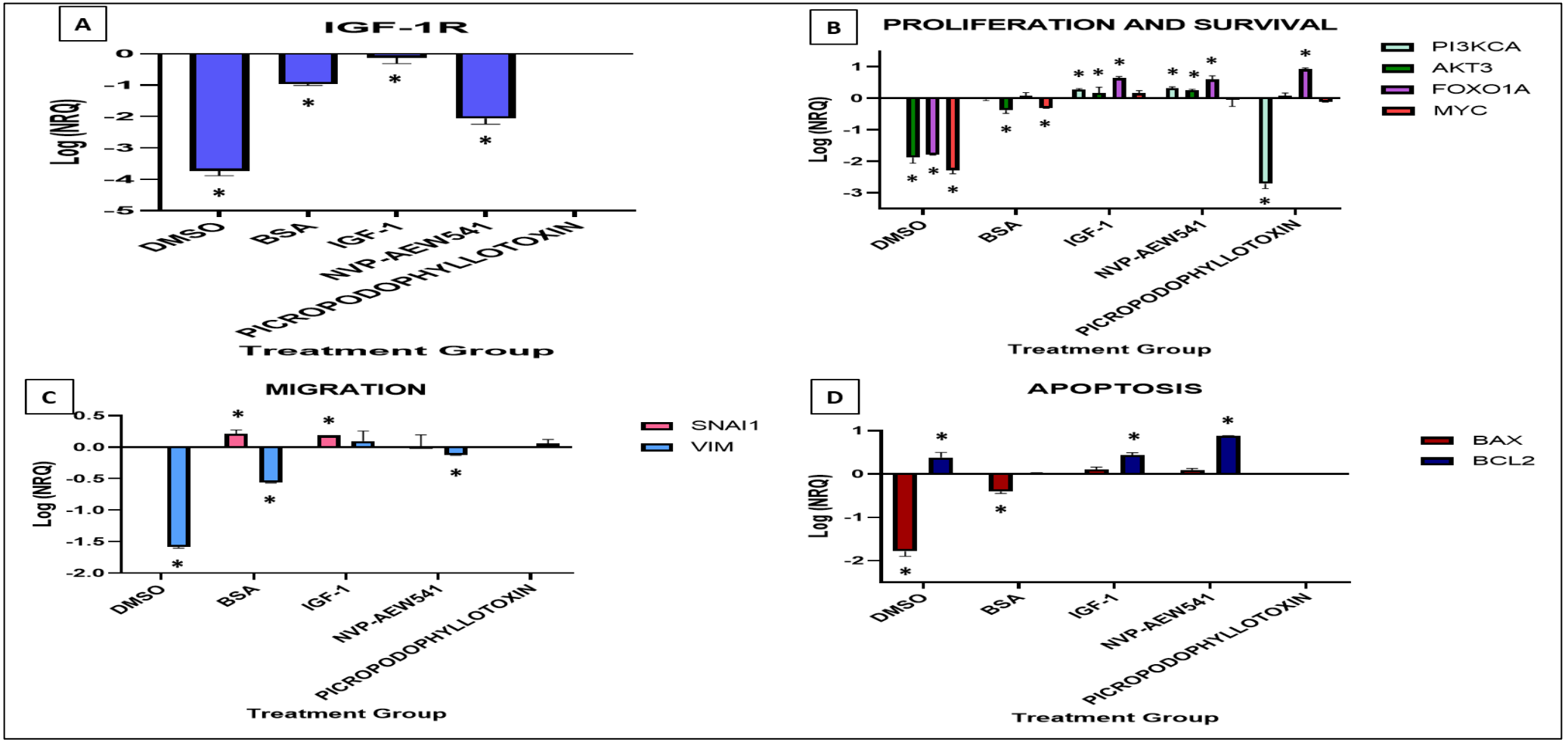

Figure 3.19: Relative gene expression of genes involved in proliferation, survival, migration, and apoptosis in the HPDE cell line. Data is presented as gene expression levels relative to untreated HPDE cells, ± SD values obtained from three independent experiments. IGF-1R gene expression was decreased in DMSO, BSA and NVP-AEW541 treated cells. Genes involved in survival and proliferation were decreased in the DMSO and BSA diluents, and increased in IGF-1, NVP-AEW541 and Picropodophyllotoxin treated HPDE cells. VIM expression was downregulated, and SNAI1 gene expression was upregulated in all treatment groups. The anti-apoptotic gene BCL-2 was upregulated in all treatments. A students t-test was performed to determine the differences between mRNA expression levels compared to the control. Asterisks represents treatments that are significantly different from the untreated control. $P<0.05$.

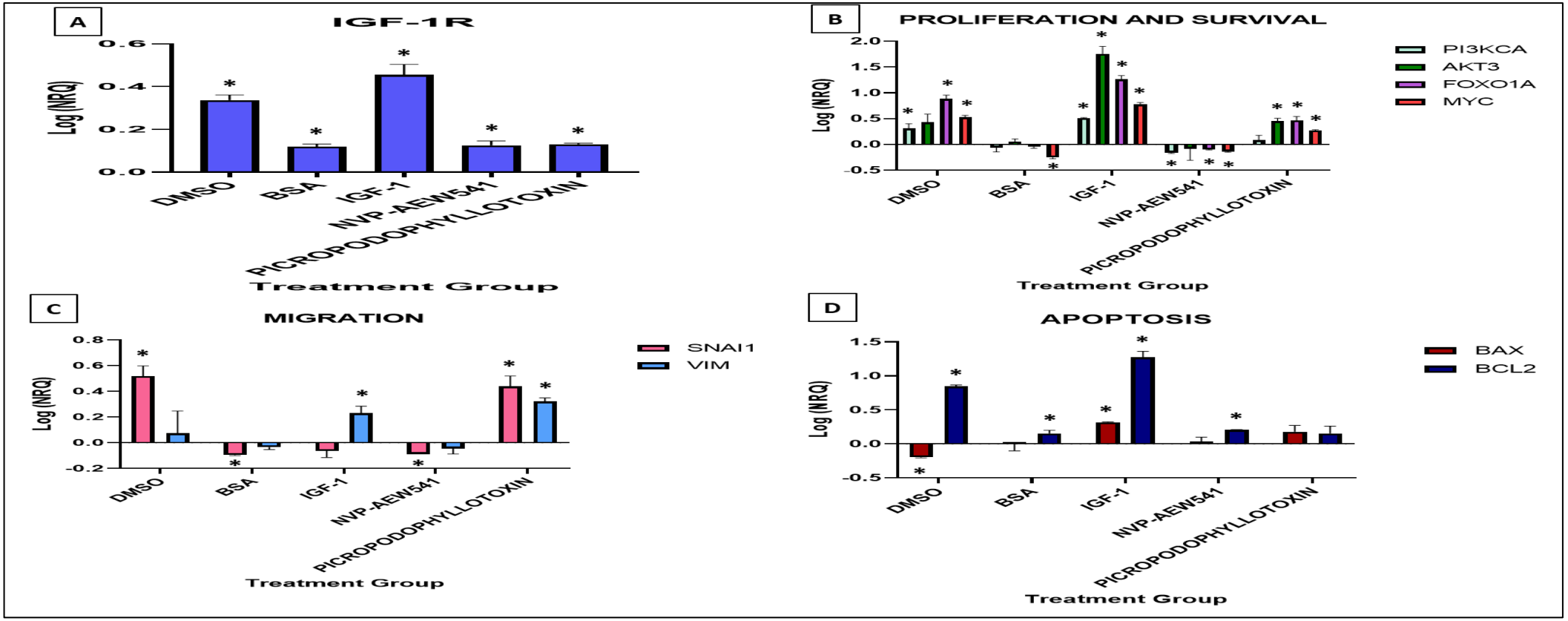

Figure 3.20: Relative gene expression of genes involved in proliferation, survival, migration, and apoptosis in PANC-1 cells. Data is presented as gene expression levels relative to untreated PANC-1 cells, ± SD values obtained from three independent experiments. IGF-1R gene expression was upregulated in DMSO, IGF-1 and Picropodophyllotoxin treatments. Correspondingly, the proliferation and survival genes, as well as the migration gene VIM, were also upregulated in these treatment groups. SNAI1 gene expression was upregulated in DMSO and Picropodophyllotoxin treatments. BCL2 was upregulated in all treatment groups, with the greatest upregulation occurring in DMSO and IGF-1 treated cells. A students t-test was performed to determine the differences between mRNA expression levels compared to the control. Asterisks represents treatments that are significantly different from the untreated control. $P<0.05$.

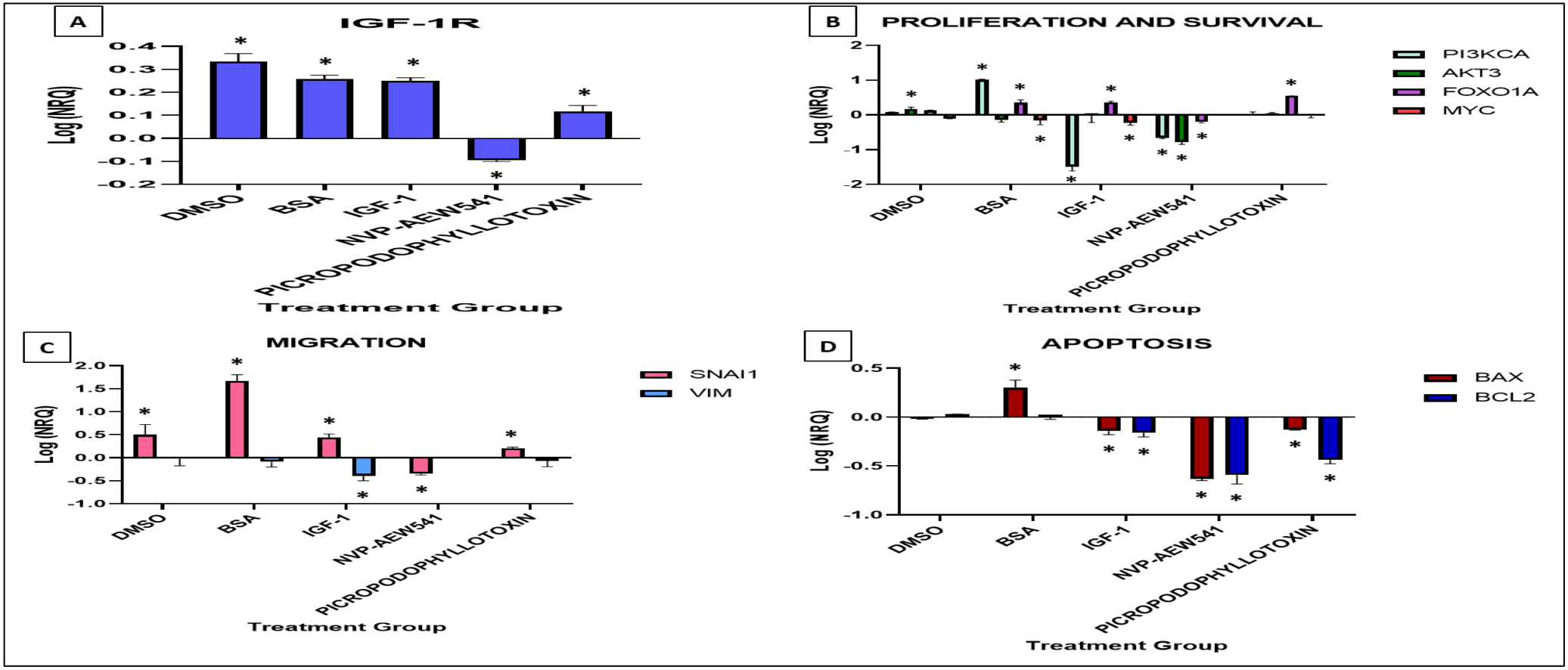

Figure 3.21: Relative gene expression of genes involved in proliferation, survival, migration, and apoptosis in Mia PaCa-2 cells. Gene expression was measured following 72-hour treatment with DMSO, BSA IGF-1, NVP-AEW541 and Picropodophyllotoxin. Data is presented as gene expression levels relative to untreated Mia PaCa-2 cells, ± SD values obtained from three independent experiments. IGF-1R gene expression was downregulated in DMSO, BSA, IGF-1 and Picropodophyllotoxin treatments. The FOXO1A proliferation and survival gene was upregulated in all treatment groups and PI3KCA and AKT3 gene expression was significantly downregulated in NVP-AEW541 treated cells. SNAI1 was upregulated in DMSO, BSA, IGF-1 and Picropodophyllotoxin treatments, while VIM was downregulated in these treatment groups. BAX was significantly upregulated in BSA-treated cells, and BAX and BCL2 genes were downregulated in IGF-1, NVP-AEW541 and Picropodophyllotoxin treated Mia PaCa-2 cells. A students t-test was performed to determine the differences between mRNA expression levels compared to the control. Asterisks represents treatments that are significantly different from the untreated control. $P<0.05$.

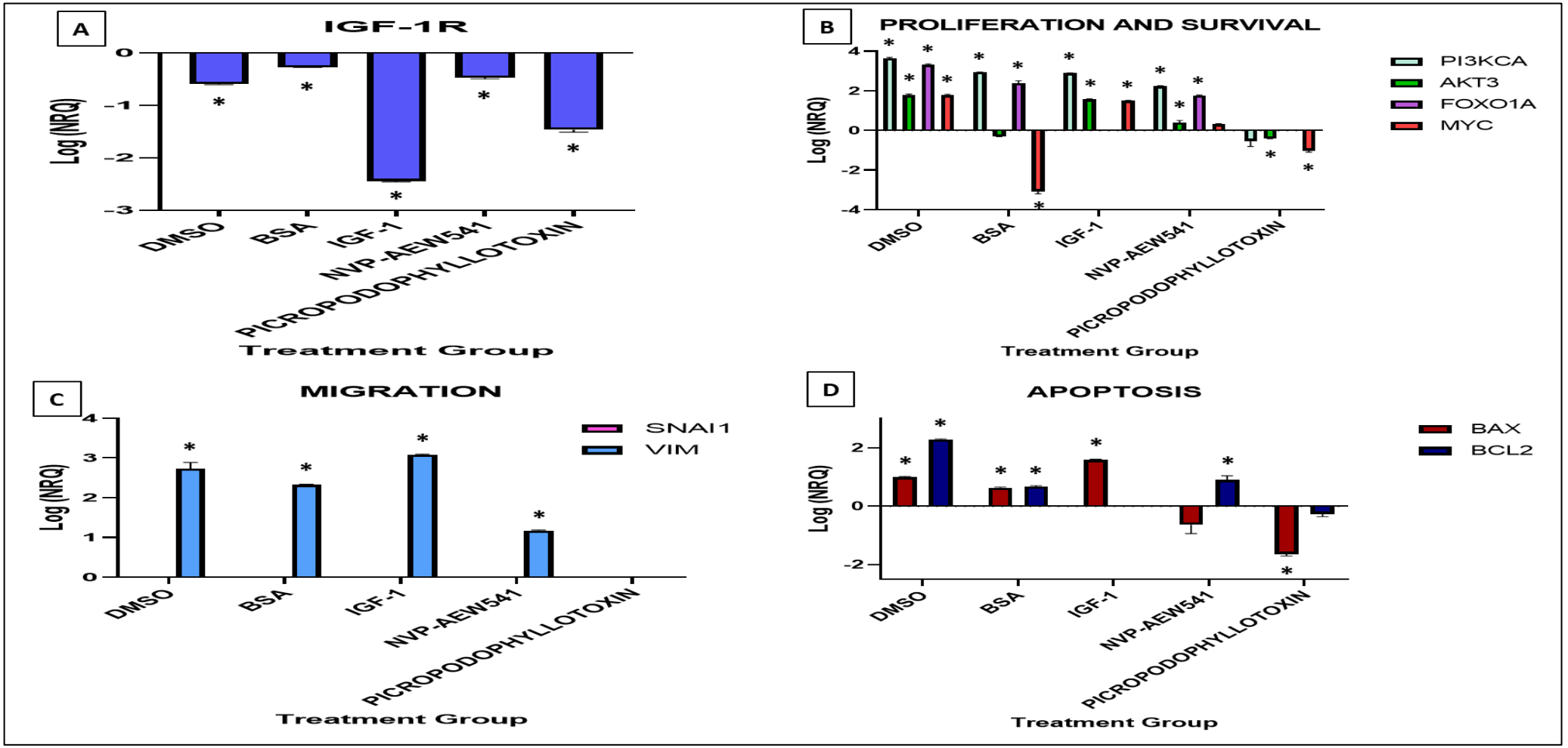

Figure 3.22: Relative gene expression of genes involved in proliferation, survival, migration, and apoptosis in the CF PAC-1 cells. Data is presented as gene expression levels relative to untreated CF PAC-1 cells, ± SD values obtained from three independent experiments. IGF-1R gene expression was upregulated in DMSO, BSA, IGF-1, NVP-AEW541 and Picropodophyllotoxin treatments. Proliferation and survival gene expression was upregulated in these treatments. VIM gene expression was upregulated in DMSO, BSA, IGF-1 and NVP-AEW541 treatments, SNAI1 expression was not detected. BCL2 expression was upregulated in DMSO, BSA and NVP-AEW541 treated cells. A students t-test was performed to determine the differences between mRNA expression levels compared to the control. Asterisks represents treatments that are significantly different from the untreated control. $P<0.05$.

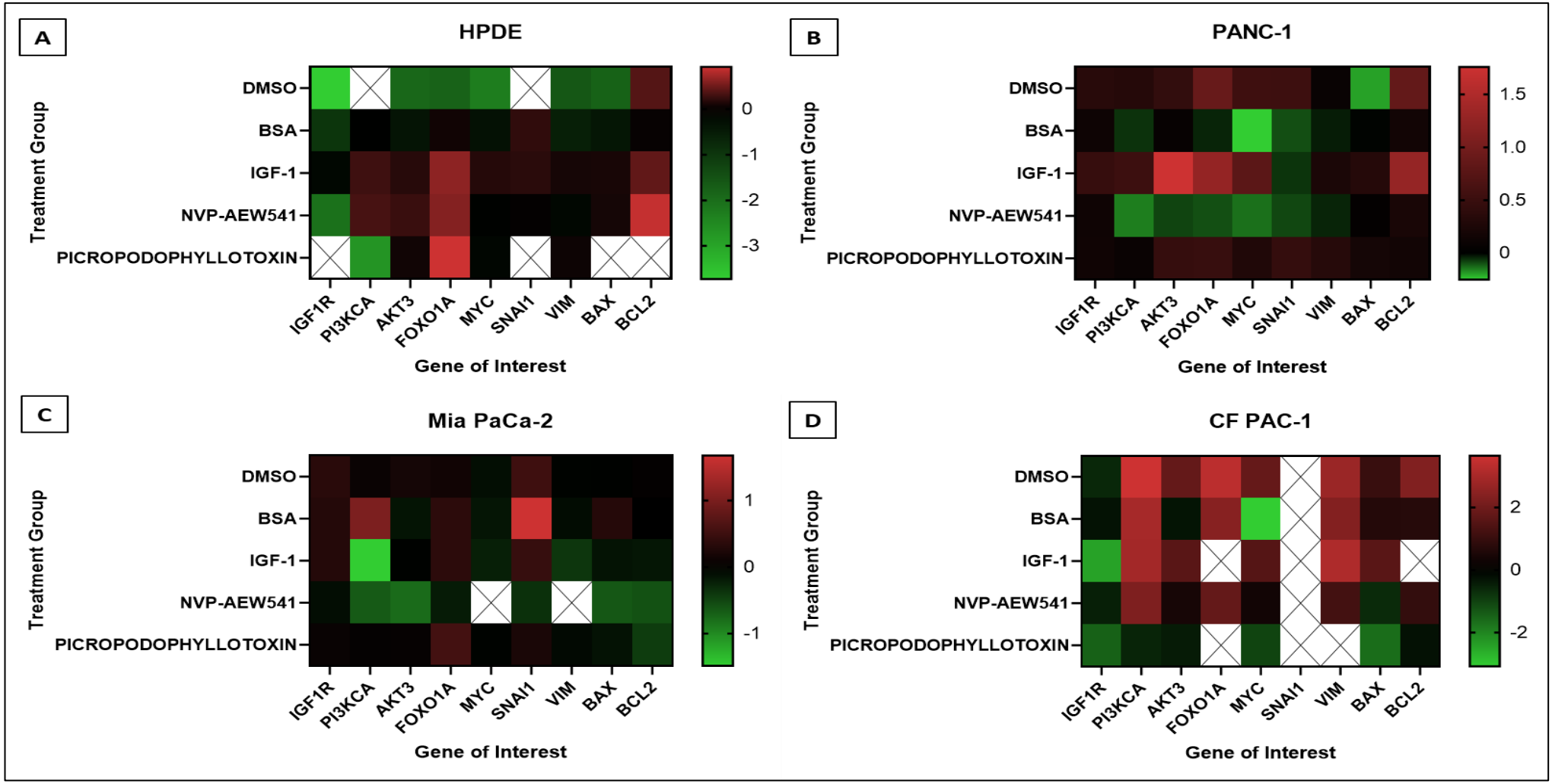

Figure 3.23: Hierarchical clustering of the average relative gene expression in a) HPDE, b) PANC-1, c) Mia PaCa-2, and d) CF PAC-1 cells. Gene expression levels are shown relative to untreated cells. Upregulated and downregulated gene expression was represented by green and red colours, respectively. Crosses represent relative gene expression that was not detected by qPCR. n=3

3.8. Western Blot Analysis

The concentrations of the antibodies used for the Western Blot analysis were determined using dot blots (**Appendix C, 9.3.**). Due to the minimal effects of IGF-1R modulation on the Mia PaCa-2 cell line, western blots were performed to determine the protein expression of targets found downstream of the IGF-1R pathway. Western blots were not performed on HPDE, PANC-1 and CF PAC-1 cell lines due to time and budget constraints.

Western blot analysis of Mia PaCa-2 cell line showed a uniform expression of pIGF-1R across all treatment groups, despite the untreated and IGF-1 treatment groups showing higher expression of IGF-1R. The mTOR antibody was detected uniformly across the untreated and diluent controls, with some expression in PPP treated cells. AKT was expressed in untreated, IGF-1 and NVP-AEW541 treated cells, and the BAD antibody was only detected in untreated cells. When the Bad protein is phosphorylated, it triggers a downstream pro-apoptotic pathway, since the antibody used can only detect non-phosphorylated Bad protein, the absence of the Bad antibody expression can be assumed that the protein is phosphorylated in the DMSO, BSA, IGF-1, NVP-AEW541 and PPP treated cells. Thus, it is speculated that apoptosis occurred in these cultures.

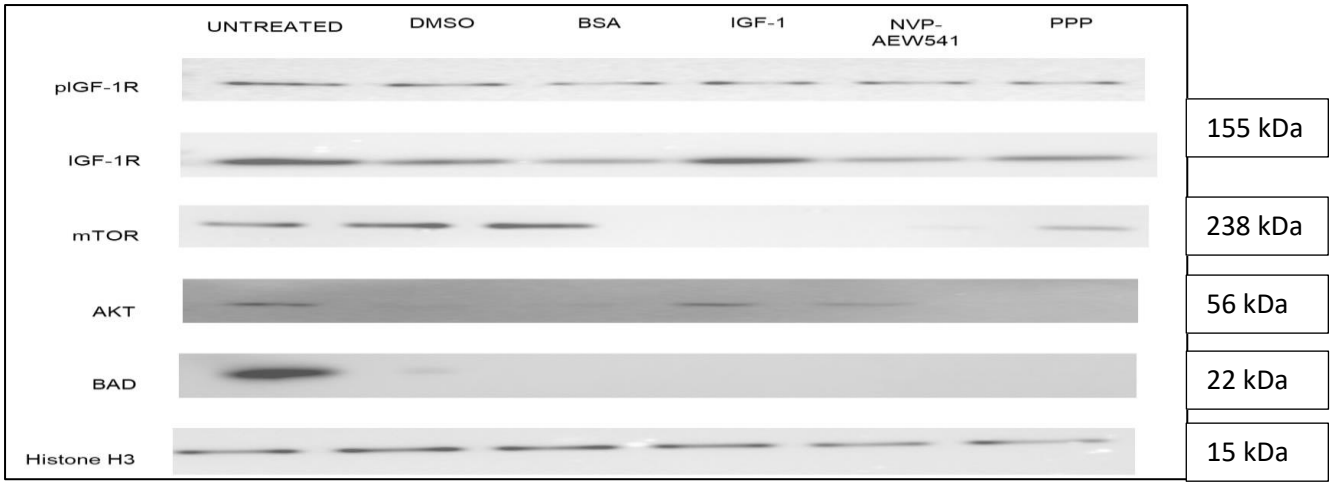

Figure 3.24: Protein expression in Mia PaCa-2 cells. Cell lysates were obtained from cells treated with DMSO, BSA, IGF-1, NVP-AEW541 and Picropodophyllotoxin (PPP) for 72 hours. Western blots were generated using pIGF-1R, IGF-1R, Akt, mTOR and BAD antibodies. Histone H3 was used as a positive control. Protein expression of pIGF-1R was constant across all treatment groups. mTOR was not detected in IGF-1 treated cells and was decreased in the NVP-AEW541 and PPP treatment groups. Akt expression was decreased in DMSO, BSA, NVP-AEW541 and PPP treatments. The BAD protein was only detected in untreated cells.

CHAPTER 4: DISCUSSION

4.1. Overview

The IGF-1R signalling pathway is an important regulator of metastatic disease, as such this study aimed to investigate the role of IGF-1R signalling in the different stages of pancreatic ductal adenocarcinoma (PDAC) using a cell line model. While IGF-1R modulation has provided information on the expression pattern of IGF-1 signal transduction in PDAC, the IGF-1R and EGFR pathways converge on multiple levels between the PI3K/Akt/mTOR and Ras/Raf/MAPK signalling cascades (Desbois-Mouthon *et al*., 2009; Valsecchi *et al*., 2012; Wong, 2015). Therefore, while the effect of IGF-1R modulation on PI3K/Akt/mTOR signalling was targeted in this study, the multiple interactions and feedback loops that exist between IGF-1R and EGFR, add another layer of complexity to the signalling networks and disease phenotype of PDAC. Moreover, it was found that tumours in PDAC patients can interchange between subtypes in order to promote tumour survival and progression (Adams *et al*., 2019). Stratified medicine is based on the identification of patient subgroups with specific mechanisms of disease, or a particular response to treatment (Jamieson *et al.*, 2014). Heterogeneity exists between tumour subtypes, moreover, with the accumulation of mutations and variation this heterogeneity increases as the tumour progresses. Based on this principle, this study hypothesized that the IGF-1R signalling pathway is differentially expressed in different stages of PDAC.

There is currently insufficient data to adequately describe the molecular characterization, phenotype and specific biomarkers that exist within different stages of the disease. Thus, the investigation of the IGF-1R signalling pathway and its downstream targets in PDAC cells representing different disease stages provides understanding of the mechanisms of resistance and thus aids in the development of effective, multi-targeting drug therapies.

4.2. The cytotoxic effects of IGF-1R inhibitors: NVP-AEW541 and Picropodophyllotoxin

This study measured used the NVP-AEW541 and Picropodophyllotoxin compounds to compare the efficacy of these inhibitors on the IGF-1R cascade and subsequent downstream signalling. It is to the best of our knowledge that this study is the first to report the assessment of a comparison of the effectiveness of these IGF-1R inhibitors.

NVP-AEW541 is a small molecular IGF-1R inhibitor that has been found to reduce proliferation and induce an apoptotic response in several cancers including pancreatic,

musculoskeletal tumours, breast, and gastrointestinal cancers (Scotlandi *et al*. 2005; EsparísOgando *et al*. 2008; Adachi *et al*. 2009; Wong *et al*. 2014). In this study we found that a similar concentration of NVP-AEW541 was required amongst all cell lines to inhibit 50 % of the cell growth, indicating that the different stages of PDAC responded similarly to the NVPAEW541 IGF-1R inhibitor. However, while it was found that NVP-AEW541 was effective in reducing the proliferative capacity of PDAC cells, it was found that Picropodophyllotoxin had a more potent cytotoxic effects on these cells.

Picropodophyllotoxin is an ATP non-competitive IGF-1R inhibitor and exerts its function by inhibiting the phosphorylation of Tyr1136 in the IGF-1R kinase activation loop. The cytotoxicity of Picropodophyllotoxin has been postulated to be associated with the inhibition of AKT activation, in conjunction with a temporary stimulation of ERK activation which occurs via IGF-1R ubiquitination (Girnita *et al*. 2004; Kwak *et al.* 2020). Thus, Picropodophyllotoxin influences two major downstream pathways of the IGF-1R cascade through different mechanisms. Interestingly, normal pancreatic cells were more sensitive to IGF-1R inhibition and therefore required lower concentrations for inhibition when compared to the different stages of PDAC.

Although NVP-AEW541 and Picropodophyllotoxin are both IGF1-R inhibitors, we found that the latter was more effective in inhibiting IGF-1R-related characteristics of the PDAC cells. The variability observed in the cellular response to these compounds could be due to the nature of the cell line and/or cell-contact survival mechanisms (Feitelson et al. 2015b). It was found that the sensitivity of IGF-1R inhibitors such as NVP-AEW541 is negatively influenced by cell-cell contact (García-Echeverría *et al.*, 2004; Feitelson *et al.* 2015). Cellcell contact is a feature of cancerous cells which rely on both autocrine and paracrine secretions for survival, therefore, cell-cell contact increases the ability of malignant cells to survive (García-Echeverría *et al.*, 2004; Crowley *et al*., 2016; Swayden *et al.*, 2018). On observation of the morphology of the PDAC cell cultures, while there were fewer cells present, these treated cells were arranged in dense colonies maintaining close cell-cell contact. Therefore, it is possible that the PDAC cells relied on the cell-cell autocrine signalling as a mechanism of survival when treated with the NVP-AEW541 inhibitor. Since NVP-AEW541 and Picropodophyllotoxin act in an ATP and ATP-independent manner, respectively (García-Echeverría *et al*., 2004; Linder *et al*., 2007), the contrast in the effectiveness of these inhibitors in PDAC cells may be due to the heterogeneity in the ATPdependent or ATP-independent IGF-1R signalling in PDAC cells.

4.3. The effects of IGF-1R modulation on PDAC cell survival

Cell survival is common as a means for resistance to chemotherapeutic, and biological agents in cancer (Grasso *et al.*, 2017) . When tumours are exposed to therapeutic agents, often tumour cells or cancer stem cells remain dormant while the actively proliferating cancerous cells are targeted (Rebucci & Michiels, 2013; Feitelson *et al*., 2015). Thus, when the stimulus is removed from the malignant environment, tumour recurrence is common. Moreover, these quiescent cancerous cells become somewhat 'resistant' to the former treatment strategy by means of microevolutionary processes. Cancer is a microevolutionary process which allows for the plasticity and the differential response of similar tumours to the same therapies. This is a common phenomenon which ultimately leads to 'heterogeneity' of tumours (Huang *et al*., 2010; Milan *et al*., 2021). This heterogeneity may be intra-tumoral, i.e., the presence of active and quiescent cells within a tumour and accumulation of epigenetic modifications, or it may be inter-tumoral, which is indicative of the differential characteristics of tumours from the same origin but at different stages of the disease, i.e., early vs late stage PDAC (Swayden *et al*., 2018; Juiz *et al*., 2019; Milan *et al*., 2021).

Cell survival mechanisms and chemo-resistance are based on the intra-tumoral heterogeneity that exists within a specific cancer type or stage of a disease (Swayden *et al*., 2018). In this study, it was found that when the stimuli or inhibitor was removed, cells were found to recover substantially and actively proliferate in the early and late stages of PDAC cells, as well as normal pancreatic cells. A study by Chen *et al*. (2021), found that some PDAC tumour cells remain in a quiescent state and do not respond to treatment. Moreover, it was found that these cells often provide a survival mechanism for damaged cancerous cells through IGF-1 autocrine release from the dormant cells. This release of IGF-1 then initiates an autophagic cell survival response in the damaged cells, resulting in the regeneration and survival of these cells (Chen *et al*., 2021). In the present study, we found that despite the effects of IGF-1R modulation on the proliferation and migration of PDAC cells, survival and regeneration of these cells were evident when the modulator was removed. This is an interesting phenomenon, which may indicate what occurs *in vivo* where a culmination of treatment regimens causes a resurgence of the cancer which is more aggressive than before treatment (Valle *et al*., 2018).

Interestingly, this was not observed in the intermediate PDAC cell line, indicating that IGF1R signalling is not a predominantly activated cascade in this stage of the disease. Of particular note is the desensitized response to IGF-1R modulation in proliferation and migration of

these cells, yet the lower survival rate in these cells when the modulator was removed. This could indicate that there may be a delayed metabolism of these compounds in these cells. The differences found in the response of the different cell lines further highlight the inter-tumoral heterogeneity that exists in IGF-1R signalling in the response of PDAC cells to treatment (Torres & Grippo, 2018).

4.4. The effects of IGF-1R modulation on PDAC migration

Studies have shown that IGF-1R is a critical regulator epithelial-to-mesenchymal transition (EMT)-mediated tumour metastasis and drug resistance (Li *et al*., 2017). Additionally, overexpression of IGF-1R was found to be associated with poor prognosis and increased mortality in cancer patients due to this enhanced potential for migration and metastasis (Seccareccia & Brodt, 2012; Subramani *et al*., 2014; Christopoulos *et al*., 2015).

In the present study we found that while NVP-AEW541 decreased the migratory rate of normal pancreatic and early stage PDAC cells, migration in these cell lines was not completely inhibited. Similar results were obtained by Esparís-Ogando *et al*. (2008) where they found that NVP-AEW541 did not completely inhibit the migration of triple negative breast cancer cells. They postulated that the continued migration in these cells may be due to insulin receptor signalling, which is not targeted by NVP-AEW541. However, this may not be the reason for the continued migration of PDAC cells, as treatment with

Picropodophyllotoxin, another IGF-1R inhibitor, completely inhibited the migration of cells. Picropodophyllotoxin is a highly specific IGF-1R inhibitor that exhibits no activity at the insulin receptor, FGFR, PDGFR or EGFR (Doghman *et al*., 2011; Kwak *et al*., 2020), therefore the suggestions made by Esparís-Ogando *et al*. (2008) may not be applicable in PDAC. Additionally, we observed that Picropodophyllotoxin had a cytotoxic effect on PDAC cells from the intermediate and late stages of the disease.

In the present study, we also found that NVP-AEW541 increased migration of intermediate and late stage PDAC cells compared to treatment with IGF-1. These results could also be due to the enhanced insulin receptor signalling or another bypass signalling pathway such as

EGFR which is known to be overexpressed in these stages of PDAC (Yuan *et al*., 2008; Valsecchi *et al*., 2012). This study reported that Picropodophyllotoxin is an effective inhibitor in preventing migration in PDAC, with potentially cytotoxic effects on tumour cells. These findings were similar to previous reports that found that Picropodophyllotoxin decreases the

motility of PDAC cell lines and that NVP-AEW541 had minimal effects on these cells (Tomizawa *et al*., 2010).

4.5. Dysregulated gene expression in PDAC

Physiologically, it was proposed that IGF-1R might increase cell proliferation while the traditional AKT and ERK pathways promote cell differentiation and survival (Lin *et al*., 2017). In this study, gene expression analysis was targeted mainly at the PI3K/Akt/mTOR signalling cascade that plays an important role in cancer growth and proliferation (Drosten *et al*. 2010). The PI3K signalling cascade has been associated with nutrient uptake, storage of energy and protein translation, as well as, IGF-1-induced cell survival, proliferation and migration in normal and malignant cells (Park *et al.*, 2005; Leger *et al.*, 2006; Finlay & Cantrell, 2010).

In PDAC, several members of the PI3K complex are upregulated, including an isoform of PI3K and Akt (Paez & Sellers, 2003; Fitzgerald *et al*., 2015; Kasprzak *et al*., 2017). A metastatic phenotype is often associated with increased expression of PI3K (Paez & Sellers, 2003).

Insulin-like growth factor receptor-1: IGF-1R

The IGF-1R is a tyrosine receptor that activates intracellular signalling cascades such as PI3K/Akt/mTOR and Ras/Raf/MAPK (Valsecchi *et al.*, 2012). The modulators used in this study were IGF-1 and NVP-AEW541 and Picropodophyllotoxin. IGF-1 was used as a stimulatory modulator for the IGF-1R, and both, NVP-AEW541 and Picropodophyllotoxin were inhibitors of IGF-1R function. While these modulators target protein expression and phosphorylation, IGF-1R gene expression is also assumed to be modulated. Therefore, the IGF-1R gene was a target for this study.

This study found that IGF-1R baseline gene expression levels were not constant in the different PDAC cell lines which represent the different stages of the disease. This is an indicator that the IGF-1R pathway may be differentially activated in the different stages of PDAC. In 1995, Freeman *et al*. showed that the PDAC Mia PaCa-2 cell line had an increased IGF-1R expression, while Nair *et al*. (2017) noted that although IGF1-R mRNA expression levels were low, the protein receptor expression was high in Mia PaCa2 cells.

Nair *et al.* (2017), therefore suggested that IGF1-R mRNA is unstable in these cells and degrades in exponentially growing cells. The study further showed that stimulation with IGF1 resulted in activation of IGF-1R although some decrease in the expression of the protein was

observed. Interestingly, the findings in this study were consistent with the findings of Nair *et al* where lower levels of IGF-1R mRNA was observed in Mia PaCa-2 cells, when compared to other PDAC cells. However, contradictory results were obtained in the phenotypic behaviour of these cells when IGF1-R was modulated. Our study found that the intermediary, Mia PaCa-2 cells were desensitized to both stimulation and inhibition of IGF-1R having a minimal effect on the phenotypic proliferative and migratory response of these cells. These results indicate that IGF-1R signalling is not a major signalling pathway in this stage of PDAC. Interestingly, we found that these cells experience the long-term effects of IGF1-R inhibition in the absence of the modulator.

It is to the best of our knowledge that this is the first instance whereby a differential expression of IGF-1R has been reported in the different stages of PDAC.

Proliferation and Survival

The PI3K gene is often amplified in human malignancies. The PI3K protein is closely associated with and activated by receptor protein kinases. The phosphorylation of PI3K leads to the phosphorylation of AKT (Cejas *et al*., 2003). Akt is a primary mediator of PI3K signalling and it is essential in the regulation of several downstream transcription factors that are involved in cancer progression, including the forkhead family of transcription factors (FOXO) and c-myc (Cejas *et al*., 2003; McCubrey *et al*., 2006; Hamacher *et al*., 2008). Microarray data has shown that the PI3K/AKT signalling pathway is activated in over 60 % of PDAC clinical samples and established cell lines (Jones *et al*., 2008). This pathway has also been shown to be a mediator of chemoresistance in most pancreatic cancers (Fitzgerald *et al*., 2015; Grasso *et al.*, 2017). The PI3KCA gene has been implicated as an oncogene is some cancers, and in PDAC the PI3KCA gene was reported to be aberrantly expressed in both clinical specimen and established cell lines (Altomare & Testa, 2005; Hamacher *et al*., 2008).

Transcription factors, such as FOXO and c-myc, that are found downstream of Akt have tumour suppressor-like and oncogene functions, respectively. FOXO transcription factors have been implicated in IGF-1 mediated cell proliferation, survival, and hypertrophy (Burgering & Medema, 2003; Stitt *et al*., 2004; Leger *et al*., 2006; Elia *et al*., 2009). In

PDAC clinical specimens it was found that an increased expression of proteins from the Forkhead family were associated with an increased average survival period of patients with PDAC (Luo *et al*., 2017).

In the present study, it was observed that in early and late stage PDAC cells an increased PI3KCA gene expression correlated with an overexpression of other genes that regulate cellular proliferation and survival, such as AKT3, FOXO1A and MYC. Moreover, it was found that an increased gene expression corresponded with the opposite phenotypic effects, i.e. decreased proliferation and migration of PDAC cells. Therefore, the increased gene expression may be as a result of an activation of a compensatory, negative feedback mechanism in order to re-establish homeostasis, where a decreased expression of these proteins increases gene expression as a compensatory mechanism when a tumour suppressor function is favoured (Ross & Pawlina, 2011; Hassan *et al*., 2013). However, this cannot be confirmed as protein expression was not measured in all PDAC cells used in this study.

It was also observed that inhibition of IGF-1R resulted in an increased expression of genes involved in cell survival and proliferation, while the stimulation of IGF-1R in PDAC cells resulted in a downregulated expression of these genes. Similar results were reported where IGF-1R silencing downregulates AKT and stimulation of IGF-1R increases AKT expression (Subramani *et al*., 2014). Additionally, it has been suggested that elevated levels of AKT3 may contribute to the aggressiveness of late stage and/or metastatic tumours and is consistently activated in PDAC (Altomare & Testa, 2005). In this study, it was noted that when IGF-1R is both, stimulated and inhibited, there is an increased AKT3 mRNA expression in early and late stage PDAC cells, but decreased in intermediate PDAC cells. These results further highlight that heterogeneity that exists both phenotypically and genetically in the different stages of PDAC.

Migration

Epithelial-to-mesenchymal transition (EMT) is a process whereby epithelial cells transdifferentiate to migratory cells that have mesenchymal characteristics (Vuoriluoto et al., 2011). EMT is often associated with the ability of cancerous cells to migrate to distant organs during metastasis (Vuoriluoto et al., 2011; Liu et al., 2019). The transcription factors that are involved in the phenotypic changes that are associated with EMT include, Snail, Vimentin and Slug. The overexpression of these genes is associated with a poor prognosis in several cancers (Wang et al., 2009; Vuoriluoto et al., 2011; Santilli et al., 2016; Liu et al., 2019).

It was found that Snail expression was overexpressed in 35-80 % of PDAC surgical samples, and has been associated with lymph node invasion and metastasis (Hotz et al., 2007). Moreover, it has been reported that Snail upregulation is associated with the EMT-like phenotype of metastatic PDAC sublines (Wang et al., 2009; Liu et al., 2019). In this study,

Snail and Vimentin gene expression was found to be decreased in early and intermediate PDAC cells but increased in late stage PDAC cells when treated with the NVP-AEW541 inhibitor. Vimentin is a mesenchymal marker that has been found in PDAC cells that are chemotherapy-resistant (Wang et al., 2009; Giovannetti et al., 2017). Since it was found that vimentin gene expression was enhanced in late stage PDAC cells treated with the NVP-AEW541 inhibitor, this may be an indicator of the resistance of these cells to IGF-1R inhibition. In addition, treatment with Picropodophyllotoxin showed an increased expression of Snail and Vimentin mRNA in early and intermediate PDAC cells. Since the Snail family of transcription factors is closely associated with PI3K/Akt/mTOR signalling, and Vimentin is transcription factor that is associated with the Ras/Raf/MAPK signalling cascade, the observations made in this study suggest that different downstream signalling cascades are activated when PDAC cells are treated with the different IGF-1R inhibitors (Cejas et al., 2003; Drosten et al., 2010; Fitzgerald et al., 2015).

This indicates that the PI3K/Akt/mTOR signalling cascade may be responsible for the regulation of migration in early and intermediate stages of PDAC via Snail, and the Ras/Raf/MAPK cascade regulates migration in the late stages of PDAC via Vimentin. These results are consistent with those reported by Zhang et al. (2020), who showed that Vimentin is overexpressed in migrating, metastatic CF PAC-1 cells in vitro.

Apoptosis

In contrast to several other cancers, in PDAC the expression of the anti-apoptotic protein BCL-2 is normal or even decreased, which may contribute to the apoptotic resistance observed (Campani *et al*., 2001; Evans *et al*., 2001). The pro-apoptotic Bcl-2-associated X protein

(BAX) protein has been found to be decreased in about 50 % of all PDACs (Evans *et al*., 2001; Hamacher *et al*., 2008). Additionally, Subramani *et al.* (2014) showed that silencing of IGF-1R decreases Bcl-2 and increases BAX expression in some PDAC cells.

However, observations made in the present study contrast with previous reports, where when the relative expression of the pro-apoptotic gene BAX was analysed relative to the expression of the anti-apoptotic Bcl-2 gene, it was found that survival was favoured across all treatment groups in the CF PAC-1 cell line, with Bcl-2 expression being higher than BAX gene expression even in the presence of IGF-1R inhibitors. Since this cell line was derived from a metastatic tumour, the enhanced expression of Bcl-2 is assumed to be a contributing factor to

tumour survival and progression of the disease (Evans *et al*., 2001; Hamacher *et al*., 2008). In addition, since multiple apoptotic pathways have been observed in PDAC, another apoptotic pathway that is independent of the Bcl-2 family of genes, such as the death receptor pathway may have been influenced (Hamacher *et al*., 2008; Hashemi *et al*., 2011).

4.6. The effect of DMSO on PDAC cell lines

Dimethyl sulfoxide (DMSO) is an organic molecule commonly used in the cryopreservation of cells, and as a solvent for pharmacological agents (Galvao *et al*., 2014; Verheijen *et al*., 2019). It is known that DMSO is a cytotoxic agent and influences the characteristics of cancerous cells at high concentrations.

In this study, DMSO was used as a diluent for the NVP-AEW541 and Picropodophyllotoxin inhibitors as per the manufacturer's instructions. As such the final working concentration of DMSO was 0.03 % and DMSO was used as a diluent control to determine whether the diluent influenced the behaviour of the PDAC cells. In this study, it was found that the DMSO diluent significantly decreased cell proliferation and colony formation and affected gene and protein expression.

Since DMSO had affected the phenotypic behaviour of PDAC cells in this study, as well as gene expression, DMSO may not be a suitable diluent for these inhibitors as the effects of the inhibitors used in this study may not be solely due to the mechanism of action of the inhibitors itself, therefore providing false positive or false negative results on the efficacy of NVP-AEW541 and Picropodophyllotoxin in modulating the IGF-1R pathway.

Published works rarely report the concentrations and results of diluent controls such as DMSO as it is so commonly used and accepted as being non-toxic below 10 % (v/v), therefore the effect of DMSO in in vitro studies is assumed to be negligible (Sumida *et al*., 2011; Galvao *et al*., 2014; Verheijen *et al*., 2019). However, this study and previous studies clearly shows that diluents such as DMSO has a severe effect on the phenotypic behaviour of cells. A study by Verheijen *et al*. (2019) reported that a concentration of 0.1 % DMSO highly affected cellular processes such as vesicle-mediated transport, cellular senescence, and DNA repair. Moreover, the study also reported that DMSO had an effect on the regulation of gene expression and translation and affected the epigenetics of cells through deregulation of the DNA methylation pathways (Verheijen *et al*., 2019). Similar results were obtained in our study where phenotypic behaviour and gene expression of cells treated with 0.03 % DMSO

was significantly altered. Therefore, we suggest that it should be standard practice for published works to report concentrations and data on the effects of diluents on cells in vitro.

4.7. Western Blotting troubleshooting

In this study, several setbacks were encountered throughout the western blotting technique whereby the proteins did not separate properly on the gel or a weak, or no signal was detected on the blot. As such, troubleshooting was done for each step of the technique to determine what caused the hindrances. Firstly, the protein did not separate on the separating gel during the gel electrophoresis phase of the technique. Therefore, the composition of the separating gel was altered. The voltages and electrophoresis run times were also adjusted, this resulted in the tanks overheating and bands that were distorted. The voltage was changed to amperes and time extended for optimal gel electrophoresis conditions.

Another problem that was encountered was that improper or no protein was transferred to the Polyvinylidene difluoride (PVDF) membrane, this was determined by Ponceau Blue S staining. To find the optimal transfer conditions, protein transfer was tested at different voltages and times. Additionally, wet, dry, and semi-dry transfer conditions were attempted to determine which transfer setup yielded the best results. The most optimal transfer conditions were determined using the semi-dry transfer setup at 10 volts, overnight at 4 °C. A few blots were generated for the Mia PaCa-2 cell line before no signal was detected in all the blots thereafter. The equipment and apparatus were properly cleaned before and after use; and buffers were remade; this did not affect the no signal detection.

A pre-stained molecular weight marker was used a positive control to determine the transfer efficacy. It was found that the marker transferred completely, and the Ponceau Blue stain of the polyacrylamide gel showed that the proteins also transferred completely. The transfer time was decreased, and voltage increased to avoid over-transfer of small proteins; this change did not yield any signal on the blot. No signal was detected when a different chemiluminescent kit was used, and a new substrate was added. The chemiluminescent substrate and blot exposure time was increased, this yielded blotchy and speckled membranes with no band signals detected. Protein concentrations were determined using the BCA assay to see if there was a problem with the protein lysates itself, such as protein degradation or poor quality of the proteins. These results showed no irregularities in protein quality.

Antibody concentrations were retested using dot blots to determine if the concentrations used were too low, it was found that a signal was detected in proteins from dot blots but not from proteins transferred from gels.

Due to time and budget constraints, the Western Blot technique could not be completed at this time and will be the focus of ongoing investigation by the laboratory.

4.8. Further Studies and Limitations

A negative aspect of the IC_{50} values in this study is that these concentrations represent the half-inhibitory concentration *in vitro* and these concentrations may not be applicable in *in vivo* studies or clinically.

An inadequate conclusion could be drawn on the effects of the IGF-1R modulation on downstream protein expression in the IGF-1R pathway due to several of the western blots not yielding results. Due to time constraints, this could not be completed in all cell lines to make apt comparisons between the expression of proteins in the different cell lines. Therefore, qPCR was used as an alternative technique to compare the gene expression of downstream genes in the IGF-1R pathway. However, post-transcriptional and post-translational modifications such as phosphorylation are not detected by qPCR. Thus, genes that appear to be up- or down-regulated may be modified post-transcriptionally affecting the phenotypic behaviour of the cells (Pan, Brentnall, and Chen 2020; Ansari *et al.,* 2019). Future studies could be done to compare gene expression with protein expression in PDAC cell lines that have been treated with IGF-1R modulators. Another possible technique to measure protein expression in cells could be performed using sequential window acquisition of all theoretical fragment ion spectra mass spectrometry (SWATH-MS) to determine the proteomic expression of IGF-1R and its downstream molecules. Expression of specific cell markers could also be measured using flow cytometry or using immunocytochemistry or immunofluorescent techniques.

PDAC is a disease that is characterized by the upregulation of several growth factors, including the epidermal growth factors and fibroblast growth factors. The EGFR pathway has been shown to be significant in PDAC development and progression. The EGFR and IGF-1R pathways converge at several downstream proteins, thus the interlink between both pathways could result as a mechanism of resistance to treatment of the disease. Thus, dual inhibition of the IGF-1R and EGFR pathways will reflect the true role of not only the IGF-1R pathway in

PDAC but also a possible mechanism of resistance to IGF-1R and EGFR inhibitor treatments observed in PDAC.

Microarray analysis based on clinical data from different online databases suggest that there is a role for insulin-like growth factor binding proteins (IGFBPs) in PDAC, and future studies on the role of these binding proteins in PDAC could provide a better understanding of the disease and possibly a novel target for a new targeted-therapy in metastatic PDAC. In addition, the microarray analysis between PDAC cell lines and PDAC clinical data showed a vast difference in gene expression patterns, thus showing a need for better *in vitro* models to mimic the PDAC tumour microenvironment (Jones *et al.*, 2008; Xu *et al.*, 2016). In this way, results obtained in *in vitro* studies will be more relevant and applicable in a clinical setting.

More research is needed to understand the behaviour of tumour cells following treatment, the survival data shown in this study indicates a possible further stimulation for the aggressive nature of metastatic PDAC cells. This could possibly explain or hint at why or how cancer recurrence occurs clinically.

CHAPTER 5: CONCLUSION

PDAC is a highly heterogeneous disease as multiple classifications exist in defining the different subtypes of the disease. Some classifications are based on inter-tumoral heterogeneity which includes histological, genomic, transcriptomic, metabolomic and stromal subtypes (Cros *et al*., 2018; Milan *et al.*, 2021). Intra-tumoral heterogeneity is driven by the epigenetic modifications which accumulate between the different stages of PDAC exhibiting differences between primary and metastatic tumours (Penchev *et al*., 2012; Cros *et al*., 2018). Stratified medicine is based on the identification of patient subgroups with specific mechanisms of disease, or a particular response to treatment (Jamieson *et al.*, 2014).

PDAC is often detected in intermediary and metastatic stages of the disease (Hezel *et al.*, 2006), therefore the development of epigenetic modification which occurs as the disease progresses may not be easily identifiable limiting the possibility of patient stratification in a clinical setting. Therefore, this study aimed to investigate the IGF-1R signalling heterogeneity which exists in different stages of PDAC cell lines derived from different clinical specimens. This comparison included the variation which exists in tumours thereby providing information on the behaviour of the different stages of PDAC, thus a possibility for patient stratification based on the dominant signalling pathway in each stage of the disease.

The present study focused on inter-tumoral heterogeneity; primarily on the histological, genomic, and transcriptomic heterogeneity which exists between the different stages of PDAC. The observation between the differences existing in the expression of IGF-1R and modulation of this pathway was assessed in cell lines representing the different stages of PDAC. This study showed that inter-tumoral heterogeneity exists between the different stages of PDAC where differences in the phenotypic and gene expression responses in the different cell lines was observed. It was found that the intermediary stages of PDAC had limited IGF1R activity, and that the early and late stages of PDAC has an increased response to IGF-1R signalling *in vitro*. It was highlighted that even though IGF-1R was not a predominant signalling cascade in the intermediate stage of PDAC, the cytotoxic effects of the compounds used may have been metabolised by the cells at a later point.

It was further shown that PDAC cells respond differently at different stages of its progression, showing that a single treatment for all stages of the disease is not sufficient in improving overall patient survival. This demonstrates an urgent need for molecular subtyping of tumours which may lead to more tailored therapies for PDAC.

REFERENCES

Abdel-Wahab, Reham, Gauri R. Varadhachary, Priya R. Bhosale, Xuemei Wang, David R. Fogelman, Rachna T. Shroff, Michael J. Overman, Robert A. Wolff, and Milind Javle. 2018. "Randomized, Phase I/II Study of Gemcitabine plus IGF-1R Antagonist (MK-0646) versus Gemcitabine plus Erlotinib with and without MK-0646 for Advanced Pancreatic Adenocarcinoma." *Journal of Hematology and Oncology* 11 (1). https://doi.org/10.1186/s13045-018-0616-2.

Abdel-wahab, Reham, Gauri R Varadhachary, Priya R Bhosale, Xuemei Wang, David R Fogelman, Rachna T Shroff, Michael J Overman, Robert A Wolff, and Milind Javle. 2018. "Randomized , Phase I / II Study of Gemcitabine plus IGF-1R Antagonist (MK-0646) versus Gemcitabine plus Erlotinib with and without MK-0646 for Advanced Pancreatic Adenocarcinoma." *Journal of Hematology & Oncology* 11 (71): 1–9.

Adachi, Yasushi, Rong Li, Hiroyuki Yamamoto, Yongfen Min, Wenhua Piao, Yu Wang, Arisa Imsumran, et al. 2009. "Insulin-like Growth Factor-I Receptor Blockade Reduces the Invasiveness of Gastrointestinal Cancers via Blocking Production of Matrilysin." *Carcinogenesis* 30 (8): 1305–13. https://doi.org/10.1093/carcin/bgp134.

Adams, Christina R, Htet Htwe Htwe, Timothy Marsh, Aprilgate L Wang, Megan L Montoya, Lakshmipriya Subbaraj, Aaron D Tward, Nabeel Bardeesy, and Rushika M Perera. 2019. "Transcriptional Control of Subtype Switching Ensures Adaptation and Growth of Pancreatic Cancer." https://doi.org/10.7554/eLife.45313.001.

Adamska, Aleksandra, Alice Domenichini, and Marco Falasca. 2017. "Pancreatic Ductal Adenocarcinoma : Current and Evolving Therapies." *International Journal of Molecular Sciences* 18 (1338). https://doi.org/10.3390/ijms18071338.

Alberts, Bruce, Alexander Johnson, Julian Lewis, David Morgan, Martin Raff, Keith Roberts, and Peter Walter. 2015. *Molecular Biology of the Cell*. Sixth Edit. New York: Garland Science.

Altomare, Deborah A., and Joseph R. Testa. 2005. "Perturbations of the AKT Signaling Pathway in Human Cancer." *Oncogene* 24 (50): 7455–64. https://doi.org/10.1038/sj.onc.1209085.

Ansari, Daniel, William Torén, Qimin Zhou, Dingyuan Hu, and Roland Andersson. 2019. "Proteomic and Genomic Profiling of Pancreatic Cancer." *Cell Biology and Toxicology*

35 (4): 333–43. https://doi.org/10.1007/s10565-019-09465-9.

Arnold, Dirk, Stefan Peinert, Wieland Voigt, Hans-joachim Schmoll, and Martin-luther-universität Halle. 2006. “Epidermal Growth Factor Receptor Tyrosine Kinase Inhibitors: Present and Future Role in Gastrointestinal Cancer Treatment: A Review.” *The Oncologist* 11: 602–11. https://doi.org/10.1634/theoncologist.11-6-602.

Artacho-cordón, Antonia, Francisco Artacho-cordón, Sandra Ríos-arrabal, Irene Calvente, and María Isabel Núñez. 2012. “Tumor Microenvironment and Breast Cancer Progression A Complex Scenario.” *Cancer Biology and Therapy* 13 (1): 14–24.

Attard, Joseph A, Alexia Farrugia, Adithya Pathanki, Keith J Roberts, Bobby Dasari, Isaac John, Yuk Ting Ma, and Nikolaos A Chatzizacharias. 2019. “Treatment Strategies and Sequencing for the Optimal Management of Locally Advanced Pancreatic Adenocarcinoma with Curative Intent.” *British Journal of Surgery* 106 (Supplement 7): 21. https://doi.org/10.1097/MPA.0000000000001694.

Balkwill, Frances R, and Thorsten Hagemann. 2012. “The Tumor Microenvironment at a Glance.” https://doi.org/10.1242/jcs.116392.

Barbieri, Michelangela, Massimiliano Bonafe, Claudio Franceschi, Giuseppe Paolisso, and Massimiliano Bonafe. 2003. “Insulin / IGF-I-Signaling Pathway : An Evolutionarily Conserved Mechanism of Longevity from Yeast to Humans.” *American Journal of Physiology, Endocrinology and Metabolism* 285 (11): 1064–71.

Baxevanos, P, and C Fountzilas. 2017. “Optimizing EGFR Targeted Therapy in Pancreatic Cancer.” *Austin Pancreatic Disorders* 1 (1): 1005–12.

Bianco, Roberto, Davide Melisi, Fortunato Ciardiello, and Giampaolo Tortora. 2006. “Key Cancer Cell Signal Transduction Pathways as Therapeutic Targets.” *European Journal of Cancer* 42 (2): 290–94. https://doi.org/10.1016/j.ejca.2005.07.034.

Biancur, Douglas E., and Alec C. Kimmelman. 2018. “The Plasticity of Pancreatic Cancer Metabolism in Tumor Progression and Therapeutic Resistance.” *Biochimica et Biophysica Acta - Reviews on Cancer*. Elsevier B.V. https://doi.org/10.1016/j.bbcan.2018.04.011.

Blankenberg, Francis Gerard. 2009. “Imaging the Molecular Signatures of Apoptosis and Injury with Radiolabeled Annexin V.” *Proceedings of the American Thoracic Society* 6

(5): 469–76. https://doi.org/10.1513/pats.200901-001AW.

Blasco, María Teresa, Carolina Navas, Guillermo Martín-Serrano, Osvaldo Graña-Castro, Carmen G. Lechuga, Laura Martín-Díaz, Magdolna Djurec, et al. 2019. "Complete Regression of Advanced Pancreatic Ductal Adenocarcinomas upon Combined Inhibition of EGFR and C-RAF." *Cancer Cell* 35 (4): 573-587.e6. https://doi.org/10.1016/j.ccell.2019.03.002.

Büth, Heiko, Pier Luigi Buttigieg, Raluca Ostafe, Maren Rehders, Stefanie R. Dannenmann, Norbert Schaschke, Hans Jürgen Stark, Petra Boukamp, and Klaudia Brix. 2007. "Cathepsin B Is Essential for Regeneration of Scratch-Wounded Normal Human Epidermal Keratinocytes." *European Journal of Cell Biology* 86 (11–12): 747–61. https://doi.org/10.1016/j.ejcb.2007.03.009.

Campani, Daniela, Irene Esposito, Ugo Boggi, Denise Cecchetti, Michele Menicagli, Ferdinando De Negri, Livio Colizzi, et al. 2001. "Bcl-2 Expression in Pancreas Development and Pancreatic Cancer Progression." *Journal of Pathology* 194 (4): 444–50. https://doi.org/10.1002/path.925.

Casa, Angelo J, Robert K Dearth, Beate C Litzenburger, Adrian V Lee, and Xiaojiang Cui. 2008. "The Type I Insulin-like Growth Factor Receptor Pathway: A Key Player in Cancer Therapeutic Resistance." *Frontiers in Bioscience* 13 (5): 3273–87.

Cejas, Paloma, Cristóbal Belda-Iniesta, Enrique Casado, Juan Ángel Fresno Vara, Javier de Castro, and Manuel González-Barón. 2003. "PI3K/Akt Signalling Pathway and Cancer." *Cancer Treatment Reviews* 30 (2): 193–204. https://doi.org/10.1016/j.ctrv.2003.07.007.

Chen, Pei Chin, Yung Che Kuo, Cheng Ming Chuong, and Yen Hua Huang. 2021a. "Niche Modulation of IGF-1R Signaling: Its Role in Stem Cell Pluripotency, Cancer Reprogramming, and Therapeutic Applications." *Frontiers in Cell and Developmental Biology* 8 (January). https://doi.org/10.3389/FCELL.2020.625943/FULL.

Christopoulos, Panagiotis F., Pavlos Msaouel, and Michael Koutsilieris. 2015. "The Role of the Insulin-like Growth Factor-1 System in Breast Cancer." *Molecular Cancer* 14 (1): 1–14. https://doi.org/10.1186/s12943-015-0291-7.

Collisson, Eric A., and Anirban Maitra. 2017. "Pancreatic Cancer Genomics 2.0: Profiling Metastases." *Cancer Cell*. Cell Press. https://doi.org/10.1016/j.ccell.2017.02.014.

Conant, Carolyn G., J. Tanner Nevill, Michael Schwartz, and Cristian Ionescu-Zanetti. 2010. "Wound Healing Assays in Well Plate—Coupled Microfluidic Devices with Controlled Parallel Flow." *Journal of Laboratory Automation* 15 (1): 52–57. https://doi.org/10.1016/j.jala.2009.08.002.

Cooperman, Avram M, Mazen E Iskandar, Michael G Wayne, and Justin G Steele. 2018. "Prevention and Early Detection of Pancreatic Cancer." *Surg Clin N Am* 98: 1–12. https://doi.org/10.1016/j.suc.2017.09.001.

Cros, Jerome, Jerome Raffenne, Anne Couvelard, and Nicolas Poté. 2018. "Tumor Heterogeneity in Pancreatic Adenocarcinoma." *Pathobiology* 85 (10): 64–71. https://doi.org/10.1159/000477773.

Crowley, Lisa C., Melinda E. Christensen, and Nigel J. Waterhouse. 2016. "Measuring Survival of Adherent Cells with the Colony-Forming Assay." *Cold Spring Harbor Protocols* 2016 (8): 721–24. https://doi.org/10.1101/pdb.prot087171.

Desbois-Mouthon, Christèle, Aurore Baron, Marie José Blivet-Van Eggelpoël, Laetitia Fartoux, Corinne Venot, Friedhelm Bladt, Chantal Housset, and Olivier Rosmorduc. 2009. "Insulin-like Growth Factor-1 Receptor Inhibition Induces a Resistance Mechanism via the Epidermal Growth Factor Receptor/HER3/AKT Signaling Pathway: Rational Basis for Cotargeting Insulin-like Growth Factor-1 Receptor and Epidermal Growth Factor Receptor in Hepatocellular Carcinoma." *Clinical Cancer Research* 15 (17): 5445–56. https://doi.org/10.1158/1078-0432.CCR-08-2980.

Dhupal, Madhusmita, Jae-min Oh, Dipti Ranjan Tripathy, Soo-ki Kim, Sang Baek Koh, and Kyu-sang Park. 2018. "Immunotoxicity of Titanium Dioxide Nanoparticles via Simultaneous Induction of Apoptosis and Multiple Toll-like Receptors Signaling through ROS- Dependent SAPK / JNK and P38 MAPK Activation." *International Journal of Nanomedicine* 13: 6735–50.

Doghman, Mabrouka, Magnus Axelson, and Enzo Lalli. 2011. "Potent Inhibitory Effect of the Cyclolignan Picropodophyllin (PPP) on Human Adrenocortical Carcinoma Cells Proliferation." *American Journal of Cancer Research* 1 (3): 356–61. http://www.pubmedcentral.nih.gov/articlerender.fcgi?artid=3180063&tool=pmcentrez&rendertype=abstract.

Drosten, Matthias, Alma Dhawahir, Eleanor Y.M. Sum, Jelena Urosevic, Carmen G.

Lechuga, Luis M. Esteban, Esther Castellano, Carmen Guerra, Eugenio Santos, and Mariano Barbacid. 2010. “Genetic Analysis of Ras Signalling Pathways in Cell Proliferation, Migration and Survival.” *EMBO Journal* 29 (6): 1091–1104. https://doi.org/10.1038/emboj.2010.7.

Eastman, Alan. 2017. “Improving Anticancer Drug Development Begins with Cell Culture : Misinformation Perpetrated by the Misuse of Cytotoxicity Assays.” *Oncotarget* 8 (5): 8854–66.

Engeland, Manon Van, Luc J.W. Nieland, Frans C.S. Ramaekers, Bert Schutte, and Chris P.M. Reutelingsperger. 1998. “Annexin V-Affinity Assay: A Review on an Apoptosis Detection System Based on Phosphatidylserine Exposure.” *Cytometry* 31 (1): 1–9. https://doi.org/10.1002/(SICI)1097-0320(19980101)31:1<1::AID-CYTO1>3.0.CO;2-R.

Eskelinen, Eeva-liisa. 2011. “The Dual Role of Autophagy in Cancer.” *Current Opinion in Pharmacology* 11 (4): 294–300. https://doi.org/10.1016/j.coph.2011.03.009.

Esparís-Ogando, A., A. Ocaña, R. Rodríguez-Barrueco, L. Ferreira, J. Borges, and Atanasio Pandiella. 2008. “Synergic Antitumoral Effect of an IGF-IR Inhibitor and Trastuzumab on HER2-Overexpressing Breast Cancer Cells.” *Annals of Oncology* 19 (11): 1860–69. https://doi.org/10.1093/annonc/mdn406.

Evans, James D., Philip A. Cornford, Andrew Dodson, William Greenhalf, Christopher S. Foster, and John P. Neoptolemos. 2001. “Detailed Tissue Expression of Bcl-2, Bax, Bak and Bcl-x in the Normal Human Pancreas and in Chronic Pancreatitis, Ampullary and Pancreatic Ductal Adenocarcinomas.” *Pancreatology* 1 (3): 254–62. https://doi.org/10.1159/000055820.

Feitelson, Mark A., Alla Arzumanyan, Rob J. Kulathinal, Stacy W. Blain, Randall F. Holcombe, Jamal Mahajna, Maria Marino, et al. 2015a. “Sustained Proliferation in Cancer: Mechanisms and Novel Therapeutic Targets.” *Seminars in Cancer Biology*. https://doi.org/10.1016/j.semcancer.2015.02.006.

———. 2015b. “Sustained Proliferation in Cancer: Mechanisms and Novel Therapeutic Targets.” *Seminars in Cancer Biology*. Academic Press. https://doi.org/10.1016/j.semcancer.2015.02.006.

Fitzgerald, Timothy L., Kvin Lertpiriyapong, Lucio Cocco, Alberto M. Martelli, Massimo

Libra, Saverio Candido, Giuseppe Montalto, et al. 2015a. “Roles of EGFR and KRAS and Their Downstream Signaling Pathways in Pancreatic Cancer and Pancreatic Cancer Stem Cells.” *Advances in Biological Regulation*. https://doi.org/10.1016/j.jbior.2015.06.003.

Franken, Nicolaas A.P., Hans M. Rodermond, Jan Stap, Jaap Haveman, and Chris van Bree. 2006. “Clonogenic Assay of Cells in Vitro.” *Nature Protocols* 1 (5): 2315–19. https://doi.org/10.1038/nprot.2006.339.

Frentzel, Julie, Domenico Sorrentino, and Sylvie Giuriato. 2017. “Targeting Autophagy in ALK-Associated Cancers.” *Cancers* 9 (161): 1–19. https://doi.org/10.3390/cancers9120161.

Galvao, Joana, Benjamin Davis, Mark Tilley, Eduardo Normando, Michael R. Duchen, and M. Francesca Cordeiro. 2014. “Unexpected Low-Dose Toxicity of the Universal Solvent DMSO.” *FASEB Journal* 28 (3): 1317–30. https://doi.org/10.1096/fj.13-235440.

García-Echeverría, Carlos, Mark A. Pearson, Andreas Marti, Thomas Meyer, Juergen Mestan, Johann Zimmermann, Jiaping Gao, et al. 2004. “In Vivo Antitumor Activity of NVP-AEW541 - A Novel, Potent, and Selective Inhibitor of the IGF-IR Kinase.” *Cancer Cell* 5: 231–39. https://doi.org/10.1016/S1535-6108(04)00051-0.

Ghaneh, P, E Costello, and J P Neoptolemos. 2008. “Biology and Management of Pancreatic Cancer,” 478–97. https://doi.org/10.1136/gut.2006.103333.

Giovannetti, E., C. L. van der Borden, A. E. Frampton, A. Ali, O. Firuzi, and G. J. Peters. 2017. “Never Let It Go: Stopping Key Mechanisms Underlying Metastasis to Fight Pancreatic Cancer.” *Seminars in Cancer Biology*. https://doi.org/10.1016/j.semcancer.2017.04.006.

Girnita, Ada, Leonard Girnita, Fabrizio Del Prete, Armando Bartolazzi, Olle Larsson, and Magnus Axelson. 2004. “Cyclolignans as Inhibitors of the Insulin-Like Growth Factor-1 Receptor and Malignant Cell Growth.” *Cancer Research* 64 (1): 236–42. https://doi.org/10.1158/0008-5472.CAN-03-2522.

Globocan, 2012. Globocan 2014: Estimated Cancer Incidence, Mortality and Prevalence Worldwide in 2014. Prediction-future burden. [Online] [Accessed 3 July 2019].

Gozuacik, Devrim, and Adi Kimchi. 2004. “Autophagy as a Cell Death and Tumor Suppressor Mechanism,” 2891–2906. https://doi.org/10.1038/sj.onc.1207521.

Grasso, Cristoforo, Gerrit Jansen, and Elisa Giovannetti. 2017. “Drug Resistance in Pancreatic Cancer: Impact of Altered Energy Metabolism.” *Critical Reviews in Oncology/Hematology*. Elsevier Ireland Ltd. https://doi.org/10.1016/j.critrevonc.2017.03.026.

Grützmann, Robert, Hans Detlev Saeger, Jutta Lüttges, Hans Konrad Schackert, Holger Kalthoff, Günter Klöppel, and Christian Pilarsky. 2004. “Microarray-Based Gene Expression Profiling in Pancreatic Ductal Carcinoma: Status Quo and Perspectives.” *International Journal of Colorectal Disease* 19 (5): 401–13. https://doi.org/10.1007/s00384-003-0563-3.

Hakam, Ardeshir, Quan Fang, and Richard Karl. 2003. “Coexpression of IGF-1R and c-Src Proteins in Human Pancreatic Ductal Adenocarcinoma” 48 (10): 1972–78.

Hamacher, Rainer, Roland M. Schmid, Dieter Saur, and Günter Schneider. 2008. “Apoptotic Pathways in Pancreatic Ductal Adenocarcinoma.” *Molecular Cancer* 7 (64): 1–10. https://doi.org/10.1186/1476-4598-7-64.

Hanahan, Douglas, and Robert A Weinberg. 2011. “Review Hallmarks of Cancer : The Next Generation.” *Cell* 144 (5): 646–74. https://doi.org/10.1016/j.cell.2011.02.013.

Hanahan, Douglas, Robert A Weinberg, and San Francisco. 2000. “The Hallmarks of Cancer Review.” *Cell* 100: 57–70.

Hanna, Thomas, and William Greenhalf. 2017. “Personalized Therapy for Pancreatic Cancer : Challenges and Opportunities.” *Clinicals in Oncology* 2 (1242): 1–10.

Hashemi, Jamileh, Claire Worrall, Daiana Vasilcanu, Mårten Fryknäs, Luqman Sulaiman, Mohsen Karimi, Wen Hui Weng, et al. 2011. “Molecular Characterization of Acquired Tolerance of Tumor Cells to Picropodophyllin (PPP).” *PLoS ONE* 6 (3). https://doi.org/10.1371/journal.pone.0014757.

Hassan, Burhan, Argun Akcakanat, Ashley M. Holder, and Funda Meric-Bernstam. 2013. “Targeting the PI3-Kinase/Akt/MTOR Signaling Pathway.” *Surgical Oncology Clinics of North America* 22 (4): 641–64. https://doi.org/10.1016/j.soc.2013.06.008.

Heidegger, Isabel, Andreas Pircher, Helmut Klocker, and Petra Massoner. 2011. “Targeting

the Insulin-like Growth Factor Network in Cancer Therapy." *Cancer Biology and Therapy* 11 (8): 701–7. https://doi.org/10.4161/cbt.11.8.14689.

Hezel, Aram F, Alec C Kimmelman, Ben Z Stanger, Nabeel Bardeesy, and Ronald A Depinho. 2006. "Genetics and Biology of Pancreatic Ductal Adenocarcinoma" 1: 1218–49. https://doi.org/10.1101/gad.1415606.PDAC.

Hotz, Birgit, Marco Arndt, Sonja Dullat, Sarah Bhargava, Heinz J. Buhr, and Hubert G. Hotz. 2007. "Epithelial to Mesenchymal Transition: Expression of the Regulators Snail, Slug, and Twist in Pancreatic Cancer." *Clinical Cancer Research* 13 (16): 4769–76. https://doi.org/10.1158/1078-0432.CCR-06-2926.

Houg, Demi S, and Maarten F Bijlsma. 2018. "The Hepatic Pre-Metastatic Niche in Pancreatic Ductal Adenocarcinoma," 1–18.

Hruban, Ralph H, Michael Goggins, Jennifer Parsons, and Scott E Kern. 2000. "Progression Model for Pancreatic Cancer 1" 6 (August): 2969–72.

Hu, Guo-fang, Xiao Han, Xia Wang, and Zhe-hai Wang. 2016. "Efficacy and Safety of Gemcitabine plus Erlotinib for Locally Advanced or Metastatic Pancreatic Cancer : A Systematic Review and Meta-Analysis." *Drug Design, Development and Therapy* 10 (6): 1961–72.

Huang, Lihua, and Liwu Fu. 2015. "Mechanisms of Resistance to EGFR Tyrosine Kinase Inhibitors." *Acta Pharmaceutica Sinica B* 5 (5): 390–401. https://doi.org/10.1016/j.apsb.2015.07.001.

Huang, Tzu-Chuan Jane, Siddhartha Kar, and Milind Javle. 2010. "Personalized Therapy for Pancreatic Cancer: Myth or Reality in 2010?" *Journal of Gastrointestinal Oncology* 1 (1): 24–33. https://doi.org/10.3978/j.issn.2078-6891.2010.009.

Ilic, Milena, and Irena Ilic. 2016. "Epidemiology of Pancreatic Cancer" 22 (44): 9694–9705. https://doi.org/10.3748/wjg.v22.i44.9694.

Jamieson, Nigel Balfour, David K. Chang, Sean M. Grimmond, and Andrew V. Biankin. 2014. "Can We Move towards Personalised Pancreatic Cancer Therapy?" *Expert Review of Gastroenterology and Hepatology* 8 (4): 335–38. https://doi.org/10.1586/17474124.2014.893820.

Jones, Siân, Xiaosong Zhang, D. Williams Parsons, Jimmy Cheng Ho Lin, Rebecca J. Leary,

Philipp Angenendt, Parminder Mankoo, et al. 2008. “Core Signaling Pathways in Human Pancreatic Cancers Revealed by Global Genomic Analyses.” *Science* 321 (5897): 1801–6. https://doi.org/10.1126/science.1164368.

Juiz, Natalia Anahi, Juan Iovanna, and Nelson Dusetti. 2019. “Pancreatic Cancer Heterogeneity Can Be Explained beyond the Genome.” *Frontiers in Oncology*. Frontiers Media S.A. https://doi.org/10.3389/fonc.2019.00246.

Kamisawa, Terumi, Laura D Wood, Takao Itoi, and Kyoichi Takaori. 2016. “Pancreatic Cancer.” *The Lancet* 388 (10039): 73–85. https://doi.org/10.1016/S0140-6736(16)00141-0.

Kasprzak, Aldona, Wojciech Kwasniewski, Agnieszka Adamek, and Anna Gozdzicka-Jozefiak. 2017. “Insulin-like Growth Factor (IGF) Axis in Cancerogenesis.” *Mutation Research - Reviews in Mutation Research* 772: 78–104. https://doi.org/10.1016/j.mrrev.2016.08.007.

Kwak, Ah Won, Goo Yoon, Mee Hyun Lee, Seung Sik Cho, Jung Hyun Shim, and Jung Il Chae. 2020. “Picropodophyllotoxin, an Epimer of Podophyllotoxin, Causes Apoptosis of Human Esophageal Squamous Cell Carcinoma Cells through ROS-Mediated JNK/P38 MAPK Pathways.” *International Journal of Molecular Sciences* 21 (13): 1–13. https://doi.org/10.3390/ijms21134640.

Law, Henry C.H., Dragana Lagundzin, Emalie J. Clement, Fangfang Qiao, Zachary S. Wagner, Kimiko L. Krieger, Diane Costanzo-Garvey, et al. 2020. “The Proteomic Landscape of Pancreatic Ductal Adenocarcinoma Liver Metastases Identifies Molecular Subtypes and Associations with Clinical Response A C.” *Clinical Cancer Research* 26 (5): 1065–76. https://doi.org/10.1158/1078-0432.CCR-19-1496.

Li, Heming, Izhar Singh Batth, Xiujuan Qu, Ling Xu, Na Song, Ruoyu Wang, and Yunpeng Liu. 2017. “IGF-IR Signaling in Epithelial to Mesenchymal Transition and Targeting IGF-IR Therapy: Overview and New Insights.” *Molecular Cancer*. BioMed Central Ltd. https://doi.org/10.1186/s12943-016-0576-5.

Liu, Menghan, Sarah E. Hancock, Ghazal Sultani, Brendan P. Wilkins, Eileen Ding, Brenna Osborne, Lake-Ee Quek, and Nigel Turner. 2019. “Snail-Overexpression Induces Epithelial-Mesenchymal Transition and Metabolic Reprogramming in Human Pancreatic Ductal Adenocarcinoma and Non-Tumorigenic Ductal Cells.” *Journal of*

Clinical Medicine 8 (6): 822–40. https://doi.org/10.3390/jcm8060822.

Luo, Xin, Zhulin Yang, Xiao Liu, Ziru Liu, Xiongying Miao, Daiqiang Li, Qiong Zou, and Yuan Yuan. 2017. "The Clinicopathological Significance of Forkhead Box P1 and Forkhead Box O3a in Pancreatic Ductal Adenocarcinomas." *Tumor Biology* 39 (5). https://doi.org/10.1177/1010428317699129.

Maitra, Anirban, and Ralph H Hruban. 2008. "Pancreatic Cancer." *Annual Review of Pathology-Mechanisms of Disease* 3: 157–88. https://doi.org/10.1146/annurev.path.

Marchetti, Antonio, Carla Martella, Lara Felicioni, Fabio Barassi, Simona Salvatore, and Antonio Chella. 2005. "EGFR Mutations in Non – Small-Cell Lung Cancer : Analysis of a Large Series of Cases and Development of a Rapid and Sensitive Method for Diagnostic Screening With Potential Implications on Pharmacologic Treatment." *Journal of Clinical Oncology* 23 (4): 857–65. https://doi.org/10.1200/JCO.2005.08.043.

McCaffery, Ian, Yanyan Tudor, Hongjie Deng, Rui Tang, Samuel Suzuki, Sunita Badola, Hedy L. Kindler, et al. 2013. "Putative Predictive Biomarkers of Survival in Patients with Metastatic Pancreatic Adenocarcinoma Treated with Gemcitabine and Ganitumab, an IGF1R Inhibitor." *Clinical Cancer Research* 19 (15): 4282–89. https://doi.org/10.1158/1078-0432.CCR-12-1840.

McCubrey, James A., Linda S. Steelman, Steven L. Abrams, John T. Lee, Fumin Chang, Fred E. Bertrand, Patrick M. Navolanic, et al. 2006. "Roles of the RAF/MEK/ERK and PI3K/PTEN/AKT Pathways in Malignant Transformation and Drug Resistance." *Advances in Enzyme Regulation* 46 (1): 249–79. https://doi.org/10.1016/j.advenzreg.2006.01.004.

Meikle, Claire K. S., Clare A. Kelly, Priyanka Garg, Leah M. Wuescher, Ramadan A. Ali, and Randall G. Worth. 2017. "Cancer and Thrombosis: The Platelet Perspective." *Frontiers in Cell and Developmental Biology* 4. https://doi.org/10.3389/fcell.2016.00147.

Michl, Patrick, and Thomas M. Gress. 2013. "Current Concepts and Novel Targets in Advanced Pancreatic Cancer." *Gut* 62 (2): 317–26. https://doi.org/10.1136/gutjnl-2012-303588.

Mihaljevic, A. L., I. Esposito, H. Friess, and J. Kleeff. 2009. "Molecular Biology, Models,

and Histopathology of Chronic Pancreatitis and Pancreatic Cancer." *European Surgery - Acta Chirurgica Austriaca* 41 (6): 250–67. https://doi.org/10.1007/s10353-009-0496-3.

Milan, Marta, Giuseppe R Diaferia, and Gioacchino Natoli. 2021. "Tumor Cell Heterogeneity and Its Transcriptional Bases in Pancreatic Cancer: A Tale of Two Cell Types and Their Many Variants." *The EMBO Journal* 40 (e107206): 1–12. https://doi.org/10.15252/embj.2020107206.

Moore, Malcolm J, David Goldstein, John Hamm, Arie Figer, Joel R Hecht, Steven Gallinger, Heather J Au, et al. 2007. "Erlotinib Plus Gemcitabine Compared With Gemcitabine Alone in Patients With Advanced Pancreatic Cancer : A Phase III Trial of the National Cancer Institute of Canada Clinical Trials Group." *Journal of Clinical Oncology* 25 (15): 1960–66. https://doi.org/10.1200/JCO.2006.07.9525.

Moore, Bence Sipos, Simonetta Orlandini, Claudio Sorio, Francisco X Real, Nicholas R Lemoine, Thomas Gress, Claudio Bassi, Analysis K-ras, and D P C Smad. 2001. "Genetic Profile of 22 Pancreatic Carcinoma Cell Lines," 798–802. https://doi.org/10.1007/s004280100474.

Moschos, Stergios J, and Christos S Mantzoros. 2002. "The Role of the IGF System in Cancer : From Basic to Clinical Studies and Clinical Applications" 02215: 317–32. https://doi.org/10.1159/000066230.

Nandy, Debashis, and Debabrata Mukhopadhyay. 2011. "Growth Factor Mediated Signaling in Pancreatic Pathogenesis." *Cancers* 3 (1): 841–71. https://doi.org/10.3390/cancers3010841.

Nijkamp, Monique M, Paul N Span, Johan Bussink, and Johannes H A M Kaanders. 2013. "Interaction of EGFR with the Tumour Microenvironment : Implications for Radiation Treatment." *Radiotherapy and Oncology* 108 (1): 17–23. https://doi.org/10.1016/j.radonc.2013.05.006.

Oliveira-cunha, Melissa, William G Newman, and Ajith K Siriwardena. 2011. "Epidermal Growth Factor Receptor in Pancreatic Cancer," 1513–26. https://doi.org/10.3390/cancers3021513.

Paez, Guillermo J, and William Sellers. 2003. "PI3K/PTEN/AKT/PATHWAY A Critical Mediator of Oncogenic Signalling." In *Cancer Treatment and Research*, 145–67.

https://doi.org/10.1007/0-306-48158-8.

Pan, Sheng, Teresa A. Brentnall, and Ru Chen. 2020. “Proteome Alterations in Pancreatic Ductal Adenocarcinoma.” *Cancer Letters* 469 (September 2019): 429–36. https://doi.org/10.1016/j.canlet.2019.11.020.

Park, Seok Ju, Mi Jin Gu, Dong Shik Lee, Sung Soo Yun, Hong Jin Kim, and Joon Hyuk Choi. 2015. “Original Article EGFR Expression in Pancreatic Intraepithelial Neoplasia and Ductal Adenocarcinoma” 8 (7): 8298–8304.

Penchev, Vesselin R, Zeshaan A Rasheed, Anirban Maitra, and William Matsui. 2012. “Heterogeneity and Targeting of Pancreatic Cancer Stem Cells.” *Clinical Cancer Research* 18 (16): 4277–84. https://doi.org/10.1158/1078-0432.CCR-11-3112.Heterogeneity.

Public Health England. Passage numbers explained. Public Health England. 2017. Available from: https://www.phe-culturecollections.org.uk/media/114565/m219_passage-numbers-explained.pdf. (Accessed July 2017)

Rajabpour, Azam, Farzad Rajaei, and Ladan Teimoori-Toolabi. 2017. “Molecular Alterations Contributing to Pancreatic Cancer Chemoresistance.” *Pancreatology*. Elsevier B.V. https://doi.org/10.1016/j.pan.2016.12.013.

Raphael, Benjamin J., Ralph H. Hruban, Andrew J. Aguirre, Richard A. Moffitt, Jen Jen Yeh, Chip Stewart, A. Gordon Robertson, et al. 2017. “Integrated Genomic Characterization of Pancreatic Ductal Adenocarcinoma.” *Cancer Cell* 32 (2): 185-203.e13. https://doi.org/10.1016/j.ccell.2017.07.007.

Rebucci, Magali, and Carine Michiels. 2013. “Molecular Aspects of Cancer Cell Resistance to Chemotherapy.” *Biochemical Pharmacology* 85 (9): 1219–26. https://doi.org/10.1016/j.bcp.2013.02.017.

Renoir, Jack Michel, Véronique Marsaud, and Gwendal Lazennec. 2013. “Estrogen Receptor Signaling as a Target for Novel Breast Cancer Therapeutics.” *Biochemical Pharmacology* 85 (4): 449–65. https://doi.org/10.1016/j.bcp.2012.10.018.

Ross, Michael H, and Wojciech Pawlina. 2011. *Histology A Text and Atlas*. Sixth.

Santilli, F., A. Boccatonda, and G. Davì. 2016. “Aspirin, Platelets, and Cancer: The Point of View of the Internist.” *European Journal of Internal Medicine* 34: 11–20.

https://doi.org/10.1016/j.ejim.2016.06.004.

Sciver, Robert E Van, Michael P Lee, Caroline Dasom Lee, Alex C Lafever, Elizaveta Svyatova, Kevin Kanda, Amber L Collier, et al. 2018. “A New Strategy to Control and Eradicate ‘ Undruggable ’ Oncogenic K-RAS-Driven Pancreatic Cancer : Molecular Insights and Core Principles Learned from Developmental and Evolutionary Biology.” *Cancers* 10 (142): 1–24. https://doi.org/10.3390/cancers10050142.

Scotlandi, Katia, Maria Cristina Manara, Giordano Nicoletti, Pier Luigi Lollini, Stella Lukas, Stefania Benini, Stefania Croci, et al. 2005. “Antitumor Activity of the Insulin-like Growth Factor-I Receptor Kinase Inhibitor NVP-AEW541 in Musculoskeletal Tumors.” *Cancer Research* 65 (9): 3868–76. https://doi.org/10.1158/0008-5472.CAN-04-3192.

Seccareccia, Erica, and Pnina Brodt. 2012. “The Role of the Insulin-like Growth Factor-I Receptor in Malignancy: An Update.” *Growth Hormone and IGF Research*. https://doi.org/10.1016/j.ghir.2012.09.003.

Sharma, Khushboo, Ngoc Le, Moureq Alotaibi, and David A Gewirtz. 2014. “Cytotoxic Autophagy in Cancer Therapy,” 10034–51. https://doi.org/10.3390/ijms150610034.

She, Qing Bai, David B. Solit, Qing Ye, Kathryn E. O’Reilly, Jose Lobo, and Neal Rosen. 2005. “The BAD Protein Integrates Survival Signaling by EGFR/MAPK and PI3K/Akt Kinase Pathways in PTEN-Deficient Tumor Cells.” *Cancer Cell* 8 (4): 287–97. https://doi.org/10.1016/j.ccr.2005.09.006.

Silva, Manuel T. 2010. “Secondary Necrosis: The Natural Outcome of the Complete Apoptotic Program.” *FEBS Letters* 584 (22): 4491–99. https://doi.org/10.1016/j.febslet.2010.10.046.

Singh, Mansher, and Anirban Maitra. 2007. “Precursor Lesions of Pancreatic Cancer : Molecular Pathology and Clinical” 21231: 9–19. https://doi.org/10.1159/000101873.

Sipos, Bence, Simone Möser, Holger Kalthoff, and Virag Török. 2003. “A Comprehensive Characterization of Pancreatic Ductal Carcinoma Cell Lines: Towards the Establishment of an in Vitro Research Platform.” *Virchows Archiv* 442 (5): 444–52. https://doi.org/10.1007/s00428-003-0784-4.

Skandalis, Spyros S, Nikolaos Afratis, Gianna Smirlaki, Dragana Nikitovic, Achilleas D Theocharis, George N Tzanakakis, and Nikos K Karamanos. 2014. “Cross-Talk between

Estradiol Receptor and EGFR / IGF-IR Signaling Pathways in Estrogen-Responsive Breast Cancers : Focus on the Role and Impact of Proteoglycans ☆." *Matrix Biology* 35: 182–93. https://doi.org/10.1016/j.matbio.2013.09.002.

Song, Yao, Tomohisa Baba, and Naofumi Mukaida. 2016. "Gemcitabine Induces Cell Senescence in Human Pancreatic Cancer Cell Lines." *Biochemical and Biophysical Research Communications* 477 (3): 515–19. https://doi.org/10.1016/j.bbrc.2016.06.063.

Subramani, Ramadevi, Rebecca Lopez-Valdez, Arunkumar Arumugam, Sushmita Nandy, Thiyagarajan Boopalan, and Rajkumar Lakshmanaswamy. 2014. "Targeting Insulin-like Growth Factor 1 Receptor Inhibits Pancreatic Cancer Growth and Metastasis." *PLoS ONE* 9 (5): e97016. https://doi.org/10.1371/journal.pone.0097016.

Sumida, Kayo, Yoshinobu Igarashi, Naoki Toritsuka, Tomochika Matsushita, Kaori Abe-Tomizawa, Mikio Aoki, Tetsuro Urushidani, Hiroshi Yamada, and Yasuo Ohno. 2011. "Effects of DMSO on Gene Expression in Human and Rat Hepatocytes." *Human and Experimental Toxicology* 30 (10): 1701–9. https://doi.org/10.1177/0960327111399325.

Swayden, Mirna, Juan Iovanna, and Philippe Soubeyran. 2018. "Pancreatic Cancer Chemo-Resistance Is Driven by Tumor Phenotype Rather than Tumor Genotype." *Heliyon*. Elsevier Ltd. https://doi.org/10.1016/j.heliyon.2018.e01055.

Tang, Hongwei, Peng Wei, Ping Chang, Yanan Li, Dong Yan, Chang Liu, Manal Hassan, and Donghui Li. 2017. "Genetic Polymorphisms Associated with Pancreatic Cancer Survival: A Genome-Wide Association Study." *International Journal of Cancer* 141 (4): 678–86. https://doi.org/10.1002/ijc.30762.

Teicher, B.A. 2003. *Cancer Drug Resistance (Cancer Drug Discovery and Development)*. Vol. 14. http://www.springer.com/series/7625.

Tomizawa, Minoru, Fuminobu Shinozaki, Takao Sugiyama, Shigenori Yamamoto, Makoto Sueishi, and Takanobu Yoshida. 2010. "Insulin-like Growth Factor-I Receptor in Proliferation and Motility of Pancreatic Cancer." *World Journal of Gastroenterology* 16 (15): 1854–58. https://doi.org/10.3748/wjg.v16.i15.1854.

Torres, Carolina, and Paul J. Grippo. 2018. "Pancreatic Cancer Subtypes: A Roadmap for Precision Medicine." *Annals of Medicine* 50 (4): 277–87. https://doi.org/10.1080/07853890.2018.1453168.

Trajkovic-Arsic, Marija, Evdokia Kalideris, and Jens T Siveke. 2013. “The Role of Insulin and IGF System in Pancreatic Cancer.” *Journal of Molecular Endocrinology* 50 (3): R67–74. https://doi.org/10.1530/jme-12-0259.

Valle, Sandra, Laura Martin-hijano, Sonia Alcal, Marta Alonso-nocelo, and Bruno Sainz Jr. 2018. “The Ever-Evolving Concept of the Cancer Stem Cell in Pancreatic Cancer.” *Cancers* 10 (33). https://doi.org/10.3390/cancers10020033.

Valsecchi, Matias E, Mary Mcdonald, Jonathan R Brody, and Terry Hyslop. 2012. “Epidermal Growth Factor Receptor and Insulinlike Growth Factor 1 Receptor Expression Predict Poor Survival in Pancreatic Ductal Adenocarcinoma.” *Cancer*, 3484–93. https://doi.org/10.1002/cncr.26661.

Vasilcanu, Daiana, Ada Girnita, Leonard Girnita, Radu Vasilcanu, Magnus Axelson, and Olle Larsson. 2004. “The Cyclolignan PPP Induces Activation Loop-Specific Inhibition of Tyrosine Phosphorylation of the Insulin-like Growth Factor-1 Receptor. Link to the Phosphatidyl Inositol-3 Kinase/Akt Apoptotic Pathway.” *Oncogene* 23 (47): 7854–62. https://doi.org/10.1038/sj.onc.1208065.

Verheijen, M., M. Lienhard, Y. Schrooders, O. Clayton, R. Nudischer, S. Boerno, B. Timmermann, et al. 2019. “DMSO Induces Drastic Changes in Human Cellular Processes and Epigenetic Landscape in Vitro.” *Scientific Reports* 9 (1): 1–12. https://doi.org/10.1038/s41598-019-40660-0.

Vincent, Audrey, Joseph Herman, Rich Schulick, Ralph H Hruban, and Michael Goggins. 2011. “Pancreatic Cancer” 378 (9791): 607–20. https://doi.org/10.1016/S0140-6736(10)62307-0.Pancreatic.

Vuoriluoto, K., H. Haugen, S. Kiviluoto, J. P. Mpindi, J. Nevo, C. Gjerdrum, C. Tiron, J. B. Lorens, and J. Ivaska. 2011. “Vimentin Regulates EMT Induction by Slug and Oncogenic H-Ras and Migration by Governing Axl Expression in Breast Cancer.” *Oncogene* 30 (12): 1436–48. https://doi.org/10.1038/onc.2010.509.

Wang, Zhiwei, Yiwei Li, Dejuan Kong, Sanjeev Banerjee, Aamir Ahmad, Asfar Sohail Azmi, Shadan Ali, James L. Abbruzzese, Gary E. Gallick, and Fazlul H. Sarkarr. 2009. “Acquisition of Epithelial-Mesenchymal Transition Phenotype of Gemcitabine-Resistant Pancreatic Cancer Cells Is Linked with Activation of the Notch Signaling Pathway.” *Cancer Research* 69 (6): 2400–2407. https://doi.org/10.1158/0008-5472.CAN-08-4312.

Welsch, Thilo, Jörg Kleeff, and Helmut Riess. 2007. “Molecular Pathogenesis of Pancreatic Cancer: Advances and Challenges.” *Current Molecular Medicine* 7 (5): 504–21. https://doi.org/10.2174/156652407781387082.

Wlodarczyk, Barbara, Anita Gasiorowska, and Ewa Malecka-Panas. 2018. “The Role of Insulin-like Growth Factor (IGF) Axis in Early Diagnosis of Pancreatic Adenocarcinoma (PDAC).” *Journal of Clinical Gastroenterology* 52 (7): 569–72. https://doi.org/10.1097/MCG.0000000000001073.

Wong, Matthew H., Aiqun Xue, Sohel M. Julovi, Nick Pavlakis, Jaswinder S. Samra, Thomas J. Hugh, Anthony J. Gill, Lyndsay Peters, Robert C. Baxter, and Ross C. Smith. 2014. “Cotargeting of Epidermal Growth Factor Receptor and PI3K Overcomes PI3K-Akt Oncogenic Dependence in Pancreatic Ductal Adenocarcinoma.” *Clinical Cancer Research* 20 (15): 4047–58. https://doi.org/10.1158/1078-0432.CCR-13-3377.

Wong, Matthew H. 2015. “Overcoming Primary and Acquired Erlotinib Resistance with Epidermal Growth Factor Receptor (EGFR) and Phophoinisitide-3 Kinase (PI3K) Co-Inhibition in Pancreatic Cancer.” *PhD Thesis*.

Wu, Liuji, Xiuli Hu, and Haitao Tang. 2014. “Valid Application of Western Blotting.” *Mol Biol Rep* 41: 3517–20. https://doi.org/10.1007/s11033-014-3215-5.

Yachida, Shinichi, and Christine A Iacobuzio-donahue. 2008. “The Pathology and Genetics of Metastatic,” 413–22.

Xu Q, Fu R, Yin G, Liu X, Liu Y, Xiang M. Microarray-based gene expression profiling reveals genes and pathways involved in the oncogenic function of REG3A on pancreatic cancer cells. Gene. 2016 Mar 10;578(2):263-73. doi: 10.1016/j.gene.2015.12.039. Epub 2015 Dec 21. PMID: 26719042.

Yang, Shenghong, Xiaoxu Wang, Gianmarco Contino, Marc Liesa, Ergun Sahin, Haoqiang Ying, Alexandra Bause, et al. 2011. “Pancreatic Cancers Require Autophagy for Tumor Growth,” 717–29. https://doi.org/10.1101/gad.2016111.pathways.

Yarden, Y. 2001. “The EGFR Family and Its Ligands in Human Cancer : Signalling Mechanisms and Therapeutic Opportunities” 37: 3–8.

Yewale, Chetan, Dipesh Baradia, Imran Vhora, Sushilkumar Patil, and Ambikanandan Misra. 2013. “Epidermal Growth Factor Receptor Targeting in Cancer : A Review of Trends

and Strategies." *Biomaterials* 34 (34): 8690–8707. https://doi.org/10.1016/j.biomaterials.2013.07.100.

Yuan, Y. L., X. H. Zhou, Jian Song, X. P. Qiu, Jun Li, and L. F. Ye. 2008. "Dual Silencing of Type 1 Insulin-like Growth Factor and Epidermal Growth Factor Receptors to Induce Apoptosis of Nasopharyngeal Cancer Cells." *Journal of Laryngology and Otology* 122 (9): 952–60. https://doi.org/10.1017/S0022215107000606.

APPENDICES

Appendix A: Ethics Waiver

UNIVERSITY OF THE WITWATERSRAND, JOHANNESBURG

HUMAN RESEARCH ETHICS COMMITTEE (MEDICAL)

Ref: W-CP-190708-2

08 July 2019

TO WHOM IT MAY CONCERN:

Waiver: This certifies that the following research does not require clearance from the Human Research Ethics Committee (Medical).

Investigator:	**Derushka Arnachellen (student no 811551)**
Co-Investigators:	**Caroline Dickens**
Supervisor:	**Martin Brand and Raquel Duarte**
Faculty:	Health Sciences
School:	Clinical Medicine
Department:	Internal Medicine
Project title:	Profiling the insulin-like growth factor receptor pathway in pancreatic ductal adenocarcinoma cell lines
Reason:	In vitro lab study using commercially available PDAC cell lines namely: HPDE-1,PANC-1,PANC-2,Capan-2,ASPC-1,RWP-1 and CF PAC-1. No humans, human data and human tissues will be used in this study.

Dr Clement Penny

Chair: Human Research Ethics Committee (Medical)

Copy – HREC (Medical) Secretariat

Research Office Secretariat: Faculty of Health Sciences, Phillip Tobias Building, 3rd Floor, Office 301, 29 Princess of Wales Terrace, Parktown, 2193 Tel +27 (0)11-717-1252 /1234/2656/2700 Private Bag 3, Wits 2050, email: zanele.ndlovu@wits.ac.za Office email: hrec-medical.researchoffice@wits.ac.zaWebsite: www.wits.ac.za/research/about-our-research/ethics-and-research-integrity/

Appendix B: Solutions

1. 0.1 % BSA

Dissolve 1 g of bovine serum albumin 10 ml of phosphate buffered saline (PBS). Filter sterilize and store solution at -20 °C.

2. 0.5 % Crystal Violet Solution

Dissolve 5 g crystal violet powder (Sigma-Aldrich) in 80 mL distilled H_2O. Then add 20 ml methanol.

Store solution in the dark at room temperature.

3. Radioimmunoprecipitation (RIPA) Buffer

The following components were combined:

5 ml 1 M Tris-HCl pH 7.4

30 ml 5 M NaCl

5 ml 20 % NP-40

5 ml 10 % Sodium deoxycholate

0.5 ml 20 % SDS (*see 8.4.*)

Adjust volume to 50 mL with dH_2O and store at 4 °C.

Add Protease Inhibitor Cocktail (1:1000) before use.

4. 20% SDS

Dissolve 20 g SDS in 10 ml dH_20 and store at RT

5. 10% SDS

Dissolve 1 g SDS in 10 mL dH_2O and store at RT.

6. 10% APS

Dissolve 1 g APS in 10 ml dH_2O and store at 4 °C.

7. Stacking Gel Buffer (0.5 M Tris-HCl)

Dissolve 6.05 g Tris in 70 ml dH_2O and adjust the pH to 6.8 using HCl.

Adjust the volume of the solution to 100 ml and store at RT.

8. Separating Gel Buffer (1.5 M Tris-HCl)

Dissolve 18.17 g Tris in 70 ml dH_2O and adjust pH to 8.8 using HCl.

Adjust the volume of the solution to 100 ml and store at RT.

9. 6x Loading Dye

Combine the following components:

3.75 ml 1M Tris-HCl (pH 6.8)

6 ml Glycerol

1.2 g SDS

0.93 g DTT

6 mg Bromophenol blue

Adjust the volume of the solution to 10 ml with dH_2O and store at –20 ˚C in

0.5 ml aliquots.

10. Sodium Dodecyl Sulphate Polyacrylamide Gel

10.1. 10% Separating Gel

3.35 ml 30 % Acrylamide

1.25 ml 1.5 M Tris-HCl buffer pH 8.8 (see 8.8)

100 µl 10 % SDS

3.95 ml dH_2O

500 µl 10% APS (see 8.6)

5 µl TEMED

Pour immediately and allow to polymerize. Pour 70% ethanol over the gel to prevent it from drying out.

10.2. 4% Stacking Gel

Mix the following together:

6.25 µl 30 % Acrylamide

1.25 ml 0.5 M Tris-HCl pH 6.8 buffer (see 8.7)

50 µl 10 % SDS

2.83 ml dH_2O

250 µl 10 % APS (see 8.6)

2.5 µl TEMED

Immediately pour over separating gel.

11. 1 x SDS Running Buffer

Dilute

50 ml Biorad Running buffer

450 ml dH_20

12. Transfer Buffer

12.1. 10x Transfer Buffer

Dissolve

30.3 g Tris base

144.1 g Glycine

In 800 ml dH_2O, adjust the volume of the solution to 1 L with dH_2O and store at RT.

12.2. 1x Transfer Buffer

100 ml 10x Transfer Buffer stock

100 ml Methanol

800 ml dH_2O

Store at 4 °C

13. 1X PBS-Tween

Add 1 ml Tween-20 to 1 L of 1X PBS and mix thoroughly and store at RT.

14. 3% BSA in 1X PBS-Tween

Dissolve 3 g BSA in 100 ml 1X PBS-Tween and store at 4 °C.

15. DNase incubation mix

Add 10 µl DNase I stock solution to 70 µl Buffer RDD. Mix by gently inverting the tube.

16. Annexin V Human ELISA

16.1. Reagent Preparation

16.1.1. 1 X Wash Buffer

Dilute 25 ml of the 20 X wash buffer concentrate with 475 ml distilled water.

Mix thoroughly.

16.1.2. 1 X Assay Buffer

Dilute 2.5 ml of the 20 X Assay Buffer in 47.5 ml distilled water.

Mix gently.

16.1.3. 1 X Biotin Conjugated Antibody

Dilute 60 µl of the Biotin Conjugated Antibody with 5.94 ml of 1 X Assay Buffer.

Use within 30 minutes of dilution.

16.1.4. 1 X Streptavidin-HRP Conjugate

Dilute 60 µl of the Streptavidin-HRP Conjugate in 11.94 ml 1 X Assay Buffer.

Use within 30 minutes of diluting.

16.2. Standard Preparations

STANDARD	SAMPLE TO DILUTE	VOLUME TO DILUTE (µl)	VOLUME OF DILUENT (µl)	STARTING CONCENTRATION (ng/ml)	FINAL CONCENTRATION (ng/ml)
1	Stock	225	225	100	50
2	Standard 1	225	225	50	25
3	Standard 2	225	225	25	12.5
4	Standard 3	225	225	12.5	6.25
5	Standard 4	225	225	6.25	3.13
6	Standard 5	225	225	3.13	1.56
7	Standard 6	225	225	1.56	0.78
8	None	-	225	-	0

Appendix C: Supplementary data

1. BCA protein Quantification

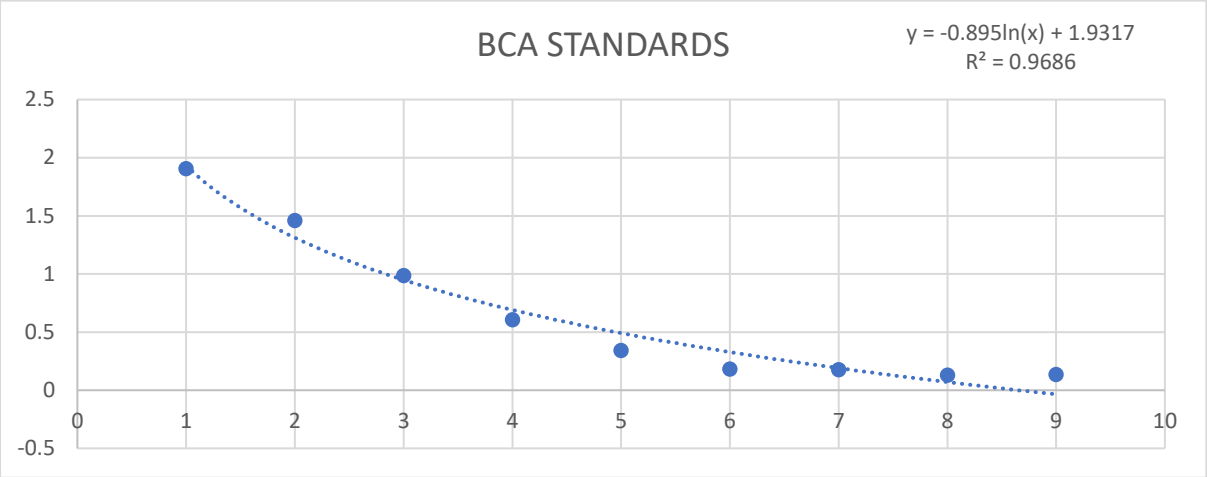

Figure C.1. Logarithmic graph showing BCA standards for protein quantification

The protein concentrations of each sample were determined using the standard curve generated in figure C.1 and the following was determined:

Table C.1: determination of protein concentrations for each sample

Sample			**mg/ml**	**5x loading dye**	**Protein concentration µg/ µl**		
	average	*x*	x *5*	x *0.8*	*10*	*25*	*50*
HPDE UT	0.151	7.312673498	36.56336749	29.25069399	0.341872231	0.854680576	1.709361153
HPDE BSA	0.101666667	7.7270718	38.635359	30.9082872	0.323537825	0.808844561	1.617689123
HPDE DMSO	0.089	7.837208259	39.1860413	31.34883304	0.31899114	0.797477851	1.594955702
HPDE Igf1	0.076666667	7.945954585	39.72977292	31.78381834	0.314625508	0.786563771	1.573127541
HPDE NVP	0.079333333	7.922314726	39.61157363	31.6892589	0.315564338	0.788910844	1.577821689
HPDE PPP	0.083333333	7.886986739	39.4349337	31.54794696	0.316977837	0.792444593	1.584889187
PANC-1 UT	1.1465	2.404443384	12.02221692	9.617773536	1.039741679	2.599354196	5.198708393
PANC-1 DMSO	0.3915	5.589522453	27.94761227	22.35808981	0.447265401	1.118163502	2.236327004
PANC-1 BSA	0.8225	3.453297629	17.26648815	13.81319052	0.723945709	1.809864272	3.619728544
PANC-1 IGF-1	0.726	3.846450742	19.23225371	15.38580297	0.649949828	1.624874571	3.229749142
PANC-1 NVP	0.659	4.15449279	20.77246395	16.61797116	0.601758175	1.504395438	3.008790876
PANC-1 PPP	0.57	4.578871242	22.89435621	18.31548497	0.545986089	1.364965222	2.729930443
Mia PaCa-2 UT	0.173333333	7.132454992	35.66227496	28.52981997	0.350510449	0.876276122	1.752552244
Mia PaCa-2 BSA	0.138	7.419662636	37.09831318	29.67865054	0.336942543	0.842356359	1.684712717
Mia PaCa-2 DMSO	0.094333333	7.790644964	38.95322482	31.16257986	0.320897694	0.802244234	1.604488468
Mia PaCa-2 Igf1	0.158333333	7.253000682	36.26500341	29.01200273	0.344684926	0.861712314	1.723424628
Mia PaCa-2 NVP	0.109	7.664017414	38.32008707	30.65606966	0.326199676	0.815499191	1.630998382
Mia PaCa-2 PPP	0.069666667	8.008345384	40.04172692	32.03338154	0.312174348	0.78043587	1.560871741

CF PAC-1 UT	0.7355	3.805838416	19.02919208	15.22335366	0.656885481	1.642213703	3.284427407
CF PAC-1 DMSO	0.1035	7.711259737	38.55629869	30.84503895	0.324201244	0.81050311	1.62100622
CF PAC-1 BSA	0.253	6.525009819	32.6250491	26.10003928	0.383141186	0.957852965	1.915705929
CF PAC-1 IGF-1	0.29225	6.245041004	31.22520502	24.98016402	0.400317628	1.000794069	2.001588139
CF PAC-1 NVP	0.526	4.809602908	24.04801454	19.23841163	0.519793432	1.299483579	2.598967158
CF PAC-1 PPP	0.268	6.41656342	32.0828171	25.66625368	0.389616659	0.974041647	1.948083293

2. Dot blots

Dot blots were used to determine the presence of the proteins of interest in each cell line as well as the optimal antibody concentrations to be used in the Western Blot Analyses. The dot blots demonstrated that Histone H3 Rabbit monoclonal antibody (1:1000) was bound by the HRP-bound anti-rabbit IgG secondary antibody (1:2000) (figure 15) and reacted with the Supersignal® West Pico Chemiluminescent substrate efficiently. Figure 10 shows that all the antibodies used sufficiently bound to the secondary antibody and reacted sufficiently with the chemiluminescent substrate. Table 3.3. Shows a summary of the final concentrations of primary antibody used for each cell line.

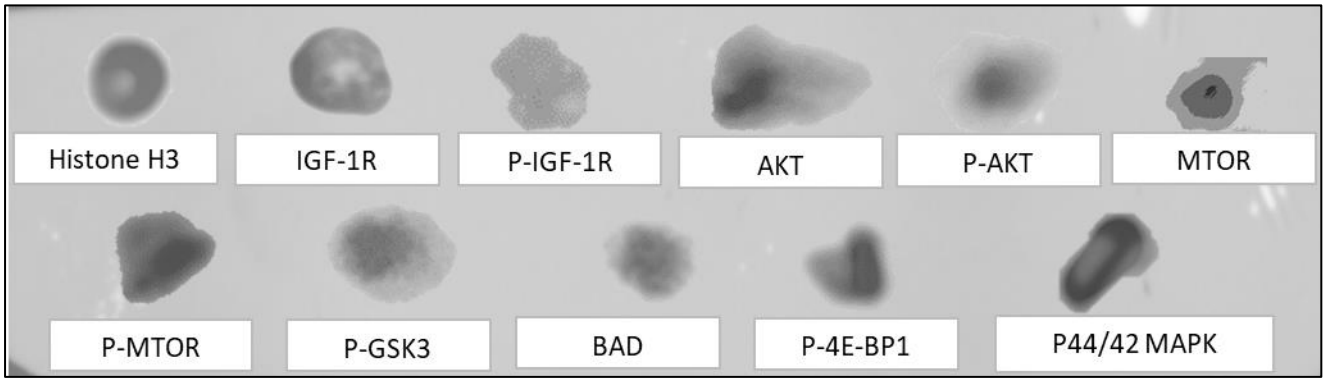

Figure C.2.: Dot Blots for the different antibodies used in Western Blotting.

Table C.2.: Summary of concentrations of antibodies used for Western Blotting as determined by dot blots.

PRIMARY ANTIBODY	OPTIMAL CONCENTRATION
HISTONE H3	1:1000
IGF-1R	1:1000
P-IGF-1R	1:2000
AKT	1:1500
P-AKT	1:1000

MTOR	1:1000
BAD	1:1000
P-4E-BP1	1:2000
P44/42 MAPK	1:1000

A concentration of 1:2000 was used throughout the optimization and western blots for the HRP-bound anti-rabbit IgG secondary antibody.

2. RNA Concentrations

Table C.3 RNA concentrations for each treatment group in PDAC cells

CELL LINE	TREATMENT GROUP	CONCENTRATION µg/µl	260/280 RATIO
HPDE	Untreated	209.6	2.07
	DMSO	0.6	1.09
	BSA	45.6	1.99
	IGF-1	212.8	2.07
	NVP-AEW541	51.2	2.2
	PPP	88.2	2.08
PANC-1	Untreated	143.9	2.09
	DMSO	62.7	2.05
	BSA	270.6	2.09
	IGF-1	15.5	2.06
	NVP-AEW541	164.5	2.09
	PPP	110.5	2.11
Mia PaCa-2	Untreated	326.1	2.09
	DMSO	389.6	2.08
	BSA	73.1	2.14
	IGF-1	322.0	2.09
	NVP-AEW541	65.7	2.06
	PPP	90.0	2.09
CF PAC-1	Untreated	5.9	2.07
	DMSO	51.8	2.08
	BSA	18.9	1.97
	IGF-1	203.4	2.12
	NVP-AEW541	7.7	1.99
	PPP	105.4	2.09

4. Statistics

Statistical analysis was done to determine if there were any differences between the treatment groups within each cell line.

4.1. HPDE

4.1.1. P-values for WST-1 proliferation

HPDE	DMSO	BSA	IGF-1	NVP-AEW541	PPP
DMSO		0.0000*	0.0000*	0.0000*	0.0001*
BSA	0.0000*		0.0000*	0.0000*	0.0824
IGF-1	0.0000*	0.0000*		0.0000*	0.0000*
NVP-AEW541	0.0000*	0.0000*	0.0000*		0.0073*
PPP	0.0001*	0.0824	0.0000*	0.0073*	

4.1.2. P-values for Clonogenic assay

HPDE	DMSO	BSA	IGF-1	NVP-AEW541	PPP
DMSO		0.0020*	0.0001*	0.0002*	0.0009*
BSA	0.0020*		0.5258	0.0333*	0.0351*
IGF-1	0.0001*	0.5258		0.0073*	0.0145*
NVP-AEW541	0.0002*	0.0333*	0.0073*		0.4983
PPP	0.0009*	0.0351*	0.0145*	0.498366	

4.1.3. P-values for gene expression

IGF1R	DMSO	BSA	IGF-1	NVP-AEW541	PPP
DMSO		0.0017*	0.0023*	0.0102*	0.0009
BSA	0.0017*		0.025*	0.9191	0.0009
IGF-1	0.0023*	0.025*		0.091	0.436
NVP-AEW541	0.0102*	0.9191	0.091		0.004
PPP	0.0009*	0.0009*	0.436	0.004*	
AKT3	**DMSO**	**BSA**	**IGF-1**	**NVP-AEW541**	**PPP**
DMSO		0.0092*	0.0075*	0.0036*	0.0052*
BSA	0.0092*		0.0624	0.0133*	0.0417*
IGF-1	0.0075*	0.0624		0.5909	0.5621
NVP-AEW541	0.0036*	0.0133*	0.5909		0.1191
PPP	0.0052*	0.0417*	0.5621	0.1191	
BAX	**DMSO**	**BSA**	**IGF-1**	**NVP-AEW541**	**PPP**
DMSO		0.004*	0.0023*	0.002*	N/A
BSA	0.004*		0.011*	0.0075*	N/A
IGF-1	0.0023*	0.011*		0.8254	N/A
NVP-AEW541	0.002*	0.0075*	0.8254		N/A
PPP	N/A	N/A	N/A	N/A	

BCL2	**DMSO**	**BSA**	**IGF-1**	**NVP-AEW541**	**PPP**
DMSO		0.2673	0.6191	0.0276*	N/A
BSA	0.2673		0.2031	0.057	N/A
IGF-1	0.6191	0.2031		0.0087*	N/A
NVP-AEW541	0.0276*	0.057	0.0087*		N/A
PPP	N/A	N/A	N/A	N/A	
FOXO1A	**DMSO**	**BSA**	**IGF-1**	**NVP-AEW541**	**PPP**
DMSO		0.0016*	0.0007*	0.001*	<0.0001*
BSA	0.0016*		0.0217*	0.0424*	0.0084*
IGF-1	0.0007*	0.0217*		0.6945	0.0218
NVP-AEW541	0.001*	0.0424*	0.6945		0.0587
PPP	<0.0001*	0.0084*	0.0218	0.0587	
MYC	**DMSO**	**BSA**	**IGF-1**	**NVP-AEW541**	**PPP**
DMSO		0.0017*	0.0016*	0.0059*	0.0469*
BSA	0.0017*		0.0131*	0.2167	0.7203
IGF-1	0.0016*	0.0131*		0.3228	0.6148
NVP-AEW541	0.0059*	0.2167	0.3228		0.8967
PPP	0.0469*	0.7203	0.6148	0.8967	
PI3KCA	**DMSO**	**BSA**	**IGF-1**	**NVP-AEW541**	**PPP**
DMSO		N/A	N/A	N/A	N/A
BSA	N/A		0.0096*	0.0122*	0.0018*
IGF-1	N/A	0.0096*		0.3745	0.0014*
NVP-AEW541	N/A	0.0122*	0.3745		0.0014*
PPP	N/A	0.0018*	0.0014*	0.0014*	
SNAI1	**DMSO**	**BSA**	**IGF-1**	**NVP-AEW541**	**PPP**
DMSO		N/A	N/A	N/A	N/A
BSA	N/A		0.8733	0.2808	N/A
IGF-1	N/A	0.8733		0.4711	N/A
NVP-AEW541	N/A	0.2808	0.4711		N/A
PPP	N/A	N/A	N/A	N/A	
VIM	**DMSO**	**BSA**	**IGF-1**	**NVP-AEW541**	**PPP**
DMSO		0.0491*	0.0232*	0.025*	0.0205*
BSA	0.0491*		0.0287*	0.0002*	0.0057*
IGF-1	0.0232*	0.0287*		0.1819	0.7734
NVP-AEW541	0.025*	0.0002*	0.1819		0.056

PPP	0.0205*	0.0057*	0.7734	0.056	

4.2. PANC-1

4.2.1. P-values for WST-1 proliferation

PANC1	**DMSO**	**BSA**	**IGF-1**	**NVP-AEW541**	**PPP**
DMSO		0.0000*	0.0005*	0.0364*	0.0000*
BSA	0.0000*		0.0000*	0.5793	0.0000*
IGF-1	0.0005*	0.0012*		0.0013*	0.0000*
NVP-AEW541	0.0364*	0.5793	0.0013*		0.0000*
PPP	0.0000*	0.0000*	0.0000*	0.0000*	

4.2.2. P-values for clonogenic assay

PANC1	**DMSO**	**BSA**	**IGF-1**	**NVP-AEW541**	**PPP**
DMSO		0.0079*	0.423	0.4537	0.0374*
BSA	0.0079*		0.1051	0.0967	0.0067*
IGF-1	0.423	0.1051		0.9192	0.3962
NVP-AEW541	0.4537	0.0967	0.9192		0.3122
PPP	0.0374*	0.0067*	0.3962	0.3122	

4.2.3. P-values for gene expression

IGF1R	**DMSO**	**BSA**	**IGF-1**	**NVP-AEW541**	**PPP**
DMSO		0.0074*	0.0925	0.0109*	0.0068*
BSA	0.0074*		0.011*	0.7541	0.3298
IGF-1	0.0925	0.011*		0.0127*	0.0113*
NVP-AEW541	0.0109*	0.7541	0.0127*		0.07476
PPP	0.0068*	0.3298	0.0113*	0.07476	
AKT3	**DMSO**	**BSA**	**IGF-1**	**NVP-AEW541**	**PPP**
DMSO		0.0909	0.0127*	0.1185	0.8605
BSA	0.0909		0.0038*	0.4714	0.0178*
IGF-1	0.0127*	0.0038*		0.01*	0.0066*
NVP-AEW541	0.1185	0.4714	0.01*		0.8
PPP	0.8605	0.0178*	0.0066*	0.8	
BAX	**DMSO**	**BSA**	**IGF-1**	**NVP-AEW541**	**PPP**
DMSO		0.1092	0.0003*	0.0393*	0.0298*
BSA	0.1092		0.0435*	0.6963	0.1953

IGF-1	0.0003*	0.0435*		0.0255*	0.1727
NVP-AEW541	0.0393*	0.6963	0.0255*		0.2133
PPP	0.0298*	0.1953	0.1727	0.2133	
BCL2	**DMSO**	**BSA**	**IGF-1**	**NVP-AEW541**	**PPP**
DMSO		0.0027*	0.1036	0.0006*	0.0121*
BSA	0.0027*		0.015*	0.235	>0.9999
IGF-1	0.1036	0.015*		0.0156*	0.0188*
NVP-AEW541	0.0006*	0.235	0.0156*		0.5364
PPP	0.0121*	>0.9999	0.0188*	0.5364	
FOXO1A	**DMSO**	**BSA**	**IGF-1**	**NVP-AEW541**	**PPP**
DMSO		0.0035*	0.0345*	0.0027*	0.0294*
BSA	0.0035*		0.0008*	0.1344	0.0114*
IGF-1	0.0345*	0.0008*		0.0014*	0.0083*
NVP-AEW541	0.0027*	0.1344	0.0014*		0.0081*
PPP	0.0294*	0.0114*	0.0083*	0.0081*	
MYC	**DMSO**	**BSA**	**IGF-1**	**NVP-AEW541**	**PPP**
DMSO		0.0017*	0.0242*	0.0018*	0.0123*
BSA	0.0017*		0.001*	0.0244*	0.0012*
IGF-1	0.0242*	0.001*		0.001*	0.0035*
NVP-AEW541	0.0018*	0.0244*	0.001*		0.0007*
PPP	0.0123*	0.0012*	0.0035*	0.0007*	
PI3KCA	**DMSO**	**BSA**	**IGF-1**	**NVP-AEW541**	**PPP**
DMSO		0.0507	0.0945	0.0193*	0.1335
BSA	0.0507		0.0107*	0.2544	0.2408
IGF-1	0.0945	0.0107*		0.0005*	0.0239*
NVP-AEW541	0.0193*	0.2544	0.0005*		0.07
PPP	0.1335	0.2408	0.0239*	0.07	
SNAI1	**DMSO**	**BSA**	**IGF-1**	**NVP-AEW541**	**PPP**
DMSO		0.0891	0.0916	0.121	0.9223
BSA	0.0891		0.7185	0.9762	0.023*
IGF-1	0.0916	0.7185		0.8658	0.0176*
NVP-AEW541	0.121	0.9762	0.8658		0.0585
PPP	0.9223	0.023*	0.0176*	0.0585	
VIM	**DMSO**	**BSA**	**IGF-1**	**NVP-AEW541**	**PPP**
DMSO		0.4702	0.3496	0.4436	0.1836

BSA	0.4702		0.0238*	0.7798	0.0004*
IGF-1	0.3496	0.0238*		0.031*	0.1707
NVP-AEW541	0.4436	0.7798	0.031*		0.0095*
PPP	0.1836	0.0004*	0.1707	0.0095*	

4.3. Mia PaCa-2

4.3.1. P-values for WST-1 Proliferation

MIAPACA	**DMSO**	**BSA**	**IGF-1**	**NVP-AEW541**	**PPP**
DMSO		0.6526	0.0817	0.6211	0.4724
BSA	0.6526		0.1074	0.4324	0.1074
IGF-1	0.0817	0.1074		0.2607	0.7948
NVP-AEW541	0.6211	0.4324	0.2607		0.6892
PPP	0.4724	0.3551	0.7948	0.6892	

4.3.2. P-values for Clonogenic Assay

MIAPACA	**DMSO**	**BSA**	**IGF-1**	**NVP-AEW541**	**PPP**
DMSO		<0.0001*	0.0006*	0.0004*	0.0327*
BSA	<0.0001*		0.0559	0.0004*	0.0559
IGF-1	0.0006*	0.0559		0.0044*	0.0044*
NVP-AEW541	0.0004*	0.0004*	0.0044*		0.0001*
PPP	0.0327*	<0.0001	0.0044*	0.0001*	

4.3.3. P-values for gene expression

IGF1R	**DMSO**	**BSA**	**IGF-1**	**NVP-AEW541**	**PPP**
DMSO		0.4429	0.5472	0.0040*	0.0672
BSA	0.4429		0.9496	0.0104*	0.1063
IGF-1	0.5472	0.9496		0	0.1161
NVP-AEW541	0.0040*	0.0104*	0.0161*		0.1298
PPP	0.0672	0.1063	0.1161	0.1298	
AKT3	**DMSO**	**BSA**	**IGF-1**	**NVP-AEW541**	**PPP**
DMSO		0	0	0	0
BSA			0.0307*	0.3248	0.0516
IGF-1		0.0307*		0.0355*	0.7046
NVP-AEW541		0.3248	0.0355*		0.0037*
PPP		0.0516	0.7046	0.0037*	

BAX	**DMSO**	**BSA**	**IGF-1**	**NVP-AEW541**	**PPP**
DMSO		0.0292*	0.0461*	0.0004*	0.0004*
BSA	0.0292*		0	0.0461*	0.0163*
IGF-1	0.0461*			0.0036*	0.7351
NVP-AEW541	0.0004*	0.0461*	0.0036*		0.0006*
PPP	0.0004*	0.0163*	0.7351	0.0006*	
BCL2	**DMSO**	**BSA**	**IGF-1**	**NVP-AEW541**	**PPP**
DMSO		0.896	0.4334	0.0923	0.1386
BSA	0.896		0.0426*	0.0125*	0.0052*
IGF-1	0.4334	0.0426*		0.0267*	0.0207*
NVP-AEW541	0.0923	0.0125*	0.0267*		0.1577
PPP	0.1386	0.0052*	0.0207*	0.1577	
FOXO1A	**DMSO**	**BSA**	**IGF-1**	**NVP-AEW541**	**PPP**
DMSO		0.0554	0.0130*	0.0042*	0.2774
BSA	0.0554		0.9468	0.0108*	0.5689
IGF-1	0.0130*	0.9468		0.0035*	0.5722
NVP-AEW541	0.0042*	0.0108*	0.0035*		0.1171
PPP	0.2774	0.5689	0.5722	0.1171	
MYC	**DMSO**	**BSA**	**IGF-1**	**NVP-AEW541**	**PPP**
DMSO		0.6188	0.1057	N/A	0.2038
BSA	0.6188		0.5537	N/A	0.3134
IGF-1	0.1057	0.5537		N/A	0.0802
NVP-AEW541	N/A	N/A	N/A		N/A
PPP	0.2038	0.3134	0.0802	N/A	
PI3KCA	**DMSO**	**BSA**	**IGF-1**	**NVP-AEW541**	**PPP**
DMSO		0.0002*	0.0033*	0.006*	0.3844
BSA	0.0002*		0.0013*	0.0002*	0.0014*
IGF-1	0.0033*	0.0013*		0.0117*	0.0039*
NVP-AEW541	0.006*	0.0002*	0.0117*		0.0031*
PPP	0.3844	0.0014*	0.0039*	0.0031*	
SNAI1	**DMSO**	**BSA**	**IGF-1**	**NVP-AEW541**	**PPP**
DMSO		0.023	0.7381	0.0319*	0.199
BSA	0.023		0.0076*	0.0022*	0.0041*
IGF-1	0.7381	0.0076*		0.0054*	0.575
NVP-AEW541	0.0319*	0.0022*	0.0054*		0.0018*

PPP	0.199	0.0041*	0.575	0.0018*	
VIM	**DMSO**	**BSA**	**IGF-1**	**NVP-AEW541**	**PPP**
DMSO		0.6866	0.1032	N/A	0.7764
BSA	0.6866		0.1042	N/A	0.8935
IGF-1	0.1032	0.1042		N/A	0.1014
NVP-AEW541	N/A	N/A	N/A		N/A
PPP	0.7764	0.8935	0.1014	N/A	

4.4. CF PAC-1

4.4.1. P-values for WST-1 Proliferation

CF PAC	**DMSO**	**BSA**	**IGF-1**	**NVP-AEW541**	**PPP**
DMSO		<0.0000*	<0.0000*	<0.0000	<0.0000*
BSA	<0.0000*		0.971544	0.0037*	<0.0000*
IGF-1	<0.0000*	0.971544		0.0123*	<0.0000*
NVP-AEW541	<0.0000*	0.0037*	0.0123*		<0.0000*
PPP	<0.0000*	<0.0000*	<0.0000*	<0.0000*	

4.4.2. P-values for Clonogenic Assay

CF PAC	**DMSO**	**BSA**	**IGF-1**	**NVP-AEW541**	**PPP**
DMSO		<0.0001*	<0.0001*	<0.0001*	<0.0001*
BSA	<0.0001*		0.0013*	0.0003*	0.0013*
IGF-1	<0.0001*	0.0013*		0.0043*	0.0005*
NVP-AEW541	<0.0001*	0.0003*	0.0043*		<0.0001*
PPP	<0.0001*	0.0004*	0.0005*	<0.0001*	

4.4.3. P-values for gene expression

IGF1R	**DMSO**	**BSA**	**IGF-1**	**NVP-AEW541**	**PPP**
DMSO		0.0005*	<0.0001*	0.0160*	0.0014*
BSA	0.0005*		<0.0001*	0.0044*	0.0007*
IGF-1	<0.0001*	<0.0001*		<0.0001*	0.0012*
NVP-AEW541	0.0160*	0.0044*	<0.0001*		0.0012*
PPP	0.0014*	0.0007*	0.0012*	0.0012*	
AKT3	**DMSO**	**BSA**	**IGF-1**	**NVP-AEW541**	**PPP**
DMSO		0.2342	0.0622	0.0039*	0.0006*
BSA	0.2342		0.0307*	0.6217	0.9443

IGF-1	0.0622	0.0307*		0.0040*	0.0040*
NVP-AEW541	0.0039*	0.6217	0.0040*		0.0006*
PPP	0.0006*	0.9443	0.0002*	0.0006*	
BAX	**DMSO**	**BSA**	**IGF-1**	**NVP-AEW541**	**PPP**
DMSO		0.0066*	0.0029*	0.0173*	0.0003*
BSA	0.0066*		0.0008*	0.0277*	0.0008*
IGF-1	0.0029*	0.0008*		0.0094*	0.0002*
NVP-AEW541	0.0173*	0.0277*	0.0094*		0.0443*
PPP	0.0003*	0.0004*	0.0002*	0.0443*	
BCL2	**DMSO**	**BSA**	**IGF-1**	**NVP-AEW541**	**PPP**
DMSO		0.0002*	N/A	0.0049*	0.0003*
BSA	0.0002*		N/A	0.1439	0.0047*
IGF-1	N/A	N/A		N/A	N/A
NVP-AEW541	0.0049*	0.1439	N/A		0.0094*
PPP	0.0003*	0.0047*	N/A	0.0094*	
FOXO1A	**DMSO**	**BSA**	**IGF-1**	**NVP-AEW541**	**PPP**
DMSO		0.0100*	N/A	0.0007*	N/A
BSA	0.0100*		N/A	0.0193*	N/A
IGF-1	N/A	N/A		N/A	N/A
NVP-AEW541	0.0007*	0.0193*	N/A		N/A
PPP	N/A	N/A	N/A	N/A	N/A
MYC	**DMSO**	**BSA**	**IGF-1**	**NVP-AEW541**	**PPP**
DMSO		0.0030*	0.0164*	0.0007*	0.0004*
BSA	0.0030*		0.0003*	0.0006*	0.0021*
IGF-1	0.0164*	0.0003*		0.0005*	0.0004*
NVP-AEW541	0.0007*	0.0006*	0.0005*		0.0016*
PPP	0.0004*	0.0021*	0.0004*	0.0016*	
PI3KCA	**DMSO**	**BSA**	**IGF-1**	**NVP-AEW541**	**PPP**
DMSO		0.0019*	0.0020*	0.006*	0.0020*
BSA	0.0019*		0.0604	0.0005*	0.0028*
IGF-1	0.0020*	0.0604		0.0012*	0.0030*
NVP-AEW541	0.006*	0.0005*	0.0012*		0.0045*
PPP	0.0020*	0.0028*	0.0030*	0.0045*	
SNAI1	**DMSO**	**BSA**	**IGF-1**	**NVP-AEW541**	**PPP**
DMSO	N/A	N/A	N/A	N/A	N/A

BSA	N/A	N/A	N/A	N/A	N/A
IGF-1	N/A	N/A	N/A	N/A	N/A
NVP-AEW541	N/A	N/A	N/A	N/A	N/A
PPP	N/A	N/A	N/A	N/A	N/A
VIM	**DMSO**	**BSA**	**IGF-1**	**NVP-AEW541**	**PPP**
DMSO		0.0674	0.5971	0.005*	N/A
BSA	0.0674		0.2955	N/A	N/A
IGF-1	0.5971	0.2955		N/A	N/A
NVP-AEW541	0.005*	0.0002*	0.0693		N/A
PPP	N/A	N/A	N/A	N/A	

Appendix D: Turnitin Report

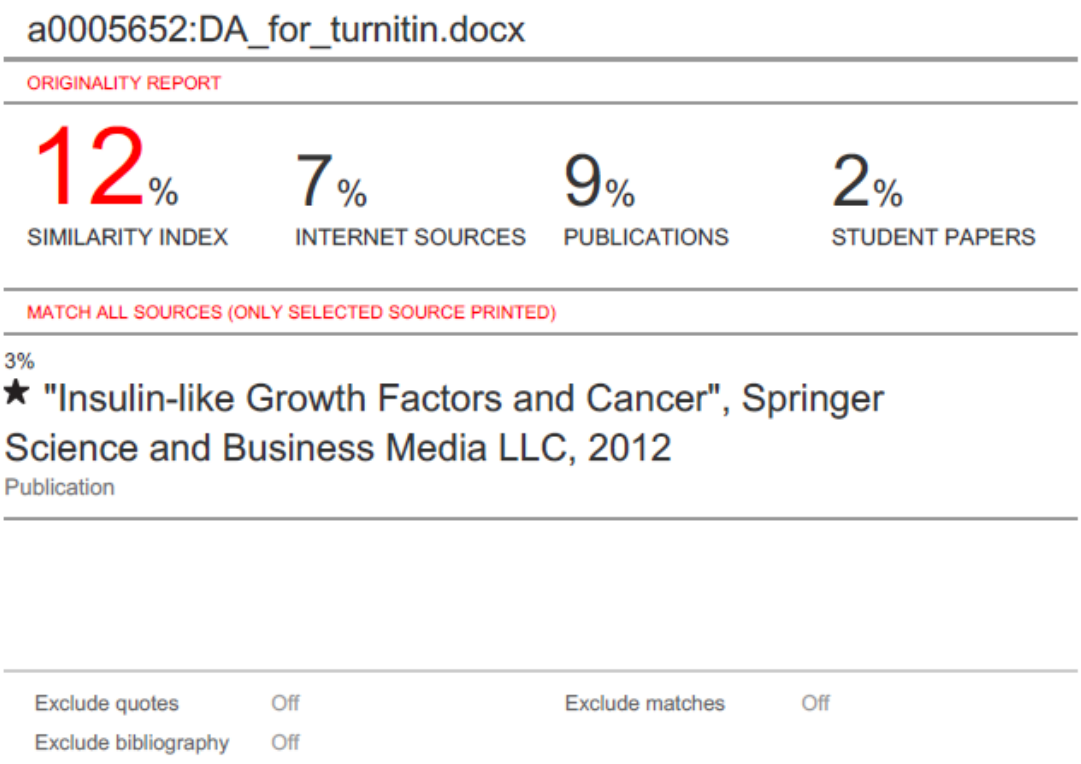

a0005652:DA_for_turnitin.docx

ORIGINALITY REPORT

12%	7%	9%	2%
SIMILARITY INDEX	INTERNET SOURCES	PUBLICATIONS	STUDENT PAPERS

MATCH ALL SOURCES (ONLY SELECTED SOURCE PRINTED)

3%

★ "Insulin-like Growth Factors and Cancer", Springer Science and Business Media LLC, 2012

Publication

Exclude quotes	Off	Exclude matches	Off
Exclude bibliography	Off		